Studies on Mre11-Ku interaction and its modulation by ionizing radiation

Inaugural-Dissertation

zur

Erlangung des Doktorgrades

Dr*. rer. nat.* der Fakultät

Biologie und Geografie

an der Universität Duisburg-Essen

Standort Essen, Germany

vorgelegt von

Aparna Sharma

aus

Neemuch, Madhya Pradesh, Indien

September 2010

Die der vorliegenden Arbeit zugrunde liegenden Experimente wurden am Institut für Medizinische Strahlenbiologie an der Universität Duisburg-Essen, Standort Essen, durchgeführt.

1. Gutachter: **Prof. Dr. George Iliakis**

2. Gutachter: **Prof. Dr. Peter Bayer**

Vorsitzender des Prüfungsausschusses: **Prof. Dr. Reinhard Hensel**

Tag der mündlichen Prüfung: **December 16, 2010**

Satisfaction does not come with achievement, but with efforts. Full effort is full victory.

Albert Einstein

Dedicated to

My Beloved Parents

Table of Contents

Abbreviation

°C	Grad Celsius
µm	Micrometer
Ab	Antibody
ATLD	Ataxia–telangiectasia-like-disorder
ATM	Ataxia-telangiectasia-mutated
B-NHEJ	Backup pathway of non-homologous end-joining
bp	Base pair
BRCA1	Breast cancer susceptibility protein 1
BRCA2	Breast cancer susceptibility protein 2
BRCT	Breast cancer C-terminus
BSA	Bovine Serum Albumin
CE	Cytoplasmic extract
CtIP	C-terminal binding protein interacting protein
DDR	DNA damage response
DNA	Deoxyribonucleic acid
DNA-PKcs	Catalytic subunit of the protein DNA-PK
D-NHEJ	DNA-PK dependent non-homologous end joining
ds	Double stranded
DSB	DNA double strand break
ECL	Enhanced Chemiluminescence
EDTA	Ethylene Diamine Tetraacetic Acid
EMSA	Electrophoretic mobility Shift Assay
et al.	et alii (and others)
EtBr	Ethidium Bromide
eV	Electron Volt
FACS	Fluorescence activated cell sorting
FBS	Fetal bovine serum
FHA	Forkhead-associated
FPLC	Fast Protein Liquid Chromatography
Gy	Gray
h	Hour
HDR	Homology directed repair

HRR	Homologous recombination repair
HSB	High salt Buffer
IP	Immunoprecipitation
IR	Ionizing radiation
k	kilo
kDa	Kilodalton
keV	Kilo electron volt
kV	Kilovolt
LSB	Low salt buffer
min	Minute
mMAb	Mouse monoclonal antibody
MOI	Multiplicity of infection
MR complex	Mre11-Rad50 complex
Mre11	Meiotic recombination11
MRN complex	Mre11-Rad50-Nbs1 complex
MW	Molecular weight
NBS	Nijmegen Breakage Syndrome
NE	Nuclear extract
ng	Nanogram
NLS	Nuclear localization signal
NP	Nuclear bound protein extract
pAb	Polyclonal antibody
PAGE	Polyacrylamide Gel Electrophoresis
PBS	Phosphate buffer saline
PCV	Packed column volume
PIKK	Phosphoinositide-3-kinase-related protein kinase
PMSF	Phenylmethylsulfonylfluoride
RNAase	Ribonuclease
RPA	Replication protein factor A
Rpm	Rotations per minute
SDS	Sodium Dodecyl Sulfate
sec	Seconds
ss	Single stranded
SSA	Single strand annealing

TEMED	N,N,N,N-Tetramethylethylenediamine
Tris	Tris- (hydroxymethyl)-aminomethane
WCE	Whole Cell extract

Abstract

The Mre11-Rad50-Nbs1 (MRN) protein complex is a well known sensor of DNA damage, functioning in signaling pathways that activate cell cycle checkpoints. The function of Mre11 is also known to be important for homologous recombination repair (HRR), and recent studies have shown that this protein may function both in HRR, as well as in the classical pathway of non homologous end joining that utilizes in addition to DNA-PK (D-NHEJ) also Ku and the Ligase IV/XRCC4 complex. Indeed, in yeast, in addition to Ku and Ligase IV homologs, also the MRN homologs are implicated in NHEJ. The Ku70/80 heterodimer is among the first proteins that recognize and bind to DNA ends. The crystal structure of Ku reveals an asymmetric ring conformation allowing the threading of the DNA and possibly facilitating rejoining. After completion of end joining, however, the protein will remain trapped on the DNA. This mode of action generates the question as to how trapped Ku is released from the DNA, and as to whether trapped protein serves somehow to the development of a full-blown DNA damage response. Hitherto, only one report suggests a ubiquitin-dependent removal and degradation of Ku80 from DNA, which is independent of the completion of NHEJ. There are no reports published to date investigating a functional role for the trapped Ku protein in the ensuing DNA damage response (DDR) signalling. The present thesis tests the hypothesis that trapped Ku contributes to DDR signalling by somehow facilitating the recruitment of the MRN complex to the site of the DSB. In support of this hypothesis, we demonstrate here that the constitutive interaction between Mre11 and Ku is enhanced after exposure to IR and that this enhancement is dose dependent. The interaction between Mre11 and Ku is studied by immunoprecipitation (IP) from nuclear extracts using an anti-Ku70 antibody while detecting Mre11 by Western blotting. IP studies are carried out using a human alveolar basal epithelium carcinoma cell line (A549), as well as CHO cells and a Ku80 deficient mutant (*xrs6*). As expected, Ku deficient cells show no detectable interaction between Mre11 and Ku70 and validate thus the specificity of the assay. An interaction between Mre11 and Ku is clearly visible in A549 cells and is markedly enhanced after exposure to 2 and 4Gy of X-rays. The interaction is resistant to EtBr and RNAase suggesting that it is not mediated by DNA or RNA. Rad50 and Nbs1 are also co-precipitated with Mre11, suggesting that the entire MRN complex is involved in the interaction. Notably, in addition to MRN, other DNA

damage sensors such as PARP-1 and ATM are part of the complex and are co-precipitated. The results point to intriguing interactions between Ku and signaling/repair proteins such as the MRN complex that warrant further investigation. The kinetics of Mre11 interaction with Ku after exposure to 4 and 8 Gy X-rays showed a weak Mre11 signal at 10 min after irradiation, but a strong signal 1-2 h after irradiation. When this interaction was tested in cells defective in PIKK family proteins, DNA-PKcs and ATM, it was found that DNA-PKcs defective cells show no Ku-MRN interaction following exposure to radiation. Treatment of extracts with bacterial alkaline phosphatase led to a decrease in the dose dependent interaction between Mre11 and Ku, while treatment with sodium ortho-vanadate and sodium azide (inhibitors of protein tyrosine phosphatases) led to an decrease in overall interaction but IR-dependent aspect remains unchanged.

The second part of my thesis focuses on the activity of PARP-1, which is a putative component of the backup pathway of non-homologous end joining (B-NHEJ), where it may function together with DNA Ligase III and histone H1. Goal of this part of the work was to examine possible interactions between Mre11 and PARP-1 and thus to establish a possible cross talk between D-NHEJ and B-NHEJ. The results show a marked increase in PARP-1 activity with increasing concentration of histone H1.

1. Introduction

1.1. DNA damage and repair

Maintenance of life depends on cell division, in which replication of millions of DNA base pairs is required. Proper DNA replication is a prerequisite of faithful chromosome segregation. However, once DNA replication faces abnormalities in the template DNA, it stops and cellular checkpoints are activated to provide time for removal of altered DNA structures. A proper restart of arrested DNA replication is vital to prevent activation of programmed cell death. However, the integrity of the genome is constantly challenged by endogenous factors, by-products of cellular metabolism, like free radicals and exogenous factors such as ionising radiation. DNA double strand breaks (DSBs) are one of the most deleterious DNA lesions, which if left unrepaired or repaired incorrectly, could lead to chromosomal aberrations including dicentrics chromosomes and acentric fragments [1, 2]. Even though DSBs is a major threat to genomic integrity, their formation also occurs naturally during meiosis [3] and in B and T-lymphocytes during V(D)J and class switch recombination. Therefore, the cell has evolved a number of mechanisms to sense, signal and repair DSBs that collectively make up the DNA damage response (DDR) [4-6].

1.2. The DNA damage Response

It is known that when inflicted with DNA damage, cells activate an intricate web of signalling pathways known as DNA damage response. Upon sensing DNA damage or stalled replication forks, cell cycle checkpoints are activated to arrest cell cycle progression and to allow time for repair. DDR comprises the stepwise activation of protein complexes involved in the detection of DNA lesions, the transduction of the generated signal to effector molecules and the activation of different repair pathways or of apoptosis (Figure 1).

DNA DSBs are one of the most powerful activators of DDR and they could be sensed by the Ku70/80 heterodimer [7] and the MRN complex [4, 8-10]. If processing of DNA ends occurs, the resulting single-stranded DNA (ssDNA) regions are immediately coated with RPA, which leads to subsequent activation of another DDR cascade with participation of ATR protein kinase [11, 12]. In the following step sensor molecules

activate a *signal transduction* system that involves members of the Phosphatidylinositol 3-OH Kinase related kinase family (PIKK) members, ATM, ATR [13, 14] and DNA-PKcs [15-17]. Once activated PIKKs phosphorylate many downstream targets including the effectors kinases Chk1 and Chk2. Finally the activation of cell cycle checkpoints culminates in the abrogation of cell cycle progression and the activation of appropriate DNA repair pathways; apoptosis ensues if the amount of damaged DNA is significant.

The key regulators of checkpoint pathways in eukaryotic cells are ATM (Ataxia Telangiectasia mutated) and ATR (ATM and Rad3-related) protein kinases. In response to initial DNA damage, ATM and ATR are phosphorylated and activate many downstream protein targets such as p53, Chk1, Chk2, BRCA1, Rad17, NBS1, 53BP1, MDC1 and many DNA repair proteins [18, 19].

It is commonly assumed that the Mre11-Rad50-Nbs1 (MRN) (Xrs2 in yeast) complex is among the earliest molecules sensing DNA damage, particularly DSBs. This complex is a paramount component of an entire signalling network and ensures DNA repair and activation of cellular response to DSBs. Main function of this complex is to recruit the ATM kinase to the damage sites, which considerably increases the ATM kinase activity. The requirement of MRN for ATM activation is also consistent with upstream MRN activation directly through the DSBs. Poly-ADP-ribose polymerase-1 (PARP-1) is another cellular enzyme with nuclear localization, which participates in sensing of DNA breaks, both single strand and double strand breaks in this case. Furthermore, the catalytic subunit of DNA dependent protein kinase (DNA-PKcs) has been proposed to be a DNA damage sensor molecule according to its ability to bind to DNA ends, either directly or through its interaction with Ku, and its activation by DSBs [20].

1.3. DNA Repair Pathways

It has now been conclusively established that cells repair DNA double strand breaks primarily by two major pathways: Non-homologous end joining (NHEJ) and Homologous recombination (HRR) [21, 22]. Since the classical NHEJ repair pathway relies on DNA-PKcs, it is referred as DNA-PKcs-dependent non-homologous end-joining (D-NHEJ). Other known pathways of DNA DSB repair are single strand annealing (SSA) and an alternative or backup pathway of NHEJ (B-NHEJ). All of the

above pathways are mechanistically and genetically distinct from each other but their functions are complementary and in some ways possibly redundant.

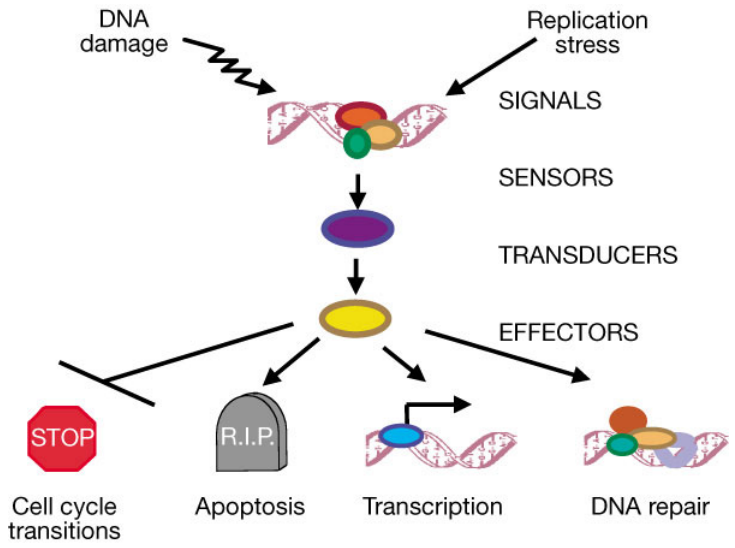

Figure 1: Schematic diagrammatic representation of DNA damage response [9]**:** This involves myriad of protein complexes. DNA damage is recognised by sensor proteins, which activate central signal transducers (for example ATM, a phosphatidylinositol-3-kinase). This ultimately results in the activation of effector proteins that execute the functions of DNA damage response, including recruitment and activation of checkpoint effectors, DNA repair proteins or induction of repair proteins.

1.3.1. Non-Homologous End-Joining (NHEJ)

Non-homologous end-joining is an error prone pathway, in which DNA ends are directly ligated without need of homologous DNA template. In mammals, NHEJ is active throughout the cell cycle but predominates particularly in G0 and G1 phase due to non-functional HRR at these cell cycle phases. Mammalian cells favour NHEJ pathway [23], although many of the components involved in this pathway are conserved from yeast to humans [24, 25]. The big difference is that mammalian cells utilize DNA-PKcs in the repair of DSBs by NHEJ, while a homolog of this enzyme in yeast and lower eukaryotes has not been found. The importance and usage of this repair process also varies greatly among species.

D-NHEJ involves of the sequential recruitment of protein complexes. In the initial step, the Ku70/80 heterodimer binds to DNA ends (initial damage detector) and recruits DNA-PKcs to DSBs activating thus its kinase function (Figure 2). DNA-PKcs, which displays serine and threonine kinase activity, becomes activated upon DNA

end binding, and phosphorylates itself as well as a number of substrates including p53, Ku heterodimer, DNA Ligase IV/XRCC4 [26] and replication protein A (RPA2) [11], all of which may facilitate NHEJ when phosphorylated. NHEJ of ends with damaged nucleotides as well as of more complex non-complementary ends requires terminal processing. End processing involves the removal of damaged or mismatched nucleotides by nucleases and/or re-synthesis of ssDNA by DNA polymerases Pol-μ and Pol-λ. DNA polymerases Pol-μ and Pol-λ (Pol4 in yeast) are from Pol-X family of DNA polymerases, which operate at aberrant DNA structures and fill the gaps during NHEJ [27]. This step can be skipped if DNA ends are compatible for ligation and have a 3'-OH and a 5' phosphate group.

There is evidence that the MRN nuclease complex could also participate in this reaction to facilitate or to regulate the further ligation step [1, 28], but the exact mechanism of engagement remains unknown. Finally, during the third step, the DNA Ligase IV/XRCC4 tetramer complex and XLF (Cernunnos) are recruited to ligate the DSBs [29-33]. The precise role of XLF is still unknown, but it interacts with DNA Ligase IV/XRCC4 and re-adenylates DNA Ligase IV after ligation, thus recharging the ligase and allowing it to catalyze a second ligation reaction [34]. BRCA1 and BRCA2, the two famous cancer genes, mutations of which are associated with breast cancer, are also associated with a number of DNA repair pathways especially NHEJ and HRR.

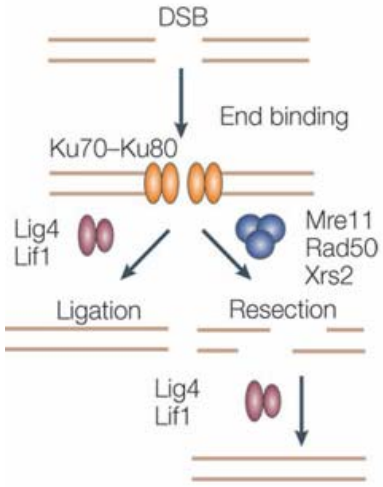

Figure 2: Non-homologous end joining pathway of DNA double strand break repair: Step1: Broken DNA ends are recognized by Ku70/80 heterodimer. Ku binds to DNA ends and recruits DNA-PKcs. DNA-PK (Ku/DNA-PKcs complex) phosphorylates other proteins involved in DNA repair or signaling. Step2: Broken DNA ends are processed to enable ligation. Mre11/Rad50/Nbs1 complex may play a role in this step. Step3: DNA Ligase IV/XRCC4 is required for stabilization and for maximum activity of DNA Ligase IV [35] .

1.3.2. Homologous recombination repair (HRR)

Homologous recombination repair (HRR) is an error free pathway, utilizing sister chromatid sequences for the restoration of the original DNA sequence in the vicinity of the DSB (Figure 3). HRR is particularly important for repairing of DSBs and Inter-strand cross links (ICLs) during G2 and S phase of the cell cycle, but it also plays an important role in the restoration of stalled or collapsed replication forks [36].

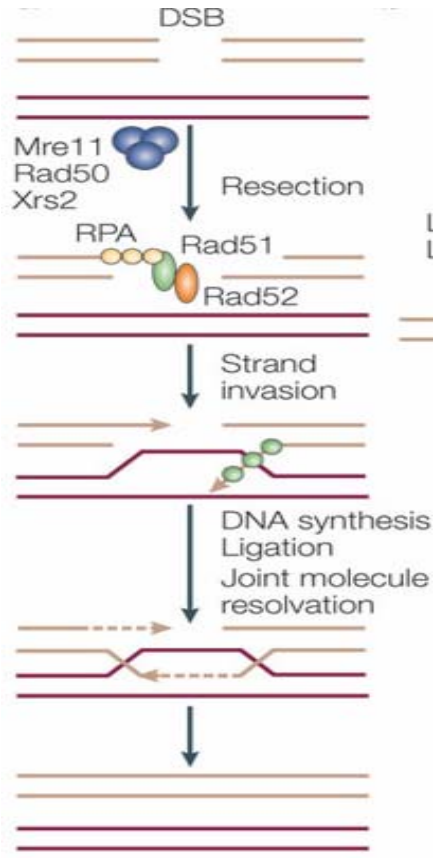

Figure 3: Homologous recombination repair: HRR is an important pathway for repairing replication lesions and it depends on the RAD51-family of proteins and makes use of homologous DNA sequences normally found in the sister chromatid. The proteins BRCA1 and BRCA2 play a key role in this pathway [35].

1.3.3. Backup (B-NHEJ) or Alternative pathway (A-NHEJ) of NHEJ

In addition to the DNA-PKcs dependent pathway of NHEJ, cells enlist another NHEJ type of double strand break repair pathway called backup pathway (B-NHEJ), which is generally utilized when D-NHEJ is compromised, or when there is chemical inhibition or mutations in any of the factors participating in the D-NHEJ. This

inactivation of D-NHEJ results in the activation of B-NHEJ that removes DSBs from the genome by performing a backup function [37]. B-NHEJ is error prone in nature [38] and operates with 20-30 fold slower kinetics in comparison to D-NHEJ, which repairs nearly half of the DSBs in the first few minutes after irradiation [39-41]. Current knowledge about B-NHEJ implicates DNA Ligase III/XRCC1 and PARP1 as the core components of this process along with the Histone H1[42].

The second part of the present thesis focuses on some aspects of Histone H1 as a stimulatory factor of B-NHEJ.

Recent data provide evidence for the cooperation of mammalian Mre11 and PARP-1 in this alternative pathway of NHEJ [43]. Our group reported that higher activity of B-NHEJ could be observed in the G2 phase of the cell cycle and that becomes apparent when measuring DSB rejoining activity in D-NHEJ deficient cells by pulse-field gel electrophoresis. The results of these experiments indicate that although the fast component of NHEJ is compromised at later time points after irradiation, residual rejoining activity fully restores genome integrity independently of HRR [44]. We also reported that B-NHEJ gets suppressed when Ku binds to DNA ends, particularly when it interacts with DNA-PKcs.

1.4. NHEJ - Still an unsolved puzzle?

1.4.1. Ku heterodimer and MRN complex: Initial players in NHEJ

The Ku70/80 heterodimer is among the first components of the classical NHEJ pathway to bind the broken DNA ends of a DSB [7]. It further recruits the 465-kDa DNA-PKcs to the DSB resulting in stimulation of DNA-PKcs kinase activity [45-47]. A consequence of this mode of end recognition is that Ku and DNA will become topologically linked on completion of the repair [48, 49]. Evidently, the Ku heterodimer becomes trapped on DNA after completion of the repair event, which raises an important question concerning the mechanism of unloading of the trapped Ku protein, as well as the possible functional importance of its presence at the site of the rejoined DSB. Several theories were proposed in this regard. It is thought that the unloading of the trapped Ku heterodimer from DNA might be achieved if the subunits could dissociate and thereby compromise the stability of the interface between α/β and β-barrel domains within a single subunit, involving some local unfolding of the β-

barrel [49] (Figure 5). Another theory proposed that there is an ubiquitin-dependent removal and degradation of Ku80 from DNA, which is independent of the completion of NHEJ. Binding of Ku to DNA induces a signal recognized by an E3 ubiquitin ligase, which then polyubiquitylates Ku80. Polyubiquitylation leads to either a conformational change in Ku, which releases it from DNA, or, more likely to the recruitment of an additional factor that actively dissociates Ku80 from the DNA. After dissociation, Ku80 is recognized and degraded by the proteasome [50].

Genetic and biochemical evidence have determined that the DNA Ligase IV/XRCC4/XLF complex is responsible for rejoining the DNA ends during NHEJ [47]. The Ku complex and MRN are known to interact to each other but the mode of their interaction and its functional significance remain unknown. In this regard, studies show that association of the Ku heterodimer with broken DNA ends inhibits recombination in MRX mutants but not in repair-proficient cells or other DNA repair single mutant [51].

One of the most intriguing questions in the field of DSB repair is how and when does a cell decide to opt for which pathway to repair a DSB. One of the recent studies demonstrate that Ku (70 and 80) is a critical regulator of pathway choice in human somatic cells, as Ku can inhibit HR at telomeres and it can inhibit HR and B-NHEJ throughout the genome [52]. There are findings which provide strong evidence that the different DNA DSB binding properties of Mre11 and Ku determine the different efficiencies of HRR and NHEJ to repair high LET induced radiation [53].

Although the Ku heterodimer and the MRN complex are the earliest molecules to be recruited to the sites of DSBs [54] and are known to interact with each other [55], the functional relevance of this interaction is not known. It is therefore particularly relevant to study the possible implications of this interaction on DNA damage repair and to determine whether induction of damage leads to positive or negative regulation of this interaction. It is possible that the nuclease activity of Mre11 has a role to play in the unloading of trapped Ku from the repaired DNA ends, but the contribution (like post translational modifications of Ku) of other MRN complex partners cannot be ruled out. For studying these aspects of the interaction, in depth knowledge of the structure of the Ku heterodimer and MRN proteins is important.

1.4.2. Biochemistry and structure of Ku heterodimer

The sequence similarity between the two Ku subunits over their entire length suggests that they originated from a common ancestor [7, 56, 57]. Each Ku subunit consists of three regions: an amino-terminal von Williebrand A domain (vWA), a central core domain and a diverged carboxy-terminal region (Figure 4). vWA domain is responsible for protein-protein interactions and is involved in the heterodimerization of Ku [7]. The carboxyl-terminal region of Ku70 consists of a SAP domain, thought to be a DNA binding domain which helps Ku translocation on linear DNA molecules [49] and ensures the ability of Ku70 to bind weakly to DNA in the absence of Ku80 [7]. The carboxy terminal domain of Ku80 is longer and contains the binding region of the DNA-dependent protein kinase catalytic subunit.

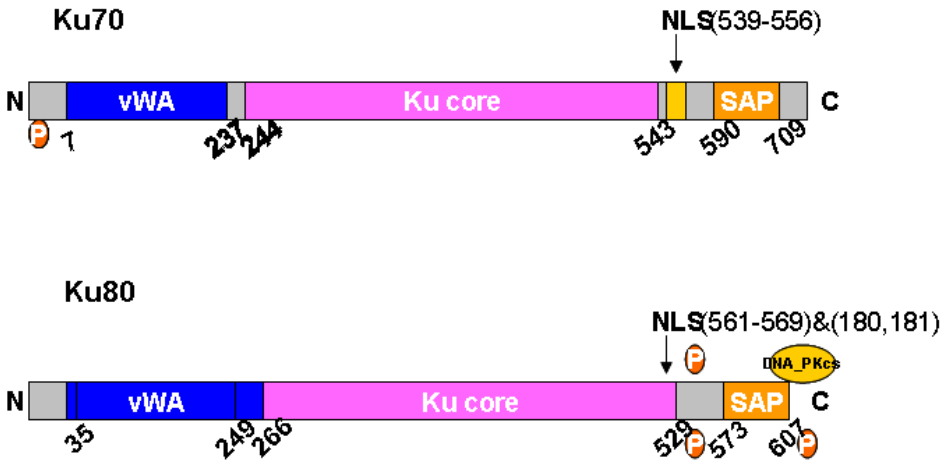

Figure 4: Structure of Ku heterodimer: Domain boundaries, phosphorylation sites (red, protein-protein interaction sites and interacting proteins (yellow ovals) are shown for (A) Ku70 and (B) Ku80. Domain boundaries for the Von Williebrand domain (vWa) (amino acids 35-249). Ku core (amino acids 266-529) and SAP domains (amino acids 573-607) of Ku70 and the vWa (amino acids 7-237), Ku core (amino acids 244-543) and C-terminal domains (amino acids 590-709) of Ku80. The location of putative nuclear localization sequences (NLS) in Ku70 (amino acids 539-556) and Ku80 (amino acids 561-569) are indicated [58].

1.4.3. The fate of Ku trapped on DNA

The Ku heterodimer is a structure specific, sequence independent DNA binding protein [7]. Ku has extreme DNA affinity and can bind to the ends of DNA, for example- 3'-5' overhangs of double stranded oligonucleotides, blunt ends and other

nucleotidic structures like nicks, gaps and bubbles in circular dsDNA, single stranded DNA and RNA [48, 59, 60]. The Kd values for DNA-end binding by Ku are in the range of 2.4x 10^{-9} - 5x10^{-10} M^{-1}. Ku is known not to require ATP for DNA binding and once bound to double stranded DNA and it can translocate along the molecule in an ATP independent way allowing multiple subunits of Ku to bind to linear DNA, at least in vitro [61]. The crystal structure of Ku bound to DNA revealed that the complex has a open-ring like shape with the DNA threaded through the aperture [49, 62]. Ku ring is designed with a base that cradles DNA, and a very narrow bridge (strand β) on each subunit that acts as a barrier to promiscuous binding to unbroken DNA [49] (Figure 5). It has been observed that Ku protein binds to the ends of DNA and then slides along DNA to offer free ends for the next Ku protein binding [7]. Therefore, the Ku protein binds DNA by adding molecules at two ends of DNA until the fragment is completely covered with protein molecules (accumulative binding) [63-65]. Ku80 requires Ku70 for binding to DNA, Ku70 has weak DNA binding activity on its own [66]. Ku binds to linear DNA much more efficiently than to closed super coiled DNA [61]. No major structural changes have been observed to the ring itself that is needed to thread a DNA end through the complex.

1.5. The biological machine: MRN Complex

The MRN complex, comprising Mre11, Rad50 and Nbs1, is a highly conserved protein complex**,** which is among the earliest molecules that sense DNA damage [67]. The reported Mre11 and Ku heterodimer interaction is in agreement with the roles proposed for these proteins in NHEJ as they are the earliest players to take a lead in the choice of the DSB repair pathway [28, 68, 69]. MRN complex is now considered to be a bridging factor or the junction between the different repair pathways available to a cell (D-NHEJ, HRR, and B-NHEJ), as probably the complexity of the DSB or the type of DNA ends generated after DNA damage induction allows MRN complex to make a pathway choice. This complex is a principal component of signalling pathways involved in cellular responses to DNA DSBs. All three complex subunits have analogues from yeast to mammals [70, 71]. The MRN components have different enzymatic activities, thus making MRN complex a sensor of DNA damage, a DNA end processing molecule and a signal transducer involved in DNA damage response signalling. The MRN complex also participates in DNA

replication, meiotic recombination, mitosis and telomere maintenance [72-74]. The importance of this complex can be gauged by the fact that null mutations in any of its components (Mre11/Nbs1/Rad50) results in embryonic lethality in mice [75]. Individuals inflicted with mutations in any of the MRN subunits suffer inherited cancer prone diseases such as NBS (Nijmegen breakage syndrome) and ATLD (Ataxia Telangiectasia like disorders) [76]. These autosomal disorders are marked with radiosensitivity and defective cell cycle checkpoints. Cells with deficiencies in MRN components are very similar to those of ATM-deficient cells with respect to the IR-induced cell-cycle arrest [77] resulting in a dramatic reduction of targeted integration frequencies, gene conversion and sister chromatid exchanges, and impaired single strand annealing [78].

The complex containing Mre11, Rad50 and Nbs1 proteins have now been implicated in all three major DNA repair pathways – HRR, D-NHEJ and B-NHEJ, even though these pathways are quite different mechanistically [79, 80]. The MRX complex in yeast plays an important role in homologous recombination, non-homologous end joining, telomere maintenance, S-phase checkpoint control and meiotic recombination [54].

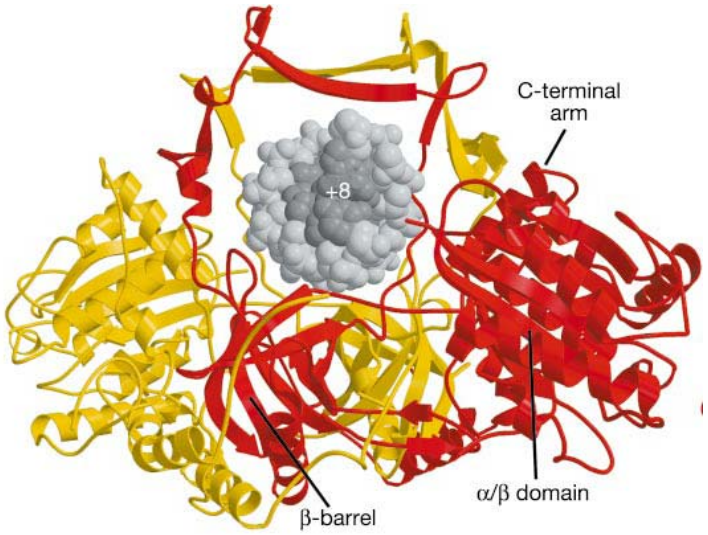

Figure 5: (A) Crystal structure of Ku heterodimer: View down of the DNA helix, Ku70 is coloured red and Ku80 orange. Only the 14bp duplex DNA is shown. The sugar phosphate backbone is coloured light grey and bases dark grey [49].

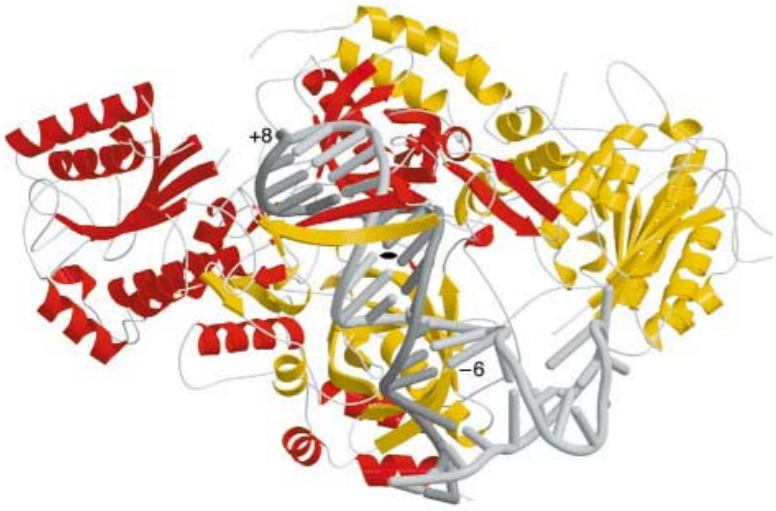

Figure 5: (B) Ribbon diagram of Ku bound to DNA: Ku70 is coloured red and Ku80 orange. The 34-residue oligonucleotide is light grey, the 21 residue oligonucleotides dark grey [49].

1.5.1. Biochemistry and structure of the MRN complex

1.5.1.1. Mre11

The human Mre11 is composed of 708 amino acids (a.a) and consists of four conserved phosphoesterase domains at the N-terminal and two DNA binding domains at the C-terminal (Figure 6). The N-terminus has an Nbs-1 binding site and the C-terminus contains a Rad50 binding site. The Phosphoesterase, or nuclease, domain is responsible for several biochemical properties of the protein such as the 3'-5' double stranded DNA exonuclease (which are Mn^{2+}, ATP and Nbs1 dependent), single stranded DNA endonuclease and DNA unwinding activities [81]. The nuclease activity of Mre11 is structure specific, the double stranded DNA exonuclease function of the protein is active on substrates with blunt or 3' recessed ends, but is poorly active on 3' protruding ends [79, 82, 83]. The endonuclease activity of Mre11 is also weakly active on hairpin DNA substrates and is stimulated by ATP [84]. It has been reported that the nuclease activity of Mre11 is only required for the purpose of DNA repair and not for DSB signalling and telomere maintenance, a point that is ambiguous when referring to budding yeast studies [85]. Mre11 has an intrinsic DNA-binding activity [81, 83] carried out by the DNA binding domain, which is stimulated by Rad50 on its own or in combination with Nbs1. The N-terminal part of Mre11 interacts with C-terminus of Ku70 and this interaction was confirmed in a yeast two-hybrid system [55].

Mre11 is known to dimerize and to form a homodimer, which is needed for the basic MRN functions and which is also required for Mre11 DNA binding in vitro, and Mre11 repair activity in vivo [86]. Scanning atomic force microscopy revealed that the MRN complex has a bipolar architecture in which human Mre11 and Rad50 bind DNA via a globular domain consisting of an Mre11 dimer and two Rad50 ATPase domains, while the coiled coil regions of Rad50 form an extended intra-molecular flexible arm. Thus, interactions between the coiled-coils of DNA bound Mre11 complexes would tether sister chromatids or DNA ends within the same chromatid [87, 88].

Mre11 (80kDa)

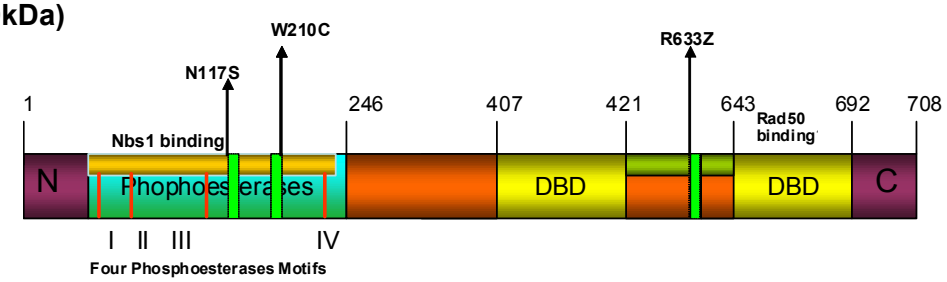

Figure 6: Domain structure of Mre11: Mre11 has an N-terminal phosphoesterase or nuclease domain, and a C-terminal DNA binding domain. The Mre11 catalytic domain (residues 1-342) bind to Mn^{2+} and the exonuclease product of Mre11, when 3'-5' exonuclease activity is catalysed [89].

1.5.1.2. Rad50

Rad50 is a 150 KDa ATP-dependent protein belonging to the "structural maintenance of chromosomes'' SMC group of proteins consisting of 1328 amino acids and containing Walker A and Walker B nucleotide (NTP)-binding motifs that confer ATPase activity [90] at its amino and carboxy-terminal ends (Figure 7). These motifs are separated by two heptad-repeat regions, which form an extended coiled-coil structure that is interrupted by a putative globular domain [79, 90]. Rad50 forms an anti-parallel homodimer that brings together the Walker A and B binding motifs of separate Rad50 molecules to create a functional ATP binding domain. Mre11 seems to bind as a dimer on the extremity of the coiled-coil region that is proximal to the catalytic domain of Rad50. The ATP binding motifs are crucial for all known activities of MRN including ATM activation. The proposed main function of Rad50 is to bind damaged DNA ends and hold them in close proximity.

Rad50 (150 kDa)

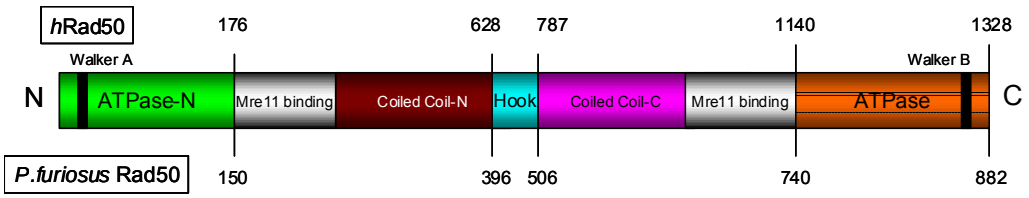

Figure 7: Domain structure of Rad50: Rad50 has ATP binding cassettes (ABC), ATPase and central Zn-hook domains. ATPase-N and ATPase-C terminal domains are separated by 600 amino acids anti-parallel coiled coil. The central Rad50 region bears a CxxC motif that reverses directionality of the coiled coil and co-ordinates Zn^{2+} to mediate hook-hook interactions [89].

1.5.1.3. Nbs1

The third subunit of eukaryotic MRN complex, Nbs1 (or its functional homolog Xrs2 in *Saccharomyces cerevisiae)* is much less sequence conserved and only found in eukaryotes [22, 91, 92]. Nbs1 is a 90 kDa protein consisting of 754 amino acids and shows three functional regions: A Fork Headed-associated Domain (FHA) at C-terminus (24-108 a.a.), which is believed to be a phospho-specific protein-protein interaction motif that recognises phosphorylation of target proteins (Figure 8). FHA domain directly interacts with the histone γ-H2AX, the phosphorylated form of H2AX, and leading to the recruitment of the MRN complex to the vicinity of DSBs. A central region, which also functions in signal transduction, consists of the BRCT domain (108-196 and 221-330 a.a.) and ATM phosphorylation sites at serine residues 278, 343 and 615, which is responsible for the intra S-phase checkpoint control [54]. The C-terminal region of Nbs1 is responsible for the interaction with Mre11 and ATM. Nbs1 regulates the Mre11 and Rad50 catalytic activity by forming a complex with them and localises Mre11 and Rad50 to the nucleus and interacts with other DNA repair proteins, for example ATM, γ-H2AX and MDC1.

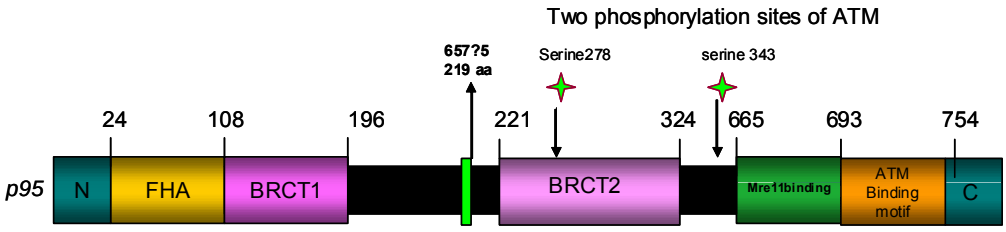

Figure 8: Domain structure of Nbs1: Nbs1 consists of an N-terminal Fork head-associated (FHA) domain. There are two important phosphorylation sites, Ser278 and Ser343 for phosphorylation by ATM. The structure also includes the Mre11-binding motif and the BRCT phosphor-peptide interaction domain [89].

1.6. How does MRN complex respond to DNA damage?

Mre11 is homogenously distributed within the nucleus in undamaged cells but migrates rapidly to the sites of DNA double strand breaks, showing association with damaged DNA within 10 min post irradiation in the form of small granular foci [22].

Initial recruitment is probably via its DNA end binding activity, but subsequently, excess MRN is recruited to the vicinity of DSBs in large focal structures regulated by its interaction with γ-H2AX. The MRN complex is thought to bind and secure the DNA ends together via its zinc hooks at the ends of the long flexible Rad50 arms, with the Mre11 molecules binding to DSBs. Upon DSB binding, the Rad50 arms undergo structural modifications, becoming rigid and parallel and bridging both DNA ends using the zinc hook. Secured in this fashion, the initial step of DSB processing is thought to take place.

In addition, the signalling cascade of DNA damage response (DDR) is activated with the initial steps being activation of ATM kinase. Inactive ATM kinase is a dimmer, which after monomerization is believed to be recruited to DSBs by Nbs1, resulting in autophosphorylation and activation of ATM kinase activity. Further, ATM kinase phosphorylates many DNA-damage response proteins including Nbs1 itself [54]. CtIP, which is an end processing nuclease, is also phosphorylated by ATM and interacts with MRN [93]. Many other DNA damage response proteins are also recruited to the sites of DNA damage and contribute to DSB processing and repair. PARP-1, which is not directly linked to checkpoint activation, is rapidly activated by DNA strand breaks (both single and double strand breaks) and signals the presence of DNA lesions by attaching ADP-ribose units to chromatin associated proteins. There is evidence [94] that Mre11 can directly bind to these ADP-ribose units via short poly ADP-ribose (PAR) binding motif localized between the two DNA-binding regions. Recent findings implicate Mre11 in backup pathways, as rapid accumulation of Mre11 and Nbs1 at the sites of DNA damage requires PARP-1, thus hinting towards a bridging role for MRN complex between D-NHEJ and B-NHEJ.

1.7. MRN complex - Role in DNA repair pathways

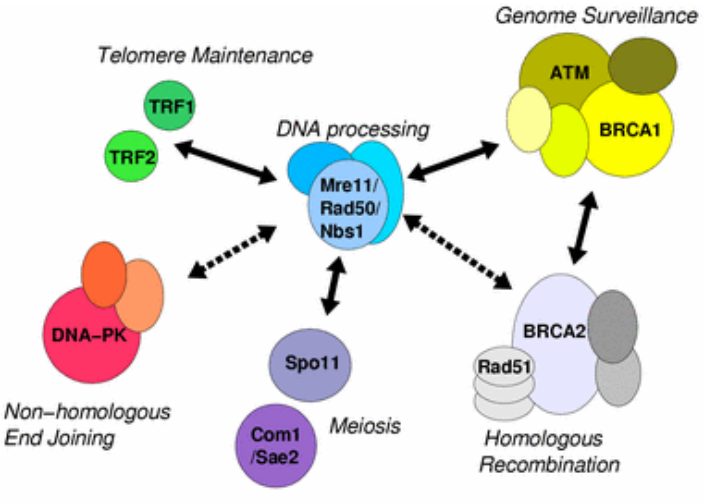

Figure 9: MRN is a key player in DDR: MRN operates in early cellular responses to DNA processing, for example in HRR, NHEJ, in meiotic recombination, telomere maintenance and ATM activation (Courtesy Hopfner lab, LMU, Munich, Germany).

1.7.1. MRN in HRR

HRR is facilitated by recognition of the DSB by CtIP (endonuclease activity) which gets phosphorylated by ATM and mediates the processing of DNA ends. CtIP has the ability to bind and promote Mre11-directed nuclease processing in the 5'-3' direction to yield 600-800 nucleotides of 3' single stranded DNA [95, 96]. These 3' single stranded tails are then coated and protected by RPA (replication protein factor A) [97]. With the help of Rad52 epistasis group members [98]: Rad52, the RAD55/57 heterodimer, Rad54 and in higher eukaryotes the breast cancer susceptibility protein BRCA2, the DNA strand exchange protein Rad51 displaces RPA generating a nucleoprotein filament that invades homologous DNA segments for polymerase mediated extension [33]. The HRR process is completed after strand resolution (resolution of Holliday junction) and ligation of the generated DNA ends. Mre11, Rad50, and XRS2 have been suggested as candidates for the nuclease that resects 5' ends in meiosis prior to homologous strand exchange in yeast [99].

1.7.2. MRN in NHEJ

It is commonly believed that the predominant pathway for DSB repair in mammalian cells is D-NHEJ. Although the nuclease activity of Mre11 is not important for accurate NHEJ, its involvement has been reported in the budding yeast [28, 69, 100-104]. Inaccurate repair has been reported in plasmid end-joining assays in the absence of Ku heterodimer on the top of Mre11 activity loss. Interaction of mammalian Ku70, which is paramount component for D-NHEJ, with Mre11 has been reported, which raises the possibility that Ku70 recruits Mre11 to the sites of DSBs. Also cells deficient in Ku70 were deficient in Mre11 foci formation after exposure to IR [55]. Furthermore, in hamster cells, co- localization of Ku protein with Mre11 has been reported and physical interactions between mouse Mre11 and Ku documented [105].

On the other hand, genetic studies suggest that in yeast Mre11 and Ku function in distinct repair pathways [106, 107]. It has also been reported that dissociation of NHEJ proteins from repaired damage sites depends on MRX and ATP binding by Rad50, indicating that the MRX complex may be the critical factor in repair pathway switching, at least at the ends that failed NHEJ [108]. The most obvious mechanism for this dissociation would be MRX-stimulated resection of DSB ends for HR, which seems incompitable with continued NHEJ protein binding protein. [108]. Loss of Ku leads to more rapid resection at the ends of the DSBs [109, 110] and increases HRR efficiency, indicating that removal of Ku from DNA is necessary to initiate HRR. Since both proteins are present in a wild type cells, the cells must engage appropriate mechanisms to ensure the proper coordination in the function between the different proteins involved in the processing by the different repair pathways.

Whether Mre11 plays a role in unloading of Ku from repaired/rejoined DNA is still not clear. Also, it is not clear whether Ku assists the recruitment of Mre11 on the DSB sites. Mre11 seems to have a bridging function for homologous stretches of DNA and/or broken DNA ends [111]. The core of Mre11-Rad50 complex exists as a heterotetrameric assembly (M2R2)2 and for non-homologous end- joining, a Zn2+-linked (M2R2)2 octamer may be responsible for bringing the two ends together. Alternatively, two broken ends might bind to the head of the same Mre11 complex that has inserted Zn2+ linkage [112]. The specific role of Mre11 in classical NHEJ is not clear as the MRN complex takes part in several processes of DNA repair

including D-NHEJ and B-NHEJ. However, it is very difficult to rationalize how MRN will be able to dominate over Ku once a DSB is induced. The models tested in the present thesis are first attempts to address this question.

1.7.3. MRN in B-NHEJ/A-NHEJ

As we have discussed above, NHEJ can be divided into two sub-pathways, one is the classical or canonical DNA-PKcs dependent NHEJ (D-NHEJ) and the other one, is a DNA-PK independent backup, or alternative pathway (A/B-NHEJ); the latter is also referred to as microhomlogy-mediated end joining (MMEJ) to indicate the higher use of microhomologies at the generated junctions. There is evidence that B-NHEJ utilizes DNA Ligase III/XRCC1, histone 1 and PARP-1. Recent studies have also implicated Mre11 as an important player in B-NHEJ. It has been observed that loss of Mre11 affects both D-NHEJ and B-NHEJ and decreases the end- joining frequencies in some experimental systems. On the other hand, Mre11 over-expression activates the resection of single stranded DNA and increases alternative end-joining. Mre11 nuclease activity was found to be an essential factor favoring A-NHEJ [43, 113]. Another study pointed out the usefulness of alternative pathways in DSB repair in mammalian cells and the role of Nbs1, which is vital for alternative NHEJ of hairpin coding ends, but suppresses the joining of signal ends in V(D)J recombination intermediates [114].

Evidence accumulates that Mre11 contributes to the regulation of DSB repair pathway choice and that it contributes to alternative NHEJ of coding ends in V(D)J recombination. However, it is not clear how Mre11 and PARP-1 interact or coordinate their functions within B-NHEJ [114].

It is known that PARP-1 and Ku compete with each other for DNA ends during DSB repair, However, in irradiated cells, the higher affinity of Ku for DNA ends and the excessive number other forms of lesions that also recruit PARP-1, limits PARP-1's contribution to DSB repair [115]. As PARP-1 and the MRN complex are important candidates of B-NHEJ and may work in conjunction with histone H1, we sought to decipher the possible interactions between the MRN complex, PARP-1 and histone H1 proteins. The structure and function of PARP-1 protein is described in the following passages.

1.8. PARP-1

PARP-1 is a member of large family of enzymes that use NAD^+ as substrate to transfer ADP-ribose units onto the glutamic acid residues of proteins. Poly ADP-ribosylation is a posttranslational modification of nuclear enzymes, which is stimulated by SSBs and DSBs and assists somehow in the repair of cells carrying this form of damage [116]. It is a DNA repair enzyme and also a chromatin associated protein mostly found in the nucleus of eukaryotic cells.

1.8.1. Structural Organization of PARP-1

PARP-1 is a monomer of 116 kDa composed of three functional domains (Figure 10). The N-terminus has a DNA binding domain which binds to SSBs, DSBs, crossovers, cruciform structures and supercoils [117]. The central region contains the auto modification domain, which has a BRCT1 at the C-terminal region and which is involved in several protein interactions related to DNA repair, recombination and cell cycle checkpoint. The catalytic domain contains an NAD^+ binding site. An immediate cellular response to DNA damage induced by alkylating agents, ionizing radiation or oxygen radicals is mediated by the activation of the catalytic domain. The targets of PARP-1's enzymatic activity includes PARP-1 itself, core histones, the linker histones and a variety of transcriptional regulatory factors that interact with PARP-1. Autoribosylation of PARP-1 is important because this property results in the release of PARP-1 from the DNA and initiates the function of other DNA repair proteins.

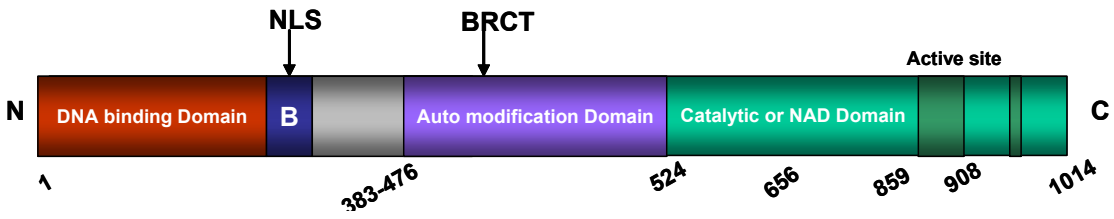

Figure 10: Domain structure of PARP-1: PARP-1 has a carboxyl terminal domain that catalyzes poly(ADP)-ribosylation reactions using NAD^+ as donor of ADP-ribose groups. PARP-1 also has an amino terminal DNA binding domain (DBD) containing three zinc finger motifs, a nuclear localization signal and an auto modification domain.

1.9. Role of PARP-1 in DNA repair

PARP-1 plays an important role in sensing DNA damage. PARP-1 is a key signaling enzyme involved in triggering the repair of single-strand DNA damage [1-3] and also in base excision repair [118]. It binds as a homodimer to SSBs through its N terminal zinc fingers and recruits XRCC1, DNA Ligase III, histone H1 and DNA polymerase β [119]. PARP-1 is also known to play a role in the remodeling of chromatin by PARylating histones and relaxing chromatin structure, thus increasing DNA accessibility to repair factors. PARP-1 together with DNA Ligase III has also been implicated in an alternative or backup pathways of NHEJ [115]. One study also observed collaboration between PARP-1, Mre11 and Nbs1 at the proximity of the DNA lesion [94]. PARP-1 deficiency is implicated in colon and liver tumorigenesis. Deficiency of PARP-1 accelerates ageing and spontaneous carcinogenesis in mice, which are hypersensitive to high doses of ionizing radiation and die within 10 days.

1.10. Aims / Objectives of the thesis

General Aim

The general aim of the thesis is to evaluate and gain deeper understanding of the interactions between Mre11 and Ku in cells exposed to IR.

Specific Aims

(I)

- To investigate the role of Mre11 as a sensor protein and to determine its function in DSB repair in cells exposed to ionizing radiation. Particular emphasis was placed on the investigation of interactions between Ku and Mre11.
- To study the effect of different X-ray doses on the interaction between Mre11 and Ku.
- To examine the stability of these interactions and to investigate whether these interactions are direct or indirect (DNA or oligonucleotide dependent).
- To monitor the kinetics of recruitment of Mre11 at the sites of DSBs after exposure of cells to ionizing radiation.
- To investigate the regulation of radiation-induced interactions between Mre11 and Ku.
- To find potential interacting partners of Ku and Mre11.

(II)

The second part of my thesis focuses on the well-known DNA damage sensor PARP-1. Here, the following objectives are tested:

- Examination of the possible interactions between Mre11 and PARP-1 in an attempt to bridge the role of Mre11 between D-NHEJ and B-NHEJ.
- Test the activity of purified PARP-1 in the presence or absence of histone H1 and analyze this function vis a vis the function of B-NHEJ.

2. Materials and Methods

2.1. Materials

2.1.1. Laboratory Apparatus

AI Filter	GE-Healthcare, Germany
AEKTA purifier 10/100 UPC-900	GE Healthcare, Germany
Avanti J-20XP	Beckman Coulter, USA
Beckman Tabletop GS-6R centrifuge	Beckman, CA, USA
BioFuge (Fresco)	ThermoScientific, USA
Cell culture Bench	Thermo Scientific, Heraeus
Coulter Counter	Beckman Coulter, USA
Electro-Transfer Unit	Bio-Rad, USA
EMSA gel apparatus	Bio-Rad, USA
Flow Cytometer	Beckman Coulter
Gel Dryer	Bio-Rad, USA
Heating unit	Peter Oehman, Germany
Incubator	Sanyo, Japan
Magnetic Stirrer	Heidolph, Germany
Microscope	Olympus, Germany
Molecular Imager VersaDoc	Bio-Rad, USA
Nanodrop	Nanodrop Technologies
Overnight Culture Shaker	Infors, Germany
Pasteur pipette	Falcon, USA
Peristaltic pump	Ismatec
pH Meter	InoLab, Germany
Pipettes	Eppendorf, Germany
Rocky	Peter Oehmen gmbh
Roller drum	Bellco Biotechnology
SDS PAGE mini gels	Mini PROTEAN, Bio-Rad
Typhoon Scanner	GE Healthcare, Germany
Ultracentrifuge	Beckman Coulter, USA

UV Spectrophotometer	UV-240IPC, Shimadzu
Vortexer(Vortex-Genie 2)	Scientific Industries, USA
Water Bath	Oehmen Laboratory
Weighing Machine	Sartorius (BP110 S)
X-ray machine (320KV)	GE Healthcare, Germany
Gel blotting Paper	Bio-Rad, USA

2.1.2. Disposable Elements

0.2 µm filter	Millipore, USA
1.5 and 2 ml tubes	Eppendorf, Germany
15 & 50 ml Centrifuge Tubes	Falcon,USA
Cell Culture Dishes	Cellstar, USA
Dounce homogenizer	KonTes, Kimble Chase LLC
Flasks and beakers	Simax, Germany
Gel blotting Paper	Bio-Rad, USA
Mouse or Rabbit True blot IgG Agarose beads	e-Biosciences, USA
Nitrocellulose membrane	Schleicher & Schuell
Pipettes	Rainin, USA
PVDF membrane	GE Healthcare, Germany
Spinner Flask	Bellco, USA
UV Cuvettes	Hellma, USA
Parafilm	Lab Depot Inc. USA

2.1.3. Chemical Reagents

The chemicals used were of analytical grade

Acrylamide-Bis-acrylamide (37:5.1)	Roth, Germany
Albumin Bovine	Sigma-Aldrich, Germany
Bromophenol Blue	Sigma-Aldrich, Germany
DMEM	Sigma-Aldrich, Germany
DTT	Roth, Germany
EDTA	Roth, Germany
Ethanol	Roth, Germany
FCS/FBS	Gibco, Germany
Glycerol	Roth, Germany
Glycine	Roth, Germany
Grace's Insect Medium	Gibco Life Sciences
Isoproponal	Roth, Germany
KCl	Roth, Germany
Lactalbumin hydrolysate	Sigma-Aldrich, Germany
McCoy's5A	Sigma-Aldrich, Germany
MEM	Gibco, Invitrogen
Methanol	Sigma-Aldrich, Germany
NaCl	Roth, Germany
Non-Fat dry milk	Roth, Germany
Nonidet P40	Roche, Germany
Propidium Iodide	Sigma-Aldrich, Germany
RNase	Sigma-Aldrich, Germany
TEMED	Roth, Germany
TRIS Base	Roth, Germany
Tris-HCL	Sigma-Aldrich, Germany
Triton X-100	Roth, Germany
Trypsin	Biochrome, Germany
Coomassie brilliant blue G250	Serva, NewYork
Tween 20	Roth, Germany
Yeastolate ultrafiltrate	Gibco, Germany

2.1.4. Commercial Kits and Columns

γ-32P	Perkin Elmer, USA
DNA cellulose resins	Sigma-Aldrich, Germany
ECL Western Blotting Reagent	GE Healthcare, Germany
Hi Load (26/60) Superdex 200	GE Healthcare, Germany
HITrap^{TM}Heparin prepacked column	Amersham Biosciences
QIAquick Nucleotide removal Kit	Qiagen, Germany
Sephadex 200	GE Healthcare, Germany
Super signal West Femto sensitive kit	Thermo Scientific, Germany
T4 polynucleotide Kinase	Fermantas, 10U/µl, Germany
T4 polynucleotide Kinase Forward buffer	Fermantas, Germany

2.1.5. Cell lines

Table 2.1: **Cell lines used in cell culture experiments.**

Name	Description	Culture Medium	Refrences
HCT116	Colorectal Carcinoma	McCoy's 10% FBS	[120]
A549	Human alveolar basal epithelial cell carcinoma	McCoy's 10% FBS	[121]
Xrs6	Chinese hamster ovary cell mutant deficient in Ku80	MEM + 10% FCS	[122]
M059 J and K	Human Glioma cell lines. M059J is DNA-PKcs mutant	DMEM+10% FCS6	[123]
AT5BIVA	Immortalized Ataxia Telangiectasia cells	McCoy's 5A + 10% FCS (20mM Hepes pH 6.85)	[124]

2.1.6. Oligonucleotide Sequences

Table 2.2: Oligonucleotides used in experiment.

Name of Oligos	Sequence(5'-3')
Oligonucleotides (EMSA)	OA-(GGC CGC ACG CGT CCA CCA TGG GGT ACA A) OB-(TTC TAC CCC ATG GTG GAC GCG TGC GGC C)

Note: Annealing of the oligonucleotides OA with OB results in blunt end double stranded DNA. This DNA was 3' end labeled using γ-P^{32} ATP with polynucleotide kinase for EMSA.

2.1.7. Antibodies

Table2.3: Antibodies used in Western Blotting analysis.

Antibodies	MW(kDa)	Type	Manufacture	Cat. number	Dilution
Primary Ab					
Ku70-N3H10	70	mAb	Kamiya Biomed	MC-351	1:1000
Mre11	81	pAb	Novus	B100-142	1:5000
Nbs1	95	pAb	Novus	NB100-143	1:5000
Rad5013B3	160	mAb	GeneTex	GTX70228	1:1000
ATM-2C1	236	mAb	GeneTex	MS-ATM-10pX1	1:1000
GAPDH	30	mAb	Chemicon	MAB374	1:100000
PARP-C-2-10	116	mAb	Sigma-Aldrich	P-248	1:1000
Secondary Ab					
Mouse IgG-HRP		mAb	Cell Signalling	7076	1:1000
Rabbit IgG-HRP		pAb	Cell Signalling	7074	1:1000

2.1.8. Software Used

Table 2.4: Software used for quantification of results.

Program	Software
Image Quant	Molecular Dynamics (Invitrogen)
Quantity One	Biorad
Illustrator	Adobe
Sigma plot	Systat
MS Office	Adobe
Unicorn	Aekta

2.2. Methods

2.2.1. Cell Culture

Tissue culture was performed in incubators at 37°C with 5% CO_2. A549 Cells were maintained in McCoy's 5A medium, M059K and M059J cells were a kind gift from Dr. J. Allalunis-Turner (Cross Cancer Center, Edmonton, Canada) and were maintained in DMEM. HCT116 DNA-PKcs$^{-/-}$ and DNA-PKcs$^{+/+}$ wild-type (wt) cells (a gift of Prof. Dr. Eric Hendrickson) were maintained in McCoy's 5A medium and AT5BIVA cells were maintained in MEM medium. Insect Sf9 cells (suspension cells) were grown in spinner cultures at 27°C in Grace's insect medium.

All adherent cells were grown in 100 ml tissue culture dishes with 15 ml growth medium. Exponentially growing cells were passaged every 3 days while avoiding confluency levels above 80%. For passage, media was removed and cells were rinsed with 1x ice cold PBS. Cells were rinsed with 2 ml Trypsin-EDTA solution and incubated for 5 min at 37°C. Detached cells were then resuspended in 10 ml cold media supplemented with 10% FBS. Single cell suspensions were obtained by passing cells through a Pasteur pipette. Cells were counted and appropriate number of cells was further incubated for experiments or for subculture, see Appendix (1). Cells were discarded after about 50 passages, since their genomic stability could not be guaranteed.

2.2.2. Ionizing radiation (IR)

Cells were exposed to X-rays generated at 320KV, 10mA after a 1.65 Al filter. Dosimetry was performed with PTW and or chemical dosimeter, which were used to calibrate an in-field ionization monitor. The doses mostly used were 2, 4 and 8 Gy. An even distribution of dose of radiation dose on the cell cultures was ensured by rotating the radiation table. Cells were returned to the incubator immediately after treatment with IR and collected at different times, from 10 min to 8 h depending on the experiment.

2.2.3. Flow cytometry

2.2.3.1. Cell cycle analysis by flow cytometry

Propidium iodide binds to DNA proportionally to its mass. Cells cycle distribution was assessed by measuring propidium iodide (PI) fluorescence in a flow cytometer. Cells were washed with cold PBS and trypsinized at 37°C for 5 min. Cell suspensions were prepared in 5 ml cold fresh media. About 1 million cells were collected and centrifuged at 1500 RPM, 4°C for 5 min. The cell pellets were washed with 1x ice cold PBS and fixed in 70% ethanol at -20°C overnight. Supernatant was removed by centrifugation at 1500 RPM for 5 min. Pellets were washed with 1x ice cold PBS and incubated in 1x PBS containing PI (40ug/ml), and RNase (62µg/ml) at 37°C for 30 min in the dark. Samples were measured in a flow cytometer according to pre-established protocols, see Appendix (1). 20,000 cells per sample were counted and the single cell population was gated to obtain standard histograms. Histogram list mode files (*.HST) were generated by counting the frequency cells with same PI signal intensity. The fractions of cells in the different phases of the cell cycle were calculated using the Wincycle® software. HST files were loaded into the Wincycle®. The parameter “S phase growing cells order” was carefully chosen between 0, 1 or 2, until the prediction model fitted the histogram shape. Cell cycle distributions were automatically calculated. G2 arrest kinetics was obtained by plotting the G2 fraction as a function of time after IR.

2.2.4. Electrophoresis

2.2.4.1. SDS-PAGE

Cell lysates and immunoprecipitation reactions were electrophoresed on 10 % SDS-PAGE gels. Cell lysates were denatured with 2X SSB and heated on 95°C for 5‘ and centrifuged for 5 min on 13000 rpm before loading. SDS-PAGE mini gels were cast according to the instructions given by the manufacturer of the apparatus. Samples were resolved for 20 min on 100V from the stacking gel and the voltage was then adjusted to 150V for a 60 min run on RT so that samples fractionate throughout the resolving gel. For further details refer to Appendix (2).

2.2.4.2. Western Immunoblots

Cell lysates and immunoprecipitates were resolved on 10% polyacrylamide gels and transferred on a PVDF membrane. PVDF membranes were activated by rinsing them for 1 minute in 100% methanol and then washing them thrice with MQ water briefly. Activated PVDF membrane and gels were incubated in 1X cold transfer buffer (Glycine 200mM, Tris 25mM, 10% methanol) at 4°C for 15-20 minutes on a rotator. Meanwhile the sponge and blotting paper were pre-soaked into transfer buffer and then all components were assembled into the electro-transfer unit according to the instructions of the manufacturer and run at 100V for 60 min. After the transfer was completed, the unit was disassembled and the side of membrane on which proteins was transferred was incubated in blocking buffer (5% non-fat dry milk dissolved into 1X TBST for 2 h at RT with gentle agitation. Membranes were incubated with primary Ab for overnight at 4°C. After incubating membranes into primary antibodies the membranes were washed gently with 1X TBST (5x 5min) and then probed with secondary antibody, linked with horseradish peroxidase, for 1 h. After incubating membranes in secondary antibodies the membrane was washed again with 1XTBST (5X 5min). For more details, refer to Appendix (2).

2.2.4.3. Western Blot detection

Western blots were developed using the ECL developing solution which is a chemiluminescence detection kit; solution A and solution B were mixed together in ratio 1000:25 µl, spread on membrane, incubated for 5 min and visualised using molecular imager VersaDoc MP 4000 System. Quantification of protein amounts was

performed using the ImageQuant software and Quantity one. For some blots which had weak signals, Super Signal West Femto Maximum sensitive Kit was also utilized for developing Western blots, in which solution A and B were mixed in 1:1 ratio.

2.2.4.4. Antibodies

The primary antibodies and secondary antibodies are given in Table 2.2 in the "Materials" section.

2.2.5. Cell Fractionation

2.2.5.1. Preparation of whole cell extract

Whole cell extract was prepared using the freeze-thaw method. First, adherent cells were washed once with 1x ice cold PBS and then the pellet was washed once with hypotonic buffer, Appendix (4); cells were centrifuged at 1500 rpm for 5 min and the pellet resuspended in three PCV hypotonic buffer. The cells were disrupted by freezing in liquid nitrogen (3x) and immediately thawing at 37°C. Then 3M KCl was added to a final concentration of 500 mM and the mix was incubated at 4°C for 30-60 min on a rotating platform. Samples were centrifuged at 14000 rpm at 4°C for 40 min. and the supernatant was dialysed against 400 mM KCl containing dialysis buffer.

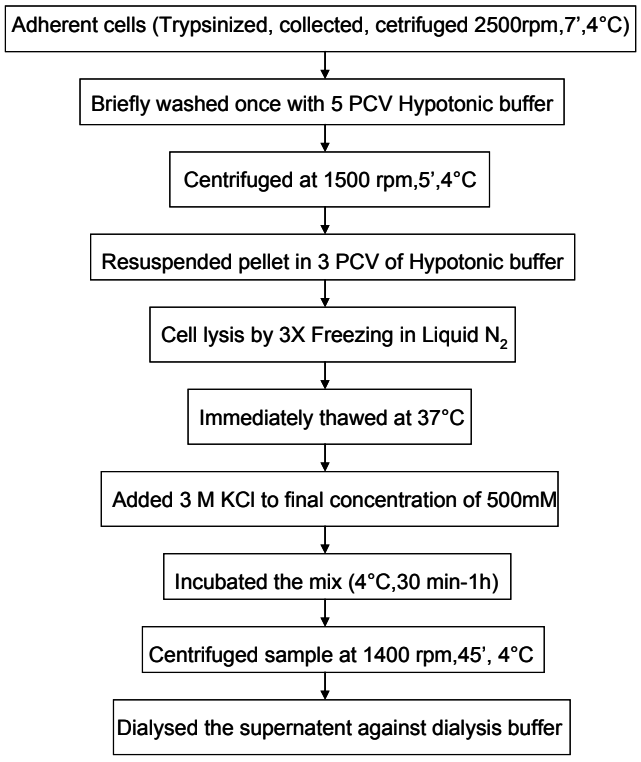

Figure 11: *Flow chart of whole cell extract preparation*

2.2.5.2. Cell Fractionation

(Cytoplasmic extract, nuclear extract and nuclear-bound-protein extract)

A549 cells were trypsinized, collected, centrifuged at 2500 rpm for 7 min and resuspended in 1 PCV of hypotonic buffer. Cells were disrupted by homogenizing in Dounce homogenizer (15-20 strokes with a B Pestle) and centrifuged at 3300 rpm for 30 min. The supernatant containing the cytoplasmic extract was collected , the pellet was resuspended into two PCV of low salt buffer (LSB), Appendix (4) and one PCV of high salt buffer (HSB) Appendix (4), and incubated for 30 min under mild rotation at 4°C. Samples were then centrifuged at 1300 rpm for 45 min and the supernatant was designated nuclear extract and collected in a new tube. The remaining pellet was processed in the same manner to obtain the nuclear-bound-protein extract. All extracts were dialysed against dialysis buffer, Appendix (4), and centrifuged for 20 min at 13000 rpm. Protein concentration was determined using the Bradford assay and BSA as a protein standard. For more information about buffers refer to Appendix (4).

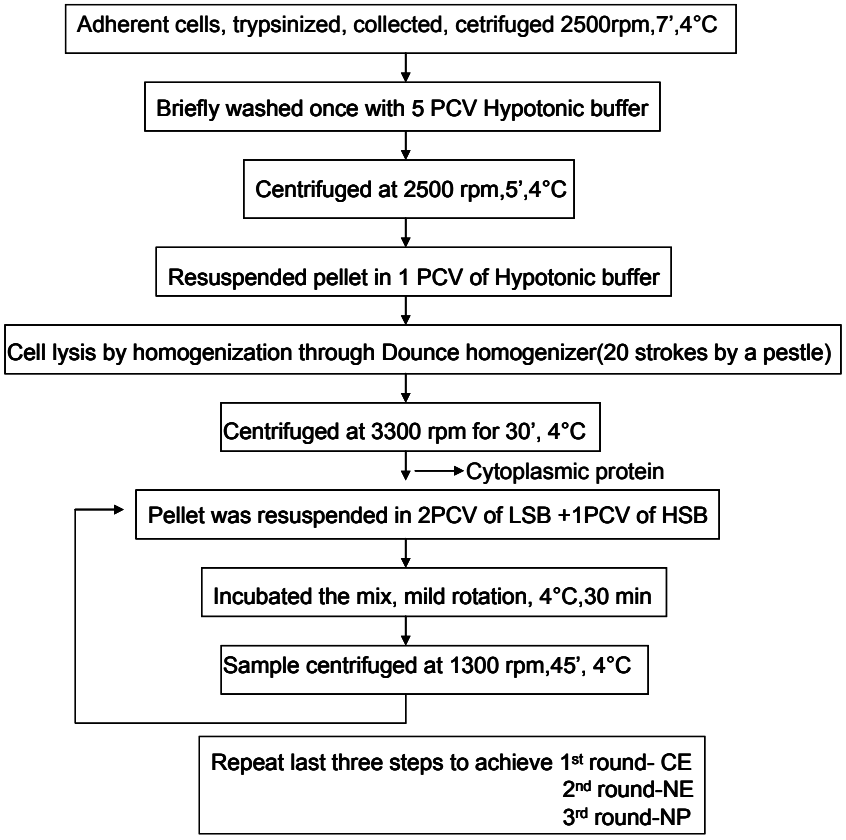

Figure 12: *Flow chart of biochemical cell fractionation*

2.2.6. Immunoprecipitation

For Immunoprecipitation reactions, we utilized mouse and rabbit TrueBlot IgG agarose beads. Immunoprecipitation was performed initially by pre-clearing of the beads with excessive protein and incubating the extract with 50 µl beads/reaction for 30 min on ice. Then samples were centrifuged at 9500 rpm for 1 min and the supernatant collected in a new eppendorf tube. Next, Ku monoclonal antibody was added at 2 µg per reaction and incubated on a rotator shaker for 2 h. Subsequently, fresh agarose beads (50 µl) were added to each tube and incubated again for 2 h under constant rotation. Non-specific proteins were removed by washing beads (3x) with 500 µl of IP lysis buffer while centrifuging each wash at 9500 rpm for 1 min. Bound proteins were denatured by adding60-100 µl Laemmli buffer to each tube, heated at 95°C and run on 10% SDS polyacrylamide gel, before blotting onto a PVDF/nitrocellulose membrane. For more information refer to Appendix (3).

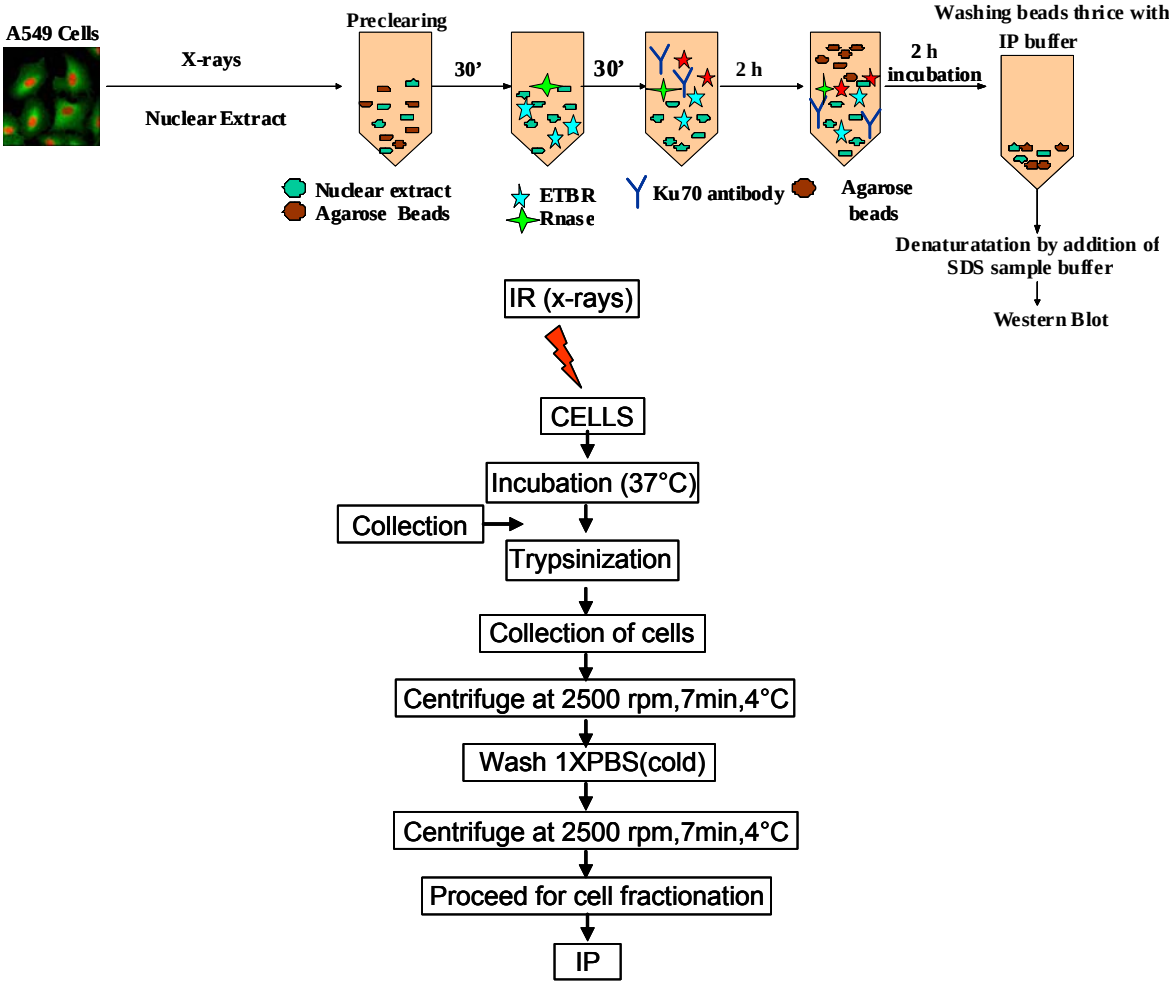

Figure13: *Diagrammatic representation of the IP procedure and flow chart of the steps from irradiation to fractionation.*

2.2.7. Phosphorylation maintenance and dephosphorylation treatments

Dephosphorylation and phosphorylation maintenance reactions were carried out using bacterial alkaline phosphatase (BAP) to mediate dephosphorylation and sodium ortho-vanadate plus sodium fluoride to maintain phosphorylation. 150 µg of nuclear extracts were incubated with 30 U of BAP for 30 min in 20 µl reactions at 25°C prior to IP. NaF and Na_3VO_4 treatment was included in all steps of NE preparation and during IP. All buffers were supplemented with 10mM of NaF and 5mM Na_3VO_4.

2.2.8. EMSA (Electrophoretic Mobility Shift Assay)

EMSA was performed to measure the activity of purified DNA binding proteins. The DNA binding assay was performed in two-step reactions as explained below (2.2.8.1 and 2.2.8.2).

2.2.8.1. End labelling of oligonucleotides with γ-^{32}P-ATP

The γ-^{32}P source vial was thawed at RT for 30min. A reaction was assembled in an eppendorf tube, which contained annealed oligonucleotides OA/OB (17, 25 ng/ul), T4 polynucleotide Kinase (10 U/µl), 10X T4 polynucleotide kinase forward buffer (buffer A), and MiliQ water (deionised, nuclease free). Reaction was placed after short centrifugation on a rack in the fume hood. Behind an acrylic shield in the fume hood, 5 µl γ-^{32}P from the source vial were removed carefully and added to the reaction mixture. The reaction was then incubated at 37°C for 30 min. After completion of the stipulated incubation period, unbound γ-^{32}P was removed from the reaction using a QIAquick nucleotide removal kit. In the first step, 250 µl of PN1 buffer was added to the reaction and mixed. Then, the reaction was placed in the QIAquick column into a clean 2 ml collection tube and centrifuged at 6000 rpm. The radioactive flow through was appropriately discarded and 500 µl buffer PE was added and centrifuged for 1 min at 6000 rpm. After discarding the radioactive flow through, the washing procedure was repeated with 500 µl of PE buffer. The column content was centrifuged in an empty tube for 1 min at 13000 rpm. Subsequently, the QIAquick column was placed in a clean 1.5 ml tube and 86 µl elution buffer was added and incubated for 1 min. Finally, the column was placed in an empty eppendorf tube and

centrifuged for 1 min at 13000 rpm. The eluate contained the radiolabelled oligos (activity was later measured in a scintillation counter).

2.2.8.2. EMSA (Assembly of the reaction)

DNA end-binding activity was assessed by incubating purified PARP-1 with 10x EMSA binding buffer, Appendix (5), 1 µl radiolabelled oligos (0.2 ng/µl) and H_2O up to 20 µl. This reaction mix was incubated for 20 min at RT in a fume hood. To achieve supershift, 1 µl (200 ng/µl) of anti-PARP-1 primary Mab was added to the γ-^{32}P-labelled DNA with the protein mixture and incubated for 15 minutes at RT. The reaction was stopped by adding 5 µl 6x DNA loading dye to the reaction. Reaction was electrophoresed on 6% polyacrylamide gel in 0.5x TBE buffer. These gels were set on pre-run for 30 min at 150 V. The samples were then loaded and run for 60 min at 150 V. Then the voltage was increased to 230 V and gels were run for another 90 min. The gels were dried, aligned and exposed on a storage phosphor screen and analysed in the Typhoon scanner. For information about buffers and oligonucleotides, refer to Appendix (5).

2.2.9. Protein purification

2.2.9.1. Expression and purification of human PARP-1

Cloning- The BAC constructs used for PARP-1 expression in Sf9 cells were a kind gift from Dr. Matthew Knight, Victorial University of Technology, Australia [125]. For the construction of this vector, PARP-1 was inserted into a pUC cloning vector. Then PARP-1 was excised from the pUC construct and cloned into pFAST BAC1 and pFastBacHTb (Invitrogen) at the XbaI restriction site.

2.2.9.2. Standard protein expression of human PARP-1

The recombinant virus expressing human PARP-1 was generated by co-transfection of Sf9 cells with pFastBac1-PARP-1 or pFastBacHTb-PARP-1 by a BAC-to-BAC® Baculovirus expression system (Invitrogen). Recombinant Baculovirus stocks were generated and stored frozen.

2.2.9.3. Medium Preparation and growth conditions

Sf9 cells were grown at 27°C in spinner flasks in Grace's insect cell medium (pH 6.1) including 100 mg/L penicillin and Streptomycin and supplemented with 10% fetal calf serum (heat-inactivated) with 50x stock (0.1665 g/ml) of Lactalbumin hydrolysate, 50x stock–200 g/L yeastolate ultrafiltrate, dissolved in water and stored in the dark.

2.2.9.4. Overproduction and identification of PARP-1

Sf9 cells were grown in spinner flasks to the concentration of 2-3 x 10^6 cells/ml, diluted to the density of 1.5 x 10^6 /ml with fresh growth medium containing virus stock at 2.5 MOI (multiplicity of infection), incubated and stirred gently for 48 hours. The expression of PARP-1 in infected cells was determined by SDS-PAGE (8%). After blotting of total cellular proteins PARP-1 was detected by Western blotting using a mouse monoclonal antibody raised against purified calf thymus PARP-1.

2.2.9.5. PARP-1 Purification

Approximately 700 x 10^6 infected cells were lysed and homogenized by vortexing (3 x 30 secs.) at 4°C with ice cold hypotonic homogenization buffer, which was enriched with protease inhibitors – 2 µg/ml aprotinin, 1mM benzamidine-HCl and 1µg/ml pepstatin. Cellular debris was removed by centrifugation for 20 min at 40,000 g at 4°C. Endogenous DNA was removed by addition of 1 mg/ml Salmon sperm protamine sulphate (Bio medicals) followed by centrifugation for 20 min at 40,000 g at 4°C. The supernatant was precipitated by two steps of ammonium sulphate precipitation; first, with 0 - 30% (5.28 g/30 ml lysate) and second with 30 - 70% saturated ammonium sulphate (8.2 g/30 ml lysate). Ammonium sulphate precipitation was performed on ice under continuous stirring. The precipitated proteins were dissolved in ice-cold chromatography extraction buffer A, Appendix (6), and kept for dialysis overnight in buffer containing 25 mM NaCl. The lysate was then loaded onto a DNA-single strand cellulose column equilibrated (five column volume) with chromatography buffer A at a flow rate of 0.2 ml/min. Elution was performed with a step gradient at 250, 750 and 1000 mM NaCl using chromatography buffer B (Buffer A + 1M NaCl). PARP-1 was eluted at 750 mM NaCl. Purified PARP-1 fractions were further used for SDS-PAGE analysis, protein concentration determination (Bradford

assay) and for determination of enzymatic activity. For further information about the buffers refer to Appendix (6).

2.2.10. Activity Assays for determination of PARP-1 activity

2.2.10.1. Non-Radioactive enzymatic assay for PARP-1 activity

The described assay is a non-radioactive Western blot-based PARP-1 assay. The activity measurment is based on the fact that when PARP-1 encounters DNA breaks, it activates itself and adds ADP-ribose units on itself using NAD^+ as a substrate. In the assay, PARP-1 auto-poly-ADP-ribosylation is measured using anti-poly-ADP-ribose antibodies. The intensity of the signal generated is proportional to the PARP-1 activity present in the sample. The standard reaction mixture contained 10x NHEJ buffer, Appendix (5), 50ng SalI-digested pSP65 plasmid, 4mM NAD^+, the indicated amount of purified histone (H1.2), 5 ng of purified Ligase3-β with 1mM ATP and 50 & 100 ng of PARP-1 in a total reaction volume of 20 µl incubated at 37°C. The reaction mixture was incubated at 37°C for 10 min. and then 5 ng of Ligase3-β with 1mM ATP was added to each reaction for a final volume of 20 µl and further incubated for 20 min at 37°C. The samples were then removed and the reaction was stopped by adding 2x SDS loading buffer and further sonicated for 15 min at 80°C. Products were analyzed on 6% PAGE at 100V for 2 hours and then blotted onto HyBond-P PVDF membrane. For immunodetection, an anti-polyADP-ribose antibody was used and was detected using the ECL Western blotting Kit.

2.2.10.2. Radioactive enzymatic assay for PARP-1 activity

EMSA was carried out with purified PARP-1 protein as described above.

2.2.10.3. Dot-Blot

Dot-Blot was performed to check the activity of purified PARP-1 in the presence and absence of histone H1. Aliquots (6 µl) from the reactions of non-radioactive PARP-1 assay were stored to run a dot-blot. The samples were diluted with SDS (5%) and sonicated for 15 min at 80°C. A nitrocellulose membrane (Protran BA 85, 0.45 µm) was activated by rinsing with water and left to semi-dry. 1 µl sample was loaded onto the semi-dried membrane. The membrane was then incubated in blocking buffer

(same as for Western blot) for 30 min and then with an anti-polyADP-ribose antibody that was detected as described above.

2.2.11. Expression and purification of human Ku

Cloning- BAC constructs for Ku70 and Ku80 were a kind gift from Dr. William S. Dynan (University of Georgia, GA). Expression of Ku70 and Ku80 was achieved by co-transfection of Sf9 cells with the corresponding recombinant viruses. Recombinant Baculovirus stocks were generated and stored frozen. The method of media preparation and the growth conditions, as well overexpression and detection of Ku was as described for PARP-1.

2.2.11.1. Ku purification

Approximately 850 x 10^6 infected cells were lysed with Ku lysis buffer, Appendix (6). The cells were then mixed gently and incubated on ice for 30 min. The lysate was then centrifuged at 4250 x g for 15 min at 4°C. The supernatant (S1) was transferred to two new tubes. The supernatant was centrifuged at 20,000 rpm (48284 x g) for 1 h in a Beckman Avanti J20XP centrifuge, rotor JA-25.50, at 4°C. The supernatant (S2) was transferred to new tubes, the volume was measured and 50 µl sample aliquots were taken for analysis. The supernatant was ultra-centrifuged at 35000 rpm for 0.5 h at 4°C (combined supernatant S3). The proteins in the lysate S3 were precipitated with 70% ammonium sulphate, for example - (27.9 g/64 ml). The samples were then centrifuged at 4°C for 10 min at 15000 rpm in a Beckman Avanti J20XP centrifuge. The ammonium sulphate precipitated pellet was then resuspended with 5 ml Ku-CB buffer + 1M NaCl and then ultracentrifuged at 35000 rpm for 0.5 h at 4°C. Supernatant (S4) was collected and aliquots removed for determining protein concentration using the Bradford assay and for SDS-PAGE analysis. The supernatant (S4) was then filtered through 0.2 µm filter before loading onto a column for purification utilizing an Aekta FPLC. For this purpose, the filtered supernatant was loaded onto a Superdex 200 column (HiLoad 26/60) equilibrated with Ku-CB + 1M NaCl. The fractions obtained were run on 10% SDS PAGE and Western blotted to check the presence of the Ku70/80 heterodimer. All fractions containing Ku70/80 heterodimer were pooled together and dialysed against 0.2 M KCl in Ku-CB buffer. The dialysed samples were filtered through 0.2 µm filter. Sample was loaded onto a single stranded (ss) DNA-cellulose column (self packed CV 2 – 3 ml) equilibrated

with 0.2 M KCl in Ku-CB buffer. A linear gradient program was designed to run from 0.2 M – 1 M NaCl, 5 CV. Ku eluted between 0.4 - 0.5 M NaCl. Fractions were collected and analysed by SDS-PAGE to determine those containing Ku. These fractions were then pooled together and dialysed against 0.1 M KCl in (Ku-CB) buffer. Dialysed samples were loaded onto a 1 ml HiTrap^{TM} Heparin HP column, pre-equilibrated in Ku-CB, 0.1M KCl. Elution was preformed with a step gradient: 0.1, 0.2, 0.3,and 1.0 M KCl. Ku eluted in the 0.3 M KCl fraction. Purified fractions were used for SDS-PAGE analysis, protein concentration determination (Bradford assay) and for determination of enzymatic activity by EMSA utilizing γ-^{32}P-labelled oligonucleotides as described earlier. For further details refer to Appendix (6).

3. Results

3.1. Introduction

3.1.1. Purpose of the Study

It is widely accepted that the MRN complex has an essential role in sensing DSBs. On the other hand, a sensing role for Ku is only occasionally suggested and it remains open how Ku and the ensuing NHEJ allows the function of MRN, either within NHEJ or HRR.

It has been reported that Mre11 physically interacts with the Ku heterodimer. However the functional significance of this interaction remains unclear. Several hypotheses can be formulated on the basis on these interactions. Although Ku is most likely the first molecule to bind and stabilize the open DNA ends, due to its ring shaped structure, it will remain trapped on the repaired DNA after completion of NHEJ. We hypothesized that Ku removal is accomplished in an Mre11 dependent manner. Trapped Ku may also help in the recruitment of the MRN complex and may also contribute to the development of a full blown DNA damage response and to DSB repair pathway selection.

To begin addressing the functional significance of Mre11/Ku interactions, we developed and performed *in vitro* and *in vivo* experiments based on immunoprecipitation reactions, in order to identify first interaction determinants. Most experiments described here are based on pull down assays utilizing purified proteins or protein extracts isolated from normal cells or from mutants with known defects in DSB repair. Our results confirm previously reported interactions between Ku and Mre11 and shed light to the role of these interactions in DSB repair process and the activation of DNA damage response cascades.

3.1.2. Purification and enzymatic activity of Ku

To study the interactions between Ku and Mre11, we utilized purified Ku. Recombinant Ku70 and Ku80 proteins were expressed in Sf9 cells using baculovirus constructs and were prepared as described under Materials and Methods. Purification was initiated with gel filtration (size exclusion chromatography) to separate large from small proteins using a Sephadex200 pre-packed column.

Indicated fractions (B9 - D2) were collected from the first chromatography step, were run on 10% SDS–PAGE to identify the fractions containing the low and high molecular weight proteins (Figure 1.1.1 A). Fractions B12 to C8 were pooled, dialysed against low salt (200mM NaCl) dialysis buffer and loaded on DNA cellulose column.

In the purification step, we utilized the DNA binding properties of Ku. Affinity purification was performed using a DNA cellulose resin (Figure 1.1.1 B). A linear gradient elution scheme was devised between 200 - 1000 mM NaCl and peak fractions (B12 - C12) of the chromatogram checked on SDS-PAGE. The presence of the Ku70 was confirmed by Western blot using an anti-Ku70 antibody (Figure 1.1.1 C). Fractions containing Ku (C4-C10) were mixed and dialysed against a buffer containing 200mM KCl, aliquoted and stored at -80°C. In further experiments, the DNA binding activity of the purified heterodimer was determined.

Electrophoretic Mobility Shift Assay (EMSA) was used to determine the enzymatic activity of purified Ku. To increase the sensitivity of detection, EMSA was performed with radio-labelled 25bp DNA oligos. This approach allows the use of small amounts of both protein and DNA.

EMSA is based on the concept that a protein-DNA complex migrates slower than the free linear DNA fragments when subjected to a non-denaturating continuous electric field polyacrylamide or agarose gel. As the rate of DNA migration is retarded and the bands appear shifted when bound to protein, the assay is also referred to as “gel shift assay” or “gel retardation assay”. A representative phosphor image of an EMSA experiment carried out with different amounts of purified Ku is presented in Figure 1.1.2.

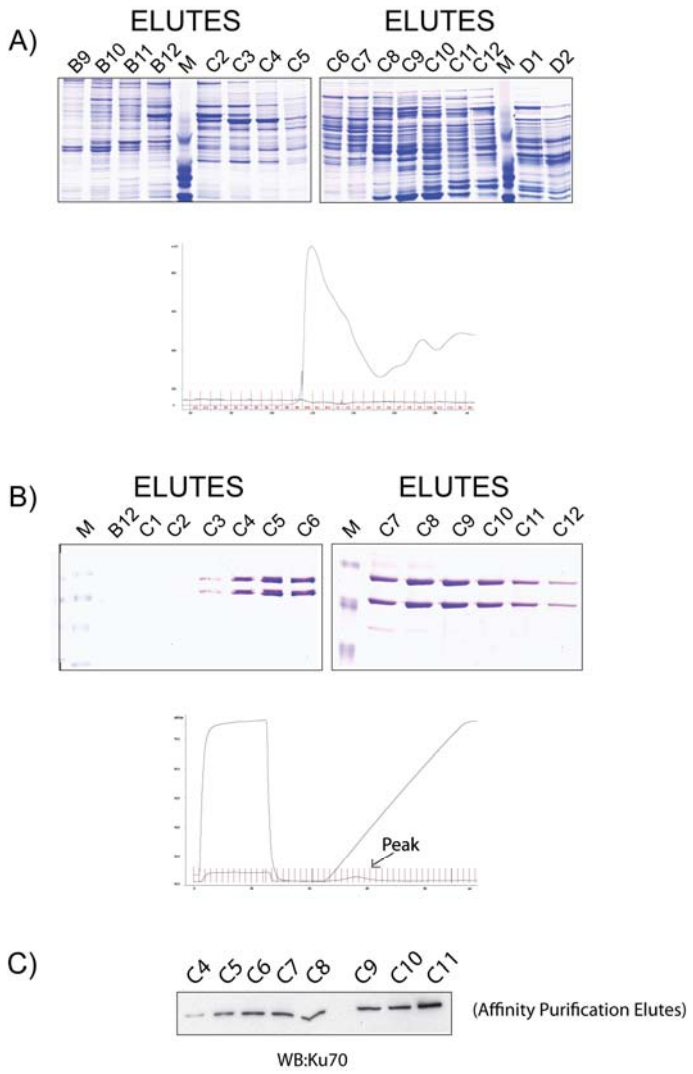

Figure 1.1.1

Purification of Ku:

A) SDS-PAGE of protein fractions collected after gel filtration chromatography. Peak fractions from the corresponding chromatogram (B9-D2) were analyzed. M – Pre-stained protein ladder.

B) SDS-PAGE of collected fractions from affinity purification. The eluted fractions from DNA cellulose column corresponding to the peak in chromatogram (B12 - C12) were run on 10% SDS PAGE and were stained with Coomassie brilliant blue.

C) Western blot with anti-Ku70 antibody of affinity purified Ku fractions.

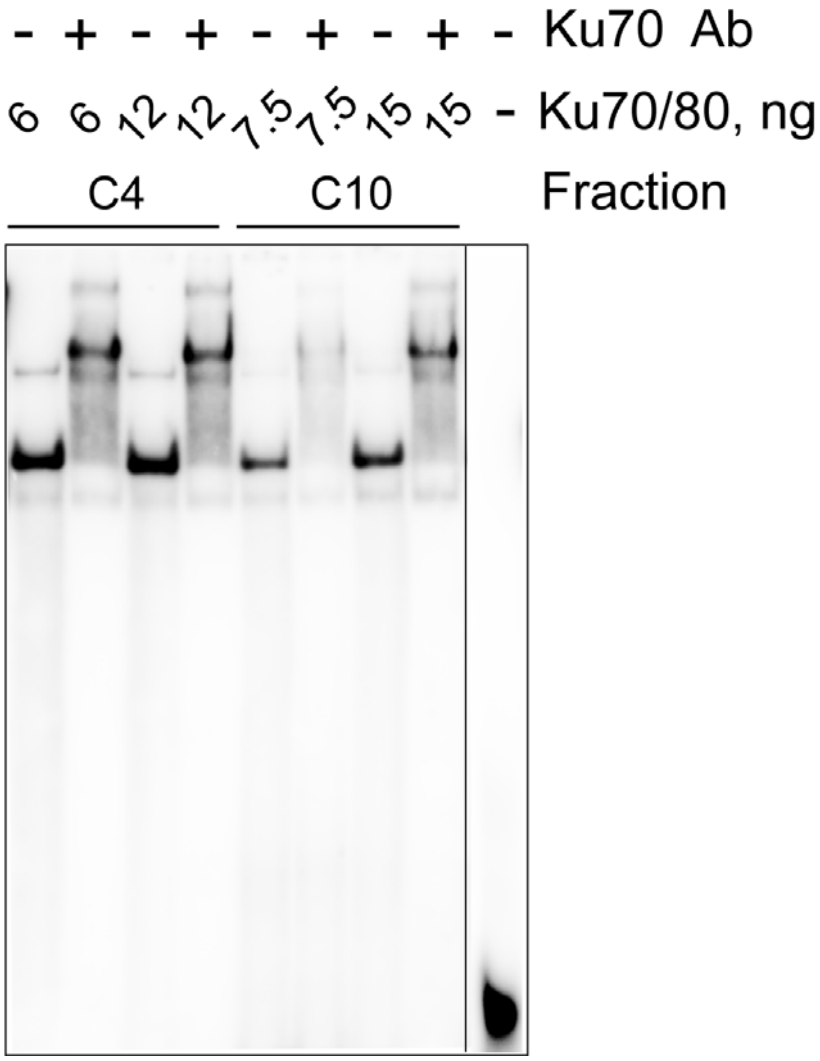

Figure 1.1.2

Determination of Ku DNA-end binding activity:

From left to right; first lane represents Ku fraction C4 (6 ng of purified Ku70/80) bound to 25 bp oligos gives a shift when compared to low molecular weight signal of only oligos (positive control) on extreme right lane. Second lane shows a super shift from C4 fraction when Ab against Ku70 was added. Third and fourth lanes are the same with C4 fraction in double the concentration (12ng). Next two lanes show again a shift and super shift with another fraction (C10). Last lane in right shows a low molecular weight signal (25bp double stranded DNA) of unbound oligonucleotides.

The Figure shows that free DNA oligos migrate at the bottom of the gel, while in the presence of Ku, a significant shift is observed. Additionally, to confirm that the DNA binding protein in our EMSA reactions is indeed Ku, the reactions were supplemented with anti-Ku70 antibody. Binding of antibody to Ku70 resulted in a super-shift, identified as a slowly migrated DNA-protein fraction above the DNA-Ku70/80 shift. The nearly complete supershift suggests the absence from the fractions of other DNA binding proteins.

3.1.3. Ku binds to DNA in a DNA length dependent manner

As mentioned above, Ku is one of the first molecules that binds to DNA ends after the generation of DSBs. The crystal structure of Ku revealed a ring shaped molecule, which contributes to its DNA interaction characteristics. Due to this conformation, Ku threads on free DNA ends and may serve as a loading platform for other factors of NHEJ, primarily though for DNA-PKcs. Additionally, Ku slides inwards the DNA thus generating space for another Ku molecule to bind.

Using purified components and protein extracts we developed an *in vitro* oligonucleotide-based assay, which in some ways mimics the situation when cells are exposed to IR. In the following experiments oligonucleotides with different lengths were utilized, assuming that larger DNA will bind a larger number of Ku molecules, thus augmenting the probability of DNA bound Ku to interact with other repair factors. To determine how different sized oligos modulate the interaction between Ku and Mre11, the IP reaction was supplemented with 25, 50 and 100 bp long oligos that were incubated with nuclear extract (NE) isolated from A549 cells or nuclear extract obtained from Ku80 (Xrs-5 and Xrs-6) deficient mutants.

The presence of Mre11 and Ku in the isolated protein extracts was determined by immunobloting. For this purpose, a nuclear extracts from A549 and Ku80 deficient cells were prepared as described under Materials and Methods and proteins were resolved on SDS-PAGE. Mre11 and Ku70 were detected by Western blot analysis with the corresponding antibodies.

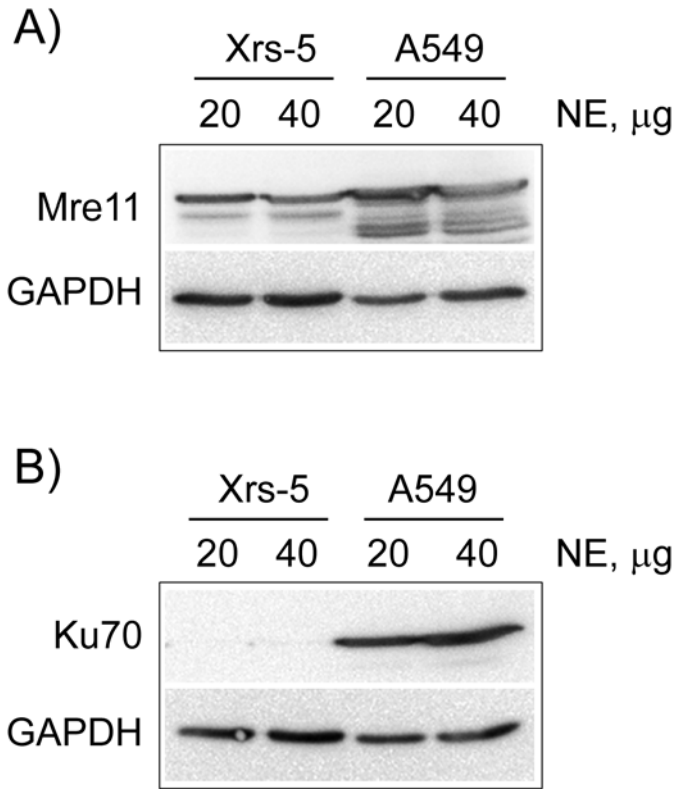

Figure 1.2.1

Western Blot analysis representing the level of Mre11 and Ku70 in nuclear extracts isolated from A549 and Xrs-5 cells:

A) Mre11 expression level in Xrs-5 (Ku80 defective CHO cells) and A549 cells.

B) Ku70 expression in Xrs-5 and A549 cells. Exponentially growing A549 and Xrs-5 cells were used for extract preparation as described under Materials and Methods. NE was resolved on 10% SDS-PAGE and blotted onto PVDF membrane for detecting the Mre11 or Ku70 (the level of this component of Ku is undetectable in the absence of the Ku80 component).

An anti GAPDH antibody was used as loading control (Figure 1.2.1). The results clearly demonstrate that the level of Mre11 in Ku70 deficient hamster cells is about 2 to 3 folds lower than the Mre11 level detected in human A549 cells. Ku70 was undetectable in xrs-5 cells as a result of the Ku80 deficiency that causes depletion of this KU component as well, while in A549 cells, a prominent band, corresponding to Ku70 was observed.

Further IP experiments were carried out with A549 or Xrs-6 NE. In the first reaction set with A549 NE, reactions were incubated in the presence of Mre11 antibody, IP beads and DNA oligos of different size. The immunoprecipitated material was resolved by SDS-PAGE and the amount of Ku co-immunoprecipitated detected by Western bloting using an anti-Ku70 antibody. In the second reaction set Mre11 was immunoprecipitated from the Xrs-6 nuclear extract and afterwards the beads containing bound Mre11 were transferred to another reaction supplemented with purified Ku and DNA oligos of different sizes. The latter protocol allows the evaluation of Ku/MRE11 interactions starting with a protein fraction enriched in Mre11, but which has not interacted with Ku. Immunoprecipitated material from the last step of this protocol was resolved on SDS PAGE and Ku was detected using an anti-Ku70 antibody. The anti-Mre11 antibody was used in both IP protocols also as a loading control and the intensity of the signal obtained with this antibody was equated to the amount of immunoprecipitated Mre11.

Western blots presented in Figure 1.2.2 clearly demonstrate that in A549 NE, Ku interacts with Mre11 even in the absence of DNA. However, in the presence of DNA the interaction observed between the two proteins increases significantly in a DNA size dependent manner. To quantify the level of Ku immunoprecipitated with Mre11, the signal corresponding to Ku70 was normalized against the Mre11 signal and the values obtained plotted as a function of the DNA oligo size (Figure 1.2.2 B). The amount of Ku70/80 immunoprecipitated together with Mre11 was highest when 100 bp oligos were used

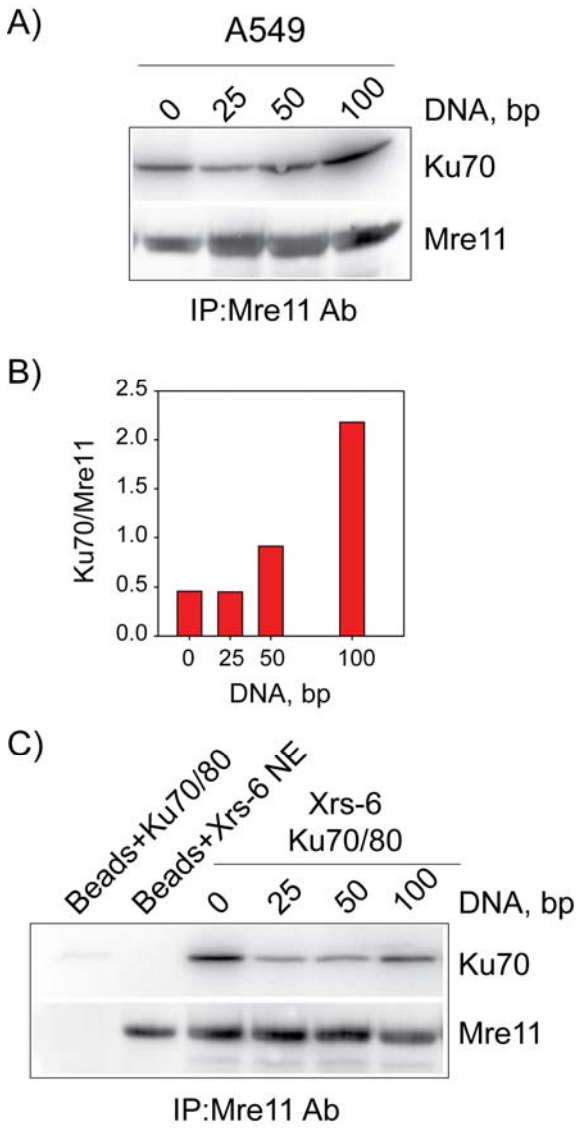

Figure 1.2.2

Ku70 binds to DNA oligos in a DNA size dependent manner:

A) Western blot analysis using a Ku70 Ab when IP was performed with Mre11 Ab in A549 NE using the indicated oligonucleotides. After Ku visualisation, the membrane was re-probed with an Mre11 Ab and the signal was used as a loading control.

B) Ku70 signal was normalized against the Mre11 signal and the values obtained are shown**.** No further absolute calibration of the Westerns was performed to derive actual amounts of protein and therefore the values obtained should only be used for the comparison between samples.

C) Western blots analysis with Ku70 Ab when IP was performed with Mre11

in our reaction. In the case of Mre11 being pulled down from Xrs-6 NE and incubated with purified Ku70/80 the pattern of interaction indicates that DNA attenuates a rather strong constitutive Mre11/Ku interaction. This observation may reflect a shift in the interaction equilibrium from Mre11/Ku to interactions between Ku and DNA. However, even under these conditions and in the presence of DNA, Mre11-Ku interactions were stronger with increasing length of the DNA oligo. This supports the view that Ku interacts with Mre11 *in vitro,* and these interactions are promoted by DNA.

3.1.4. Introduction to *in vivo* experiments

The results of our *in vitro* experiments lead to the following conclusions: First, the interaction between Mre11 and Ku is influenced by the presence of DNA; and second, that this interaction is influenced by the size of the DNA oligos used.
Since the interaction between Mre11 and Ku has been previously reported [55], we decided to examine whether these interactions are DNA damage dependent and also how these interactions are influenced by the proteins involved in the DDR response. To begin with our experiments, we selected the human lung carcinoma cell line (A549), which exhibits decreased repair of mismatched DNA bases, but express a wild type p53 - contrary to most human carcinoma cell lines available. The presence of a functional p53 in A549 cells is beneficial to our studies, since it leaves intact several important DNA damage signalling cascades. This property enables us to investigate the role of Ku/Mre11 interactions in developing full checkpoint response and in modulating DSB repair by switching or selecting between available repair pathways. Xrs-6 cells are Chinese hamster ovary (CHO) with a defect in Ku80, mutant in p53, highly radiosensitive and defective in DSB repair (D-NHEJ) [122].

3.1.4.1. Investigation of Ku/Mre11 interactions in intact cells

To investigate the functions of Mre11 and Ku, the initial players of DNA damage response in DSBs repair, and to elucidate the significance of their interaction, we carried out IP reactions in extracts of irradiated A549 cells. We utilized agarose beads pre-coated with mouse/rabbit IgG antibody, which have high binding specificity towards mouse/rabbit-originated antibodies - e.g. mouse monoclonal anti-Ku70 Ab or

rabbit polyclonal anti-Mre11 Ab. Initially, immunoprecipitation was carried out with an Ku70 Ab in non-irradiated A549 whole cell extract and Mre11 was detected in the immunoprecipitates by Western bloting. As expected, Mre11 was detectable in A549 cell WCE, but not in Xrs-6 cells WCE (Figure 1.3). This preliminary experiment revealed an IR independent interaction between Ku and Mre11, which served as a platform for further investigations.

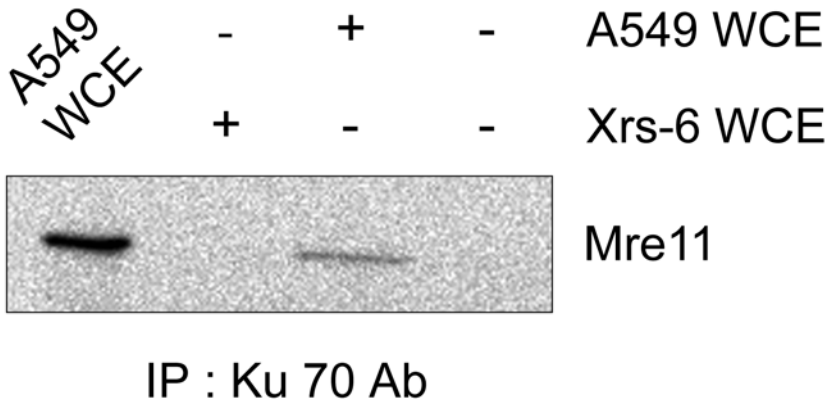

Figure1.3

***Co-Immunoprecipitation of Ku and Mre11 from non-irradiated cells*:**

Western blot signal detected with and anti-Mre11 Ab when IP with a anti-Ku70 AB was carried out in WCE prepared from exponentially growing A549 and Xrs-6 cells. The first lane represents 10 µg of A549 WCE which was loaded as a positive control. The second lane shows absence of Mre11 signal when immunoprecipitation is carried out in Xrs-6 WCE. The third lane represents the Mre11 signal detected after IP in A549 cell extracts. Last lane depicts the singal obtained when only beads are loaded.

3.1.5. The Ku/Mre11 interaction is enhanced in NE of A549 cells.

Most proteins involved in DDR exhibit predominantly nuclear localization. To check, Ku/MRE11 interactions in different sub-cellular compartments, irradiated or non-irradiated A549 cells were biochemically fractionated into cytoplasmic (CE), nuclear (NE) and chromatin bound (NP) extracts and the interaction between MRE11 and Ku examined using procedures similar to those outlined above.

Figure1.4.1 A shows a representative Western blot indicating that the maximum binding of Mre11 to the IP beads was observed in NE, a result that could also be confirmed by densitometry analysis, Figure 1.4.1 B. Here, it is necessary to mention that the more prominent Mre11 binding to IP beads in the NE extracts, may be due to minute differences in the amount of CE, NE ad NP loaded in each lane . Nevertheless, the same pattern of Mre11 binding to IP beads was observed in extracts of irradiated cells.

In the next experiments the ability of Mre11 antibody to immunoprecipitate Ku70 from the different A549 sub-cellular fractions was tested. The results from these experiments show that Ku70 immunoprecipitation does not strictly depend on the origin of the protein extracts, especially when the cells were irradiated (10 Gy) (Figure 1.4.2). Based on these results all further co-immunoprecipitation reactions we carried out in NE.

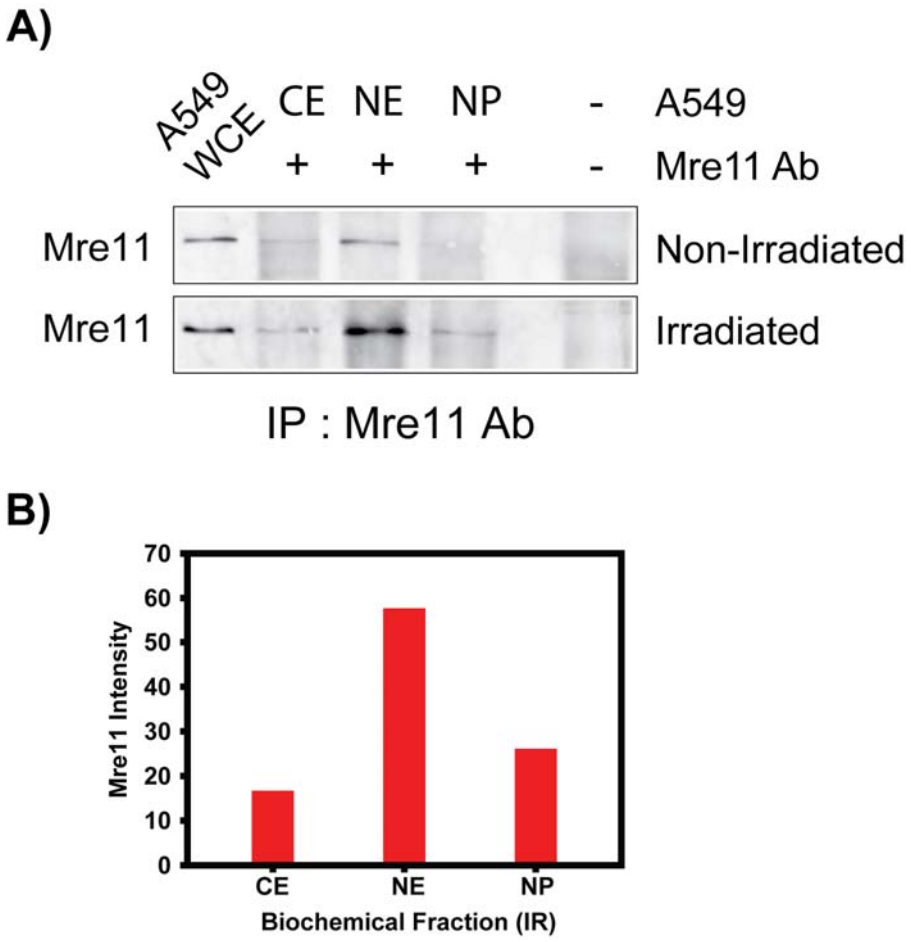

Figure 1.4.1

NE is ideal for IP experiments:

A) Detection of Mre11 binding to IP beads. CE, NE and NP were used and after IP Mre11 was detected by Western blotting. Extracts from irradiated (lower panel) and non-irradiated (upper panel) A549 cells were tested.

B) Bar graph showing the quantification of the above results based on the intensity of Mre11 signal.

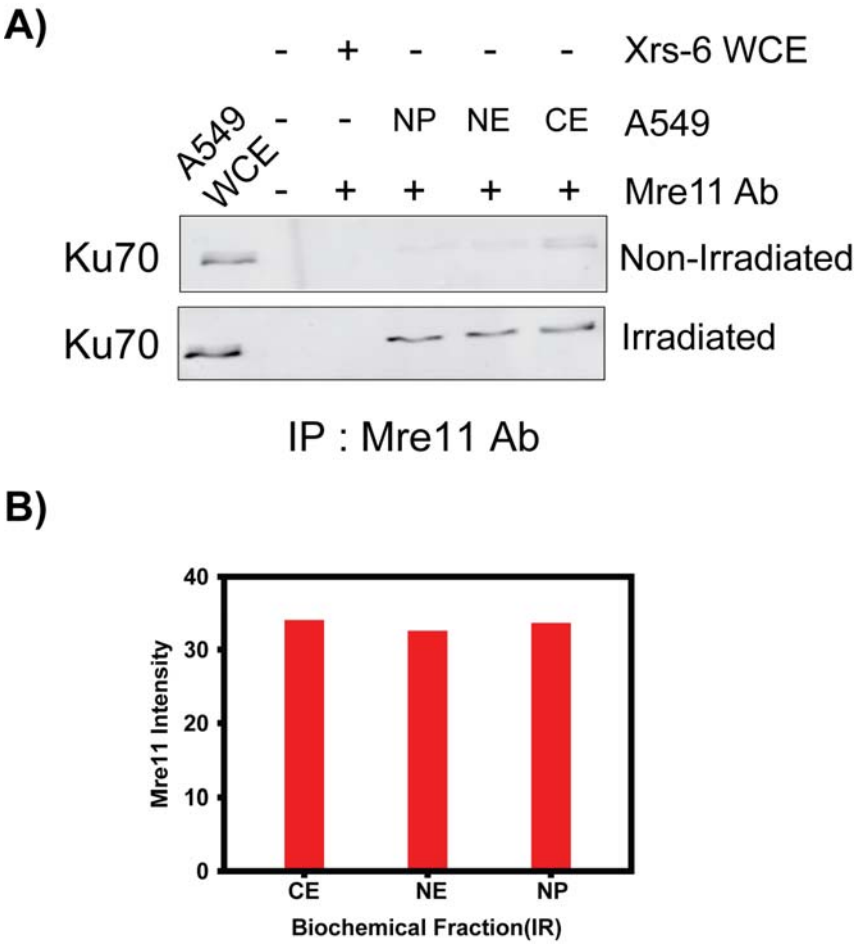

Figure 1.4.2

Interdependency between Mre11 and Ku interactions:

A) Western Blot for Ku70 when IP was performed using an anti-Mre11 Ab in A549 CE, NE and NP. The Upper panel represents IP performed with non-irradiated A549 cells and the lower panel IP in irradiated cells. The first lane in the upper and lower panels represent positive controls, where A549 WCE is directly loaded. Samples were run on SDS-PAGE and blotted onto PVDF membrane for the detection of Ku70 protein.

3.1.6. The interaction of Mre11 and Ku70 is enhanced after IR

The above results confirm the constitutive interaction between Ku and Mre11 and suggest that this interaction is enhanced after induction of DNA damage by IR. Since the latter finding is novel and has important ramifications for our understanding of the DDR, we designed experiments to analyze further this effect.

In the following experiment, we exposed cells to 2 and 4 Gy of IR and after 10 min incubation cells were processed for NE preparation. The short incubation time after IR was chosen on the assumption that both interacting partners are recruited to DSBs within minutes after IR [108]. Indeed, fast kinetics of Mre11 foci formation and the nearly immediate recruitment of Ku to DSBs have been reported [94].

The Western blot results shown on Figure 1.5 A clearly demonstrate that in the absence of radiation only a small amount of Mre11 co-immunoprecipitates with Ku70. This amount increases significantly after IR even for short incubation times.

To validate further this interaction, we performed the same experiment as above but instead of immunoprecipitating with an anti-Ku70 antibody and checking for Mre11 in the immunoprecipitated material, an Mre11 antibody was used in the IP reactions and the immunoprecipitates were checked for Ku70 (Figure 1.5 B). The results of this experiment are similar to the results obtained from above.

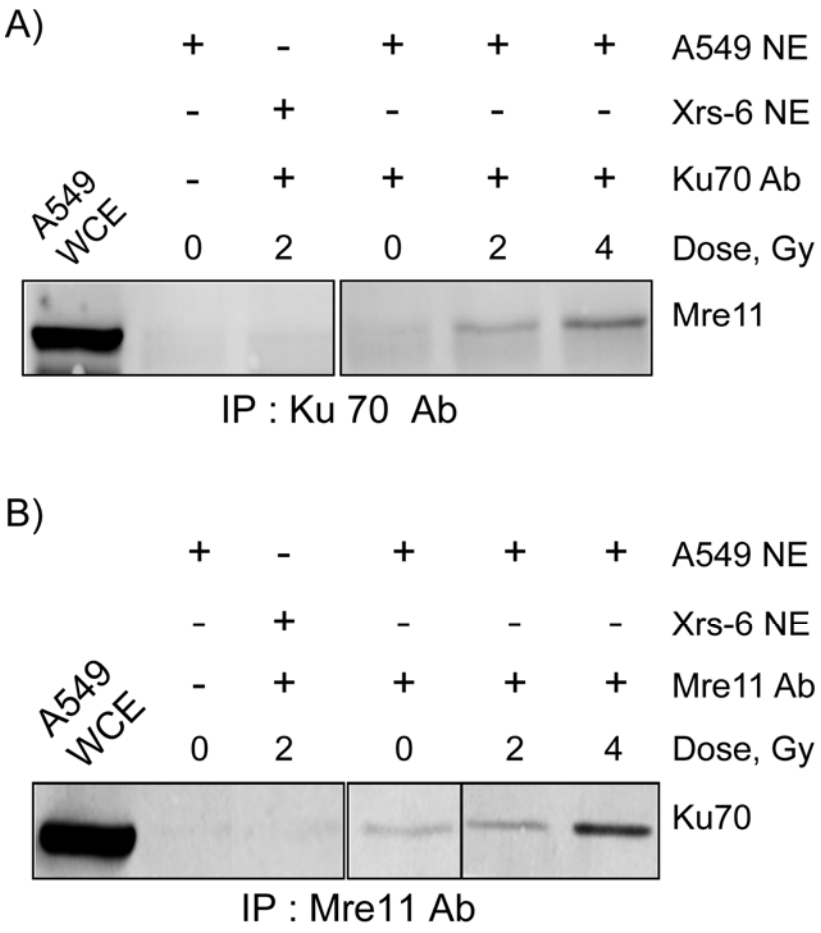

Figure 1.5

***The interaction between Mre11 and Ku is enhanced after IR*:**

A) Western blot of Mre11 in IP reactions carried out with and anti-Ku70 Ab using A549 NE from cells exposed to 2 and 4 Gy IR. The first lane shows a positive control signal of Mre11 in A549 WCE, the second lane shows a control reaction, exclusing nonspecific binding of Mre11 to IP beads, the third lane shows a negative control showing no MRE11 signal in Xrs-6 NE, the fourth lane shows IP with non-irradiated cells and the fifth and sixth lanes the IPs performed in irradiated samples.

B) Western blot of Ku/Mre11 interaction using an anti-Mre11 Ab for IP and and anti-Ku antibody for detection. Lanes are as explained in A.

3.1.7. The Ku/Mre11 interaction persists after IR

In the previous experiments, the dose dependent effect of IR on Ku/Mre11 interaction was investigated at 10 min after irradiation. This time was selected on the assumption that the interaction between the two proteins should be most prominent immediately after the induction of DSBs in the DNA. The fast formation of the Ku/Mre11 complex also suggests that the two proteins could modulate the efficiency of DSB repair by somehow regulating either NHEJ or HRR. To examine for how long the interactions between Ku and Mre11 persist after IR, we followed Ku/Mre11 interaction as a function of time after irradiation with 4 and 8 Gy. Results summarized in Figure 1.6 show a time dependent interaction between the two proteins, when IP was performed with a anti-Ku70 antibody. Densitometric analysis of Western blot data shows that the Ku/Mre11 interaction increases with time after IR reaching a plateau at 4h in the case of 8 Gy with no significant decrease at later times. However, at later times, the signal generated from irradiated samples was similar to that measured in non-irradiated samples at the same time suggesting recovery. Curiously, the signal measured in non-irradiated samples increased during the course of the experiment and it was not possible to identify parameters responsible for this unexpected response. As the peak of interaction was achieved at 2h, it was decided to perform all subsequent experiments after this incubation time.

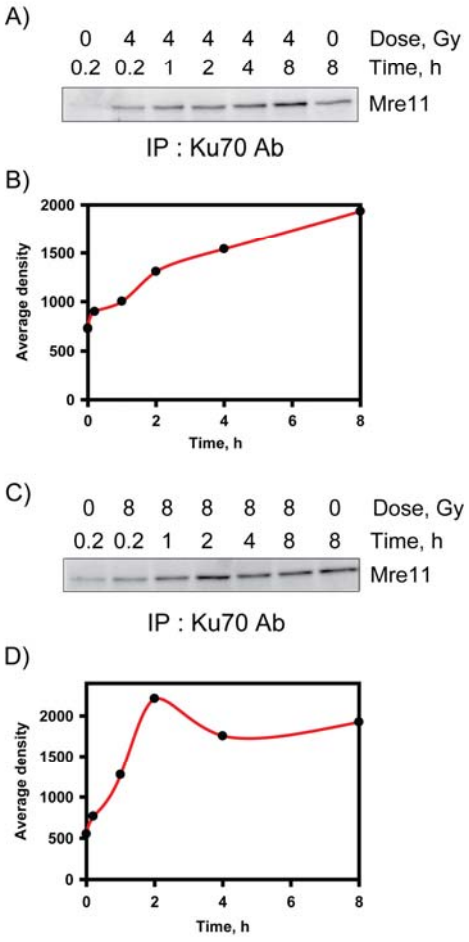

Figure 1.6

Kinetics of Mre11/Ku interaction at different time points post irradiation:

A) Western blot analysis with Mre11 Ab showing the kinetics of Mre11/Ku interaction as detected by IP performed with an anti-Ku70 Ab from A549 NE prepared at different times post IR. First lane (0Gy, 0hr) and last lane (0Gy, 8hr) show Mre11 signal in reactions of non irradiated cells.

B) Values from densitometric analysis of the signal intensity of Mre11.

C) Western blot analysis with Mre11 Ab depicting recruitment kinetics obtained when IP was performed with Ku70 Ab and 8 Gy IR.

D) Densitometric analysis of Mre11 signal intensity plotted in line graph format.

3.1.8. The Ku/Mre11 interaction is stable and is not mediated by DNA

Both Ku and Mre11 are DNA binding proteins; therefore the next step was to investigate whether the observed interaction and effects are DNA dependent events. For the following assay, we selected the well known DNA intercalating agent ethidium bromide (EtBr) to investigate whether DNA or RNA serve as a binding scaffold for both proteins. In other words, we wished to exclude that the observed interaction did not derive from the independent binding of each protein on DNA or RNA. Nuclear extracts were incubated with EtBr and RNAase prior to IP (For concentrations of EtBr and RNase used, see under Materials and Methods). Although the interaction between Ku and Mre11 was somewhat attenuated in the presence of EtBr, the interaction was not completely abrogated and the effect of radiation remained clearly detectable. Thus, we conclude that Mre11/Ku interaction is not indirect, mediated by the independent binding of the proteins on DNA. The results obtained are summarized in (Figure 1.7)

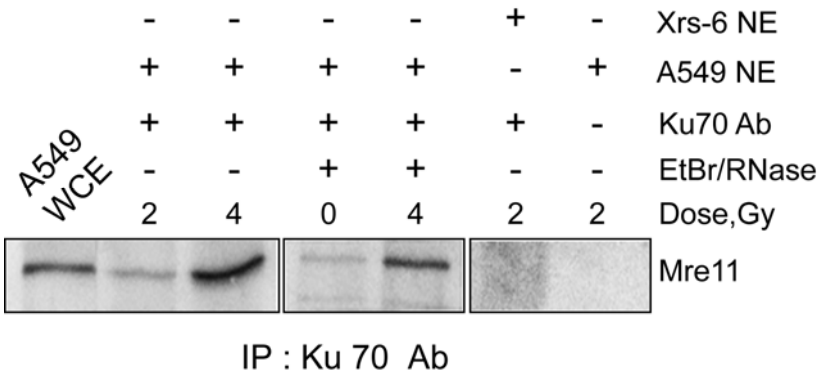

Figure 1.7

Validation of Mre11/Ku interaction:

Western blot of interacting Mre11 when IP with an anti-Ku70 Ab using A549 cells was carried out in the presence or absence of EtBr and RNase. First lane shows a positive control signal of Mre11 in A549 WCE, second and third lanes show Mre11 signal when cells were radiated with 2 and 4 Gy of X-rays in absence of EtBr and Rnase. The next two lanes show the same reactions carried out in the presence of EtBr and RNase. The last two lanes show control reactions with Xrs-6 NE and A549 NE showing the lack of non-specific binding of Mre11 to the IP beads.

3.1.9. The entire MRN complex takes part in the interaction with Ku

In the cellular environment the Mre11 protein does not exist as a single molecule but is in a complex with Nbs1 and Rad50. All three proteins form the MRN complex, which has an important function in DSB repair and DDR signalling. The aim of the next experiments was to investigate whether other partners from the MRN complex take part in the interaction with Ku. After immunoprecipitation with an anti-Ku70 antibody the immunodetection of Rad50 and Nbs1 was accomplished. It can be observed from Figure 1.8 that Nbs1 and Rad50 also take part in the interaction, thus implicating the whole MRN complex in the interaction with Ku.

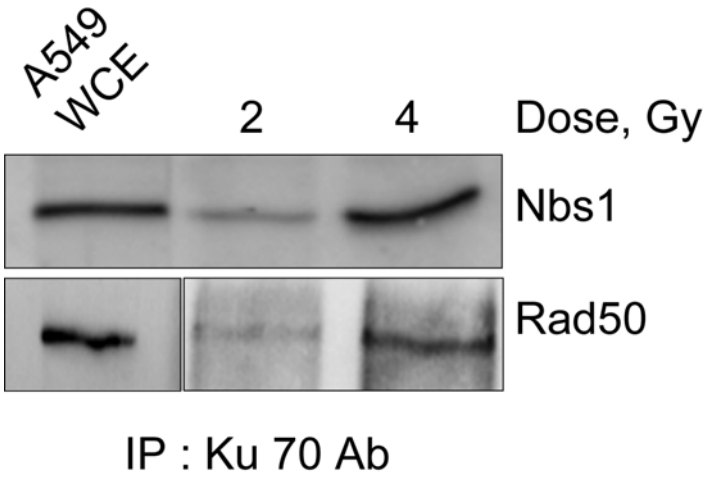

Figure 1.8

***Western Blot analysis of Rad50 and Nbs-1 after IP of Ku*:**

Western blot of Nbs1 and Rad50 when IP was performed with an anti-Ku Ab. First lane in both panels shows the positive control with A549 WCE, the second and third lanes represent IP with an anti-Ku70 Ab performed with cells irradiated with 2 and 4 Gy.

3.1.10. Are other partners involved in the KU/MRN interaction?

To check the specificity of the interaction between MRN and Ku and to investigate whether other proteins are also involved in this interaction, further IP experiments were performed. The blots were probed with antibodies against proteins involved in DDR, such as ATM, PARP-1, 53BP1 and Mdc-1. It was found that along with the MRN complex, other DNA damage sensors such as PARP-1 and ATM were also involved in the complex (Figure 1.9 A). These proteins are known interacting partners of Mre11 and Ku, so it is not surprising that the signals of those proteins are found in the Ku70 immunoprecipitated material. Surprisingly, Mdc-1 and 53BP1, which are involved in the mediation of DDR, were not found in the Ku/MRN complex, suggesting that the observed interactions may reflect the initial DSB response.

The specificity of the interaction between Mre11 and Ku was confirmed by analyzing the immunoprecipitates with anti-Rad51 antibody. It is known that the active form of the Rad51 protein forms a right helical nucleoprotein filament along the ssDNA regions surrounding the processed DSBs. The formation of a Rad51 nucleoprotein filaments needs extensive processing of the ends and it is now known that the MRN complex, together with CtIP plays an important role in this process. As a result of the participation of the MRN complex in the processing of DNA ends during DSB repair, it is reasonable to speculate that the entire repair machinery may interact with the primary DSB sensors, especially if they persist at the damaged sites. The Rad51 recombinase, which does not participate in NHEJ, failed to interact with Ku, which strengthened the significance of Ku/MRN interaction for D-NHEJ and signaling (Figure 1.9 B).

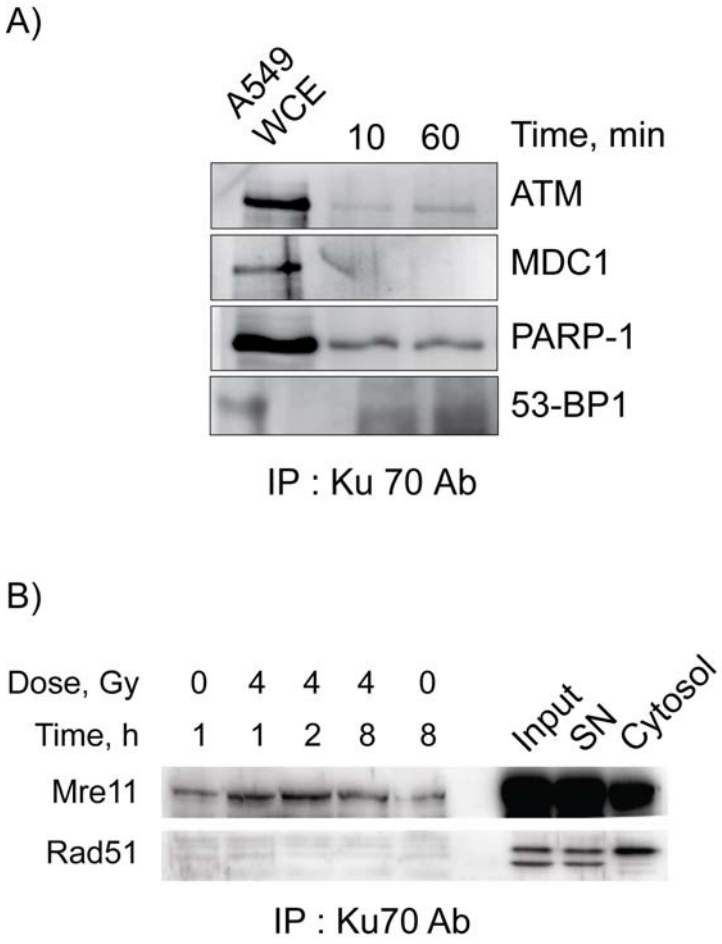

Figure 1.9

***DDR proteins involved in the Ku/MRN interaction*:**

A) IP reactions with an anti-Ku70 Ab were resolved on 10% SDS-PAGE and the blots were probed with anti-ATM, anti-MDC1, anti-PARP-1 and anti-53BP1 antibodies.

B) Rad51 is not part of the KU/MRN complex. The membranes from Western blots showing the dose and time dependent interaction of Mre11 and Ku were stripped and re-probed with anti-Rad51 antibody.

3.1.11. Cells defective in DNA-PKcs show no radiation-dependent enhancement of Ku/Mre11 interaction

It is well known that Ku participates in a complex with DNA-PKcs to form the DNA-PK holoenzyme, which is functional in D-NHEJ. As DNA-PKcs is a kinase that phosphorylates a number of proteins including Ku and itself, we investigated whether the interaction between Ku and Mre11 requires DNA-PKcs. For this purpose we used M059J and M059K cells. These cells originate from the same glioblastoma tumour, but have widely different DNA-PKcs levels. Thus, as a result of a frame-shift mutation, the expression level of DNA-PKcs is in M059J cells about 200 times lower than in M059K cells and are deficient in D-NHEJ.

For experiments, we prepared NE from M059J and M059K cells and used them in IP reactions with an anti-Ku70 antibody. Interestingly, we found that DNA-PKcs defective cells fail to show any enhancement in Mre11/Ku interaction after IR. On the other hand, a dose dependent increase in the interaction between Ku and Mre11 was observed in the DNA-PKcs proficient M059K cells (Figure 1.10 A). This result suggests possible regulation of the Mre11/Ku interaction by DNA-PKcs. The quantification of the Western blots demonstrates that in DNA-Pkcs deficient cells, the Mre11/Ku70 interaction becomes attenuated with dose as compared MO59K cell, which express functional DNA-PKcs and where a clear increase is observed (Figure 1.10 A). On the other hand, a higher level of constitutive (IR-independent) interaction between Mre11 and Ku is observed in M059J cells, suggesting multi-level regulation of this interaction by DNA-PKcs.

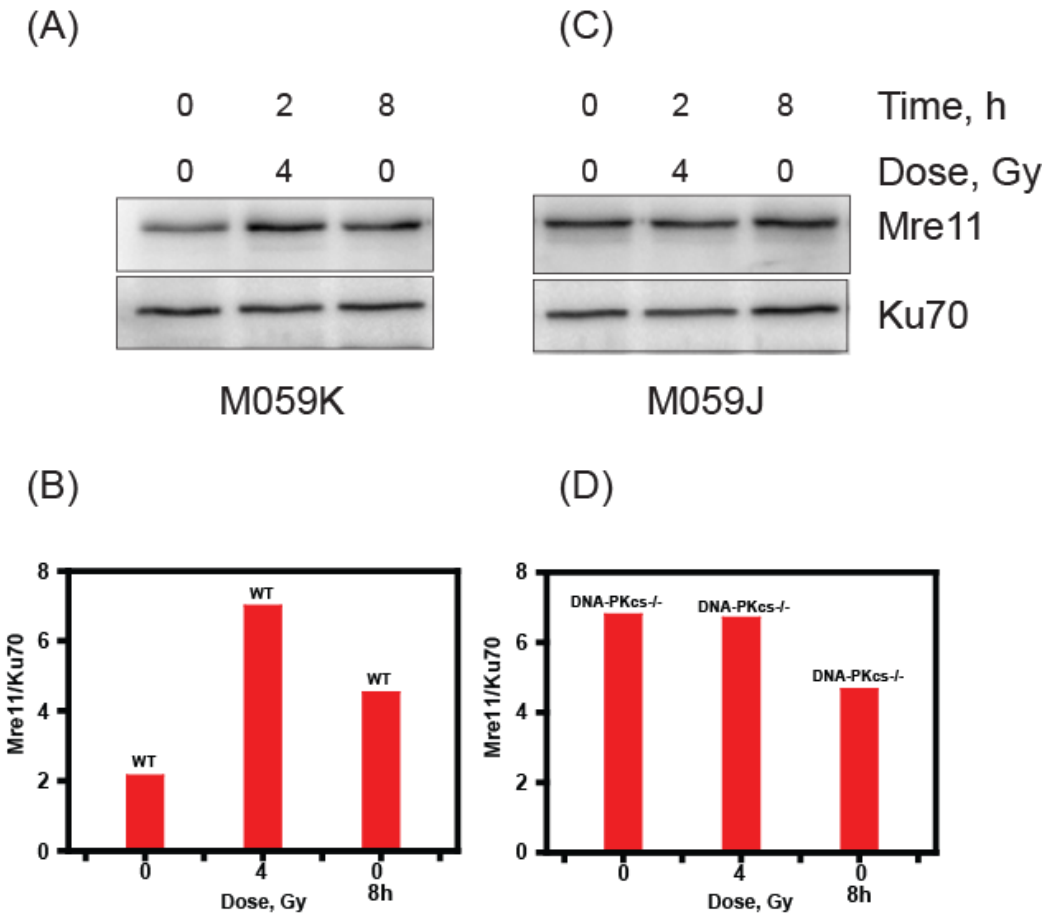

Figure 1.10

(A) Mre11/KU interaction in DNA-PKcs deficient cells:

A) Western blot analysis of Mre11 in DNA-PKcs$^{+/+}$ cells when IP was performed with an anti-Ku70 Ab.

B) The ratio of Mre11 to Ku signal intensity, determined by densitometric analysis of M059J and K Western blots, shown in bar graph form.

C) Mre11 signal detected through Western blot in DNA-PKcs$^{-/-}$cells.

D) Bar graph generated by calculating the ratio between Mre11 and Ku70 signal intensities.

As it was observed in M059J and K cell lines that the interaction between Mre11 and Ku is dependent on DNA-PKcs in irradiated cells, we carried out an experiment utilizing another DNA-PKcs deficient cell line, HCT116 DNA-PKcs$^{-/-}$ along with its wild type counterpart. These cells are human adenocarcinoma cells and the defect was generated by disrupting DNA-PKcs through gene targeting (exon 81-83 was deleted) [126]. HCT116 wild type is an immortalized and transformed cell line; it is diploid, has a stable karyotype and is wild type for most known DNA repair mechanisms. For the following experiment, we prepared NE of HCT116 wild type and HCT116 DNA-PKcs deficient cells and utilized them to perform an IP with an anti-Ku70 Ab. The results obtained in this pair of cells were similar to those of M059J and M059K and show that DNA-PKcs deficiency attenuates the radiation-dependent interaction between Ku and Mre11. The results of this experiments are summarized in Figure 1.10 B. Western blots were densitometrically analysed and the ratio of Ku70 to Mre11 signal, plotted as a bar graph (Figure 1.10 B). The quantitation of the Western blots clearly shows that the level of Mre11-Ku70 interaction is more than 4-fold decreased in comparison to signal in HCT116 wild type cells, which expresses functional DNA-PKcs (Figure 1.10 B).

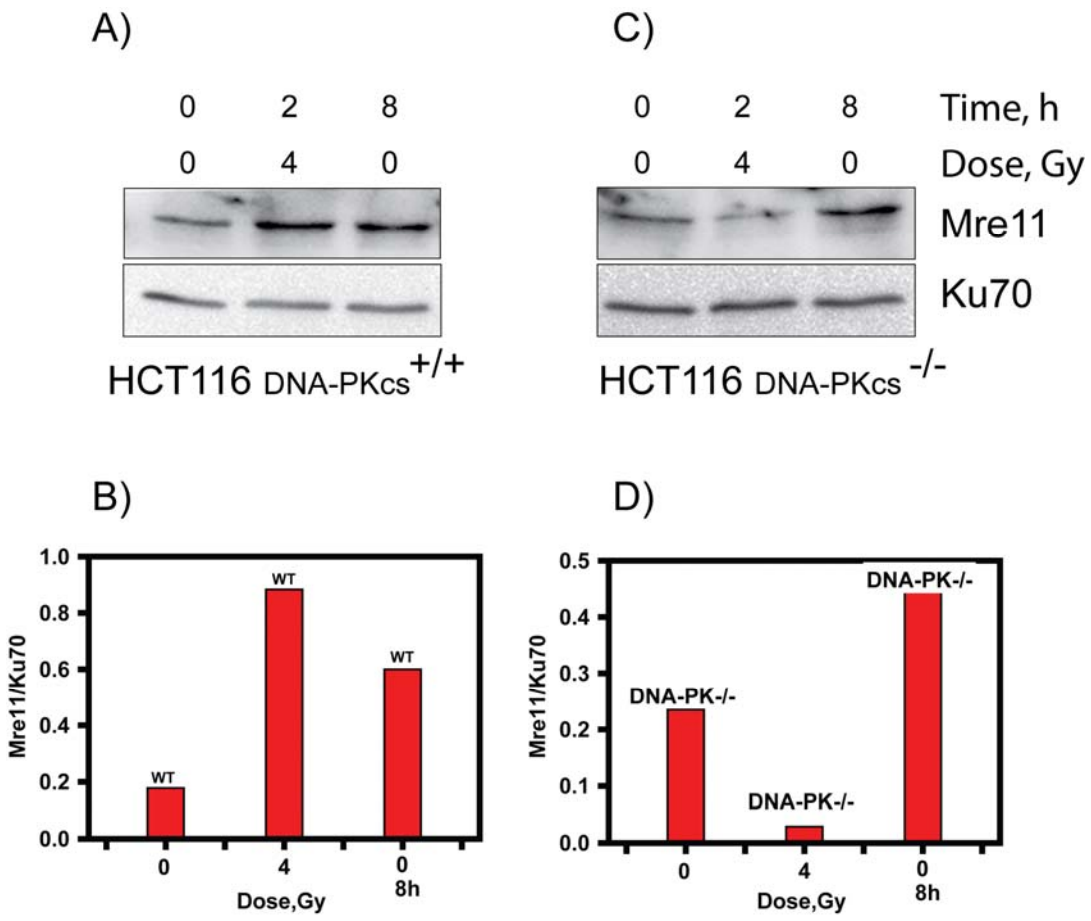

Figure 1.10

(B) Effect of DNA-PKcs on Mre11/KU interaction (continued):

A) Western blot analysis of IP performed with an anti-Ku70 Ab and detection with Mre11 Ab in DNA-PKcs$^{+/+}$ HCT116 cells.

B) The ratio of Mre11 to Ku signal, as determined by densitometric analysis and plotted in the form of a bar graph.

C) Mre11 signal detected through western blotting in DNA-PKcs$^{-/-}$cells.

D) Bar graph was plotted by calculating the ratio between Mre11 and Ku70 signal intensities.

3.1.12. ATM defective cells shows no radiation-dependent Mre11/KU interaction

A key signalling function of the MRN complex is the recruitment and activation of ATM (ataxia-telangiectasia-mutated) kinase, which then initiates a cascade of phosphorylation events that leads to signal amplification, cell cycle arrest and DNA repair. The MRN complex acts as DNA damage sensor and an upstream regulator of ATM activity. The MRN complex also plays a crucial role downstream of ATM in DSB checkpoint signalling. Since the MRN complex seems to be important in the activation of ATM, we investigated the effect of ATM on KU/MRN interaction. For this purpose, we utilised an ATM deficient cell line, AT5BIVA. AT5BIVA are skin fibroblasts derived from AT individuals and were immortalized by transfection with the SV40 large T-antigen [124]. For experiments, we prepared NE of A549 and AT5BIVA cells and used them to perform IP with an anti-Ku70 Ab. Time course analysis of extracts of irradiated AT5BIVA cells shows the same response for Ku/Mre11 interaction as DNA-PKcs deficient cells. Quantitative Western blot analysis for both Ku and Mre11 signal, confirms this observation. Figure 1.11 shows that there is no IR-dependent boost in Mre11/Ku interaction in ATM defective cells when compared to their wild type counter part.

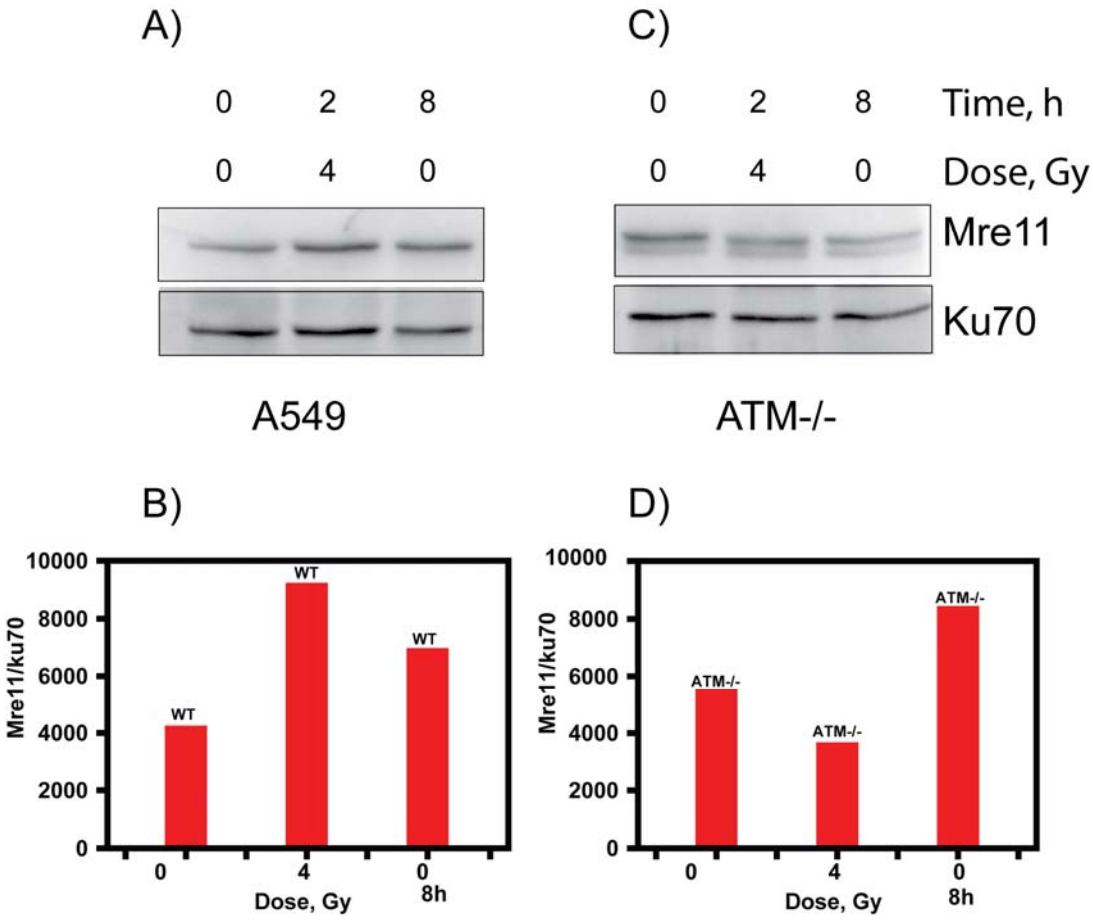

Figure 1.11

Effect of ATM on IR-dependent Mre11/KU interaction:

A) Western blot analysis of IP performed with an anti-Ku70 Ab and detection with anti-Mre11 Ab in A549 NE, in cells exposed to 4 Gy X-rays.

B) The ratio of Mre11 to Ku signal (A549) was determined by densitometric analysis and plotted as a bar graph.

C) Mre11 signal detected by Western blot in ATM deficient AT5BIVA cells.

D) Bar graph plotted on the basis of Western blot densitometric analysis for ATM deficient cells.

3.1.13. Preservation of phosphorylation compromises MRE11/KU interaction

The above experiments suggest that DNA-PK and ATM mediated phosphorylation regulate somehow the Mre11/Ku interaction. Hence, we designed an experiment to investigate whether maintaining phosphorylation with phosphatase inhibitors such as sodium orthovanadate (Na_3VO_4) with sodium azide (NaF) modulates the effect. We also determined the effect of dephosphorylation using bacterial alkaline phosphatase (BAP). For all experiments, A549 cells were used. The treatment schemes used in these reactions are outlined under Materials and Methods. Figure 1.12 demonstrates the effect of phosphorylation and de-phosphorylation on the radiation dependent interaction between Mre11 and Ku. A control reaction which is carried out without any treatment shows the expected dose-dependent interaction of Mre11 with Ku. The presence of BAP in the IP reaction completely abrogates and even reverses this interaction. IP performed in the presence of Na_3VO_4 and NaF shows a decrease in the overall the interaction but the IR-dependent aspect remains unchanged or even more pronounced. Interestingly, when BAP is used in conjunction with Na_3VO_4 + NaF the effect of the latter cocktail dominates and a robust IR-dependent Mre11/KU interaction is observed.

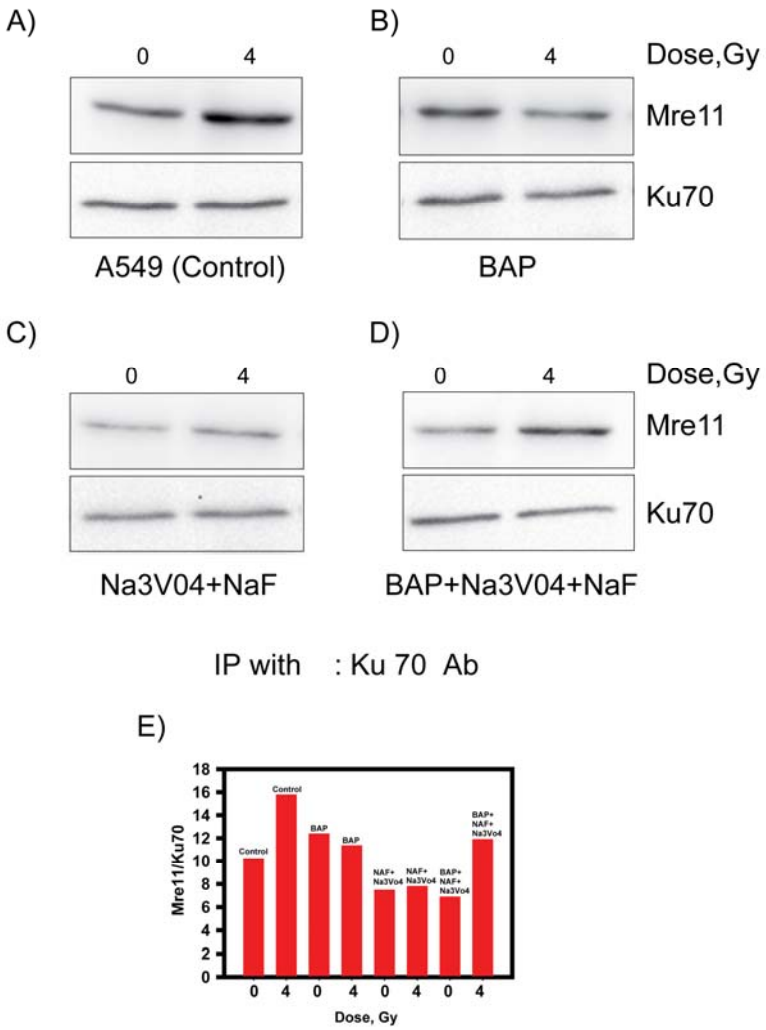

Figure 1.12

Effect of phosphorylation status on Mre11/Ku interaction:

A) Western blot analysis of Mre11 in control reaction when IP with an anti-Ku70 Ab was carried out in extracts of cells exposed to 0 and 4 Gy IR.

B) Mre11 signal when IP was performed in presence of BAP.

C) Mre11 signal when IP was performed in the presence of Na3V04 and NaF.

D) Mre11 signal when IP was performed in presence of BAP + Na3V04 and NaF.

E) Bar graph showing the quantification of above results based on the ratio of Mre11 to Ku signal for all four treatments.

PART-II

3.2. Introduction

As discussed above the MRN complex plays a key role not only in D-NHEJ and HRR, but also in B-NHEJ [114] The above experiments indicate that PARP-1 and Mre11 interact, which is in agreement with results showing that accumulation of Mre11 and Nbs-1 at the sites of DNA damage requires PARP-1 [94]. Previous results from our group have shown Ku and PARP-1 competition for DNA ends and implicated histone H1 as a factor contributing to DSB repair by B-NHEJ. These results raise several important questions: (1) Does the competition for DNA ends between proteins belonging to different repair pathways determines how the cell decides which pathway to engage? (2) Is there a synergism in the function of histone H1, PARP-1 and the MRN complex in B-NHEJ?

PARP-1, is a potential component of B-NHEJ and is thought to function together with XRCC1/DNA Ligase III and histone H1. As mentioned above, our results implicate histone H1 as an accessory factor of DNA Ligase III and thus a putative component of B-NHEJ. We, therefore, investigated whether the activity of PARP-1 is modified by histone H1. For this purpose, we designed an in vitro PARP-1 activity assay utilizing purified proteins (PARP-1 protein and histone H1).

3.2.1. Purification of PARP-1 protein

To facilitate the analysis of possible interactions between PARP-1 and histone H1, we utilized purified recombinant PARP-1 and histone H1. As purified histone H1 was commercially available, we purified only PARP-1. For this purpose we expressed recombinant PARP-1 in Sf9 cells and purified the protein as outlined under Material and Methods. The initial purification strategy relied on affinity purification utilizing DNA cellulose resin, owing to the DNA binding properties of PARP-1. A step gradient elution scheme was established with a buffer containing 250-1000mM NaCl and bound proteins were eluted at 750mM NaCl. Fractions containing protein peaks were analyzed on SDS-PAGE (Figure 1.13). Indicated fractions (B1-B9) from first round of chromatography and were run on SDS-PAGE to determine the purity of PARP-1. Although affinity purification led to 80% purity of PARP-1, it was necessary to remove some low molecular weight contaminating proteins. Hence, a second step of

purification was included in the protocol.

In the second round of purification, we utilized gel filtration (size exclusion) chromatography to remove small molecular weight proteins. Fraction B7 from the affinity purification was selected for further purification by Gel Filtration. Indicated fractions (B5-B9) from the second round were analyzed on SDS-PAGE and Western blot to identify PARP-1 and determine purity (Figure 1.13). The fractions containing PARP-1 (B5-B9) were dialysed against CB buffer (300mM KCl), aliquoted and stored in -80°C. In further experiments, the enzymatic activity of PARP-1 was determined by using short radiolabeled DNA oligonucleotides and non-radioactive assays.

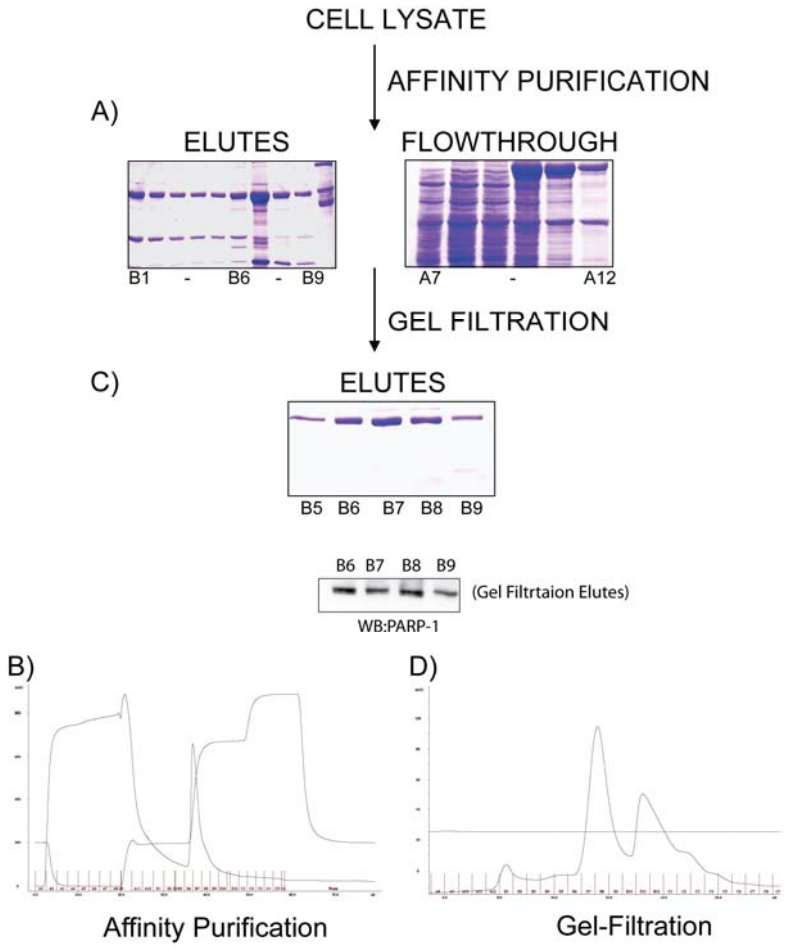

Figure 1.13

Purification of PARP-1:

A) SDS-PAGE of fractions collected after affinity chromatography. SDS-PAGE fractions from the corresponding peak in chromatogram (B1-B9).

B) Representative chromatogram plot of affinity chromatography. Fractions (A1-A12) are wash and flow through fractions, and (B1-B12) were eluted from DNA cellulose column. X-axis denotes the volume (ml) of buffer passed through column and Y-axis denotes the UV absorbance (mAU) at 280nm.

C) SDS-PAGE of fractions from gel filtration. Fractions from the Gel filtration column corresponding to the peak in the chromatogram (B5 –B9) were run on SDS PAGE and on a Western blot. The purity of PARP-1 (113kDa) after gel filtration is clearly seen.

D) Representative chromatogram of PARP-1 gel filtration using sephadex 200.

3.2.2. Enzymatic activity of purified PARP-1

To determine the activity of purified PARP-1, two functional assays were utilized. First, a non-radioactive Western blot assay which is based on the quantification of PARP-1 auto-poly–ADP-ribosylation using an anti-poly(ADP-ribose) antibody, and EMSA. Both assays are described under Materials and Methods. In presence of oligonucleotides, PARP-1 utilizes NAD^+ as a substrate to ribosylate itself, thus causing the high molecular weight smear in the Western blot. The auto-ribosylation of PARP-1 is a post-translational modification recognized by the anti-poly-(ADP-ribose) antibody.

Figure 1.14 illustrates the activity of PARP-1 under various conditions. The Figure shows PARP-1 activity (Figure 1.14 A and B) with increasing concentration of purified enzyme. Figures 1.14 C and D show that PARP-1 activity is influenced by the presence of oligonucleotides. As PARP-1 was purified from DNA cellulose column, the possibility of contamination with small fragments of DNA cannot be ruled out, which might explain the activity observed in the absence of oligonucleotides. PARP-1 auto-poly–ADP-ribosylation increases with time and as shown in Figures 1.14 E and F, it increases significantly from 5 to 10 min reaching a plateau at later times. Increasing the concentration of NAD^+ also increases PARP-1 auto-poly–ADP-ribosylation (Figure 1.14 G and H).

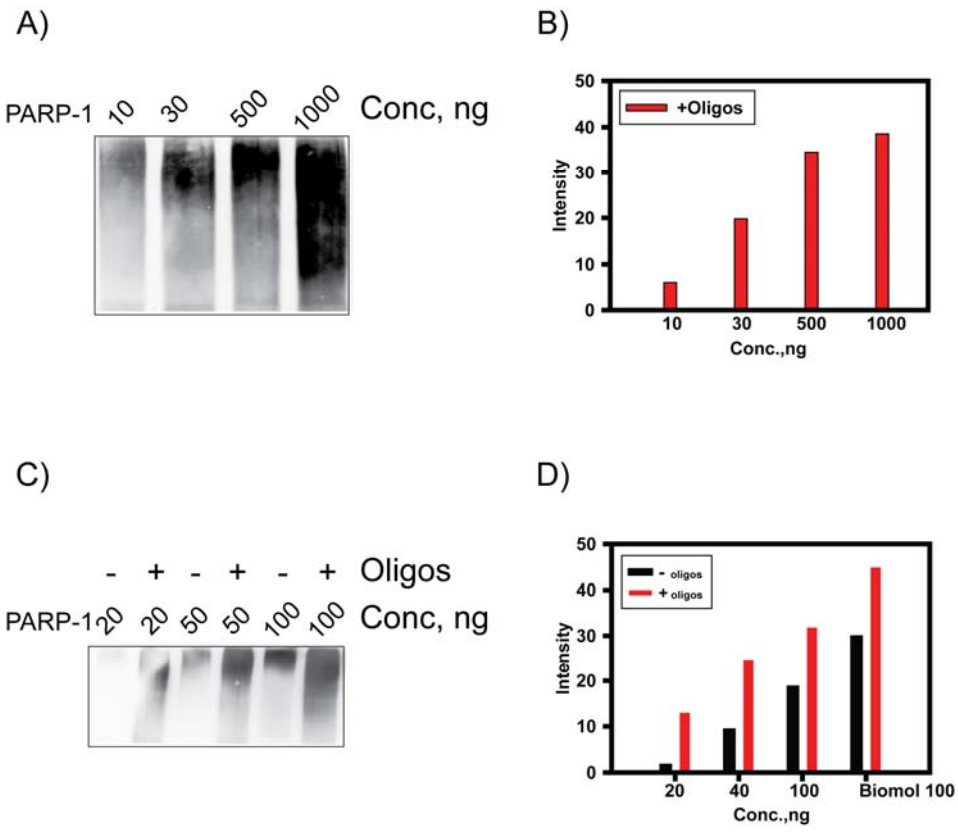

Figure 1.14

***(A) Analysis of PARP-1 activity*:**

A) Western blot showing PARP-1 activity when blotted with an anti-PAR Ab at four different PARP-1 concentrations in the presence of an oligonucleotide 2 ng).

B) Bar graph representing densitometric analysis of PAR signal intensity.

C) PARP-1 auto-poly–ADP-ribosylation determined by Western blotting at different concentrations of oligonucleotides.

D) Bar graph representing the values calculated from the signal intensity in **C.**

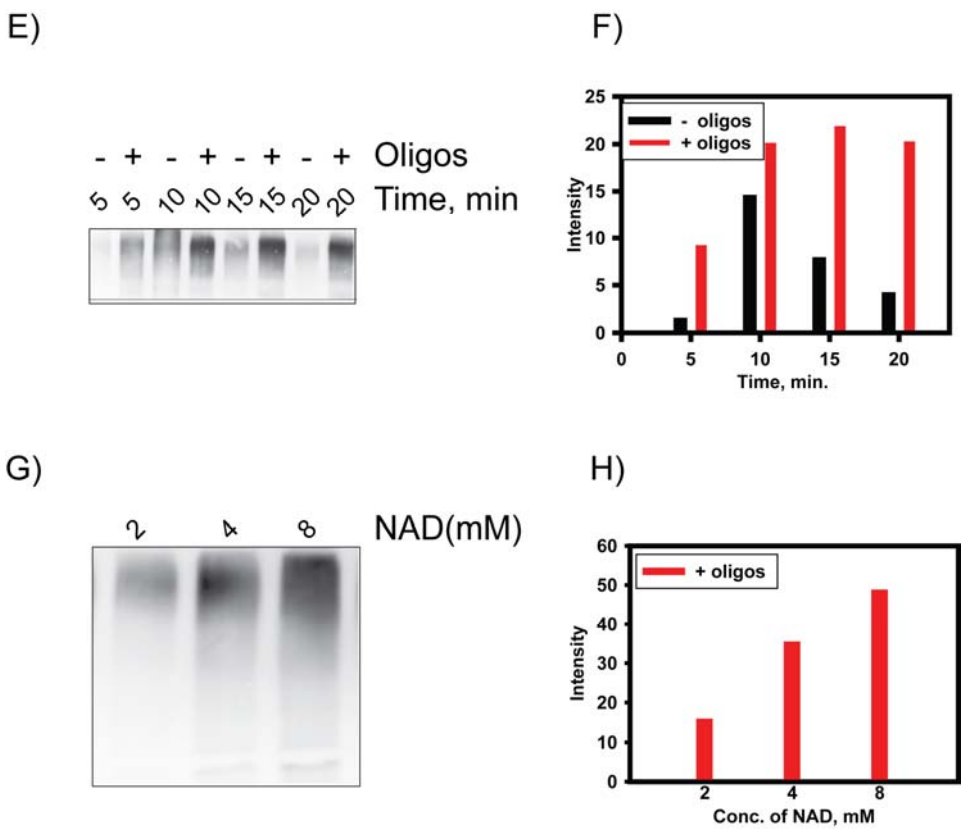

Figure 1.14

***Analysis of PARP-1 activity (Continued)*:**

E) Western blot showing PARP-1 auto-poly–ADP-ribosylation determined with an anti-PAR Ab at four different time points of incubation.

F) Bar graph showing densitometric analysis of PAR signal intensity from **E**.

G) PARP-1 auto-poly–ADP-ribosylation with increasing concentration of NAD^+ in the presence of 2 ng oligonucleotides.

H) Bar graph representing the values calculated from the signal intensity in **G**.

3.2.3. PARP-1 activity determined by EMSA

We employed EMSA to examine DNA end binding activity of purified PARP-1. PARP-1 effectively binds a radioactively labeled double-stranded DNA oligonucleotide substrate causing a mobility shift that is clearly detectable above 1 pmol protein concentration. We chose blunt-ended oligonucleotide substrates (OA/OB) to test the enzymatic activity of our purified PARP-1. OA/OB avidly binds PARP-1 and gives a measurable shift at 0.2 pmol of oligonucleotide. Representative phosphor images of the EMSA experiments carried out under different conditions are summarized in Figure 1.15. The control reaction with free DNA alone shows a band at low molecular weight that migrates at the bottom of gel. On addition of purified PARP-1 to the reaction mixture containing the oligos, a significant shift in the oligos band is observed. To confirm that the DNA binding protein in our EMSA assays is PARP-1, the reactions were supplemented with anti-PARP-1 antibody. Binding of antibody to PARP-1 results in a super shift, identified as a slowly migrating band in Figure 1.15. As a control, we also used purified Ku to indicate shift and super-shift of bands, since both Ku and PARP-1 show the same pattern of shift and super-shift bands in EMSA. As a positive control, we used semi-purified, commercially-available PARP-1 from Biomol, which also shows the expected gel shift. Our purified PARP-1 displayed very high levels of activity and lead to the formation of complexes which were unable to enter the gel, (Figure 1.15). A super-shift was visible with our purified fraction when used at low concentrations (5ng).

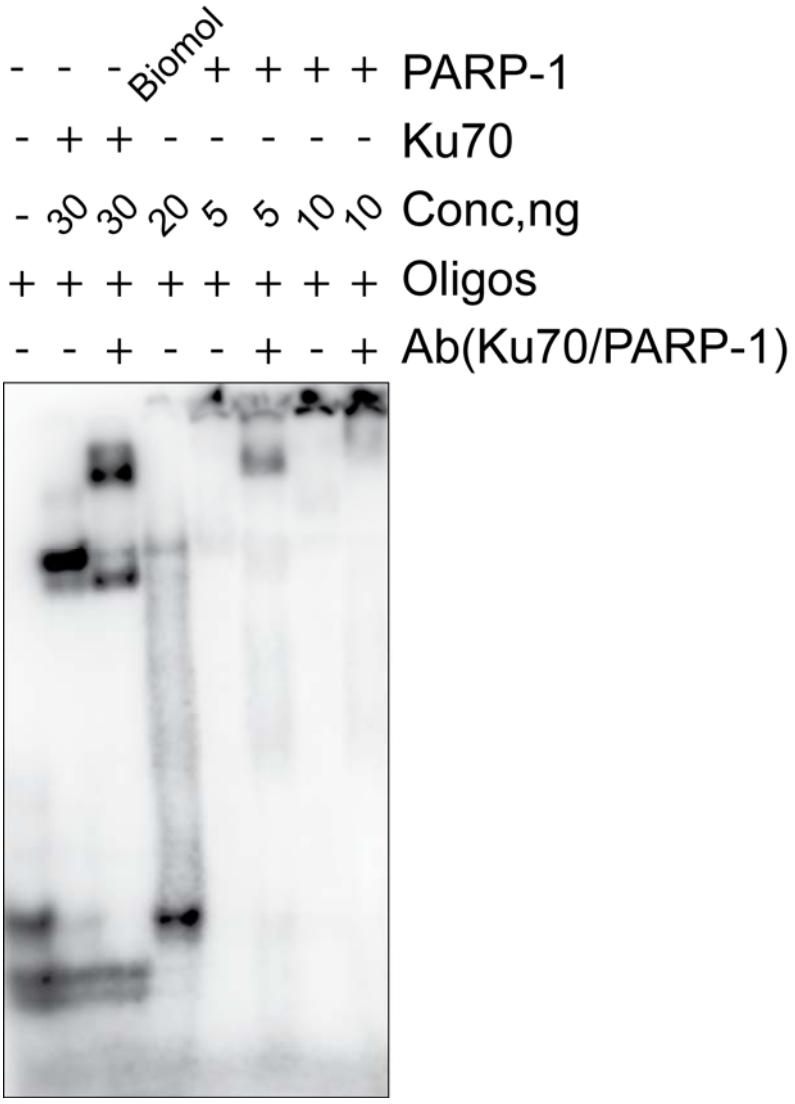

Figure 1.15

Analysis of PARP-1 activity by EMSA:

EMSA gel depicting activity of PARP-1 when bound to oligonucleotides. Starting from left, the first lane shows signal of only radiolabeled oligonucleotide (25bp), the second depicts the signal of purified Ku when bound to the same oligonucleotide, next lane shows super-shift signal by an anti-Ku 80 Ab, the fourth lane shows Biomol PARP-1 bound to oligonucleotides, the fifth lane shows purified PARP-1 (5ng) when bound to oligonucleotides, next is with purified PARP-1 (5ng) plus an anti-PARP-1 antibody, the seventh lane is with purified PARP-1 (10ng) bound to oligonucleotides and the last lane shows purified PARP-1 (10ng) with an anti-PARP-1 antibody bound to oligonucleotides.

3.2.4. Histone H1 activates PARP-1

Fractionation studies combined with proteomic analysis of active fractions identified histone H1 as a component of B-NHEJ, possibly functioning as an alignment factor or DNA end-joining factor [42]. This postulate is supported by the observation that DNA end ligation activity of LigIII is strongly and relatively specifically enhanced by histone H1. We inquired, therefore, whether the activity of other candidate components of this pathway such as PARP-1 is modified by histone H1. For this purpose, we assembled a reaction in the presence of NAD^+ and different amounts of purified PARP-1 and its activity was measured using an antibody against poly-(ADP ribose).
The results show a marked increase in PARP-1 activity with increasing concentration of histone H1, measured either by Western blot (Figure 1.16 A) or by dot blot (Figure 1.16 B), although the increase was more evident in the dot blot. Thus, a marked stimulation is observed at low concentrations of histone H1 reaching a maximum at about 10 – 20 ng and a decline at higher concentration**.** These results indicate that histone H1 can markedly influence PARP-1 activity.

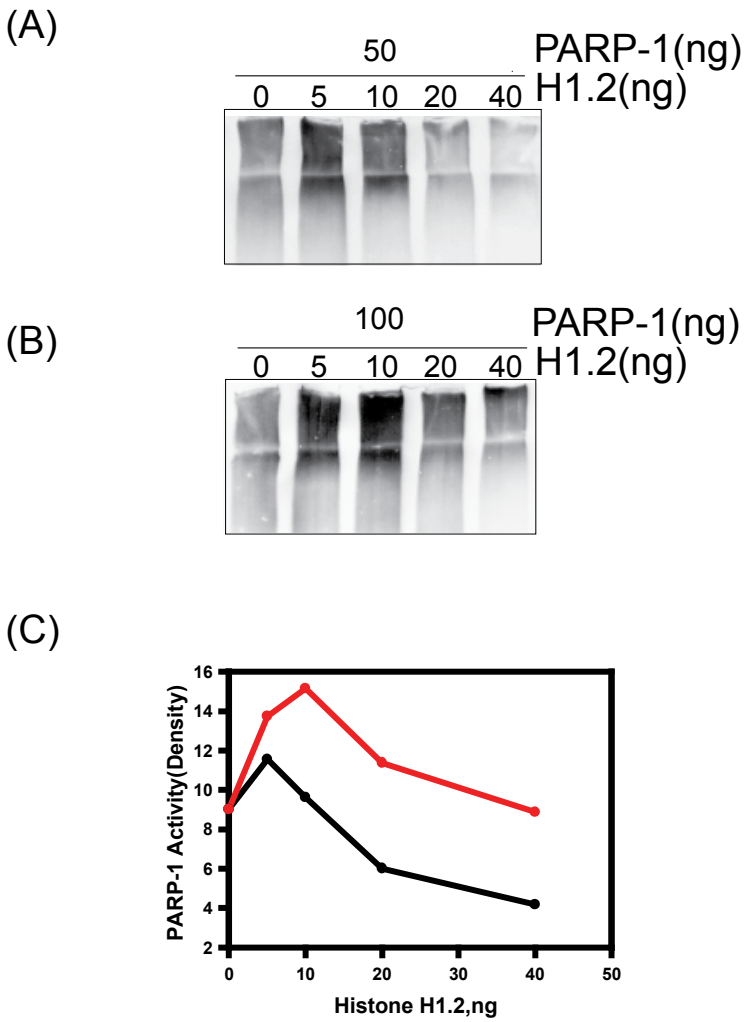

Figure 1.16

(A) Histone H1 activates PARP-1(Western blot):

A) Western blot depicting PARP-1 activity measured by auto-poly-(ADP-ribosylation), detected by an antibody against poly-(ADP-ribose) using 50 ng of purified PARP-1.

B) Western blot detected by an anti-PAR Ab to evaluate PARP-1 activity using 100 ng of purified PARP-1.

C) Line graph representing the densitometric quantification of results shown in the corresponding blots.

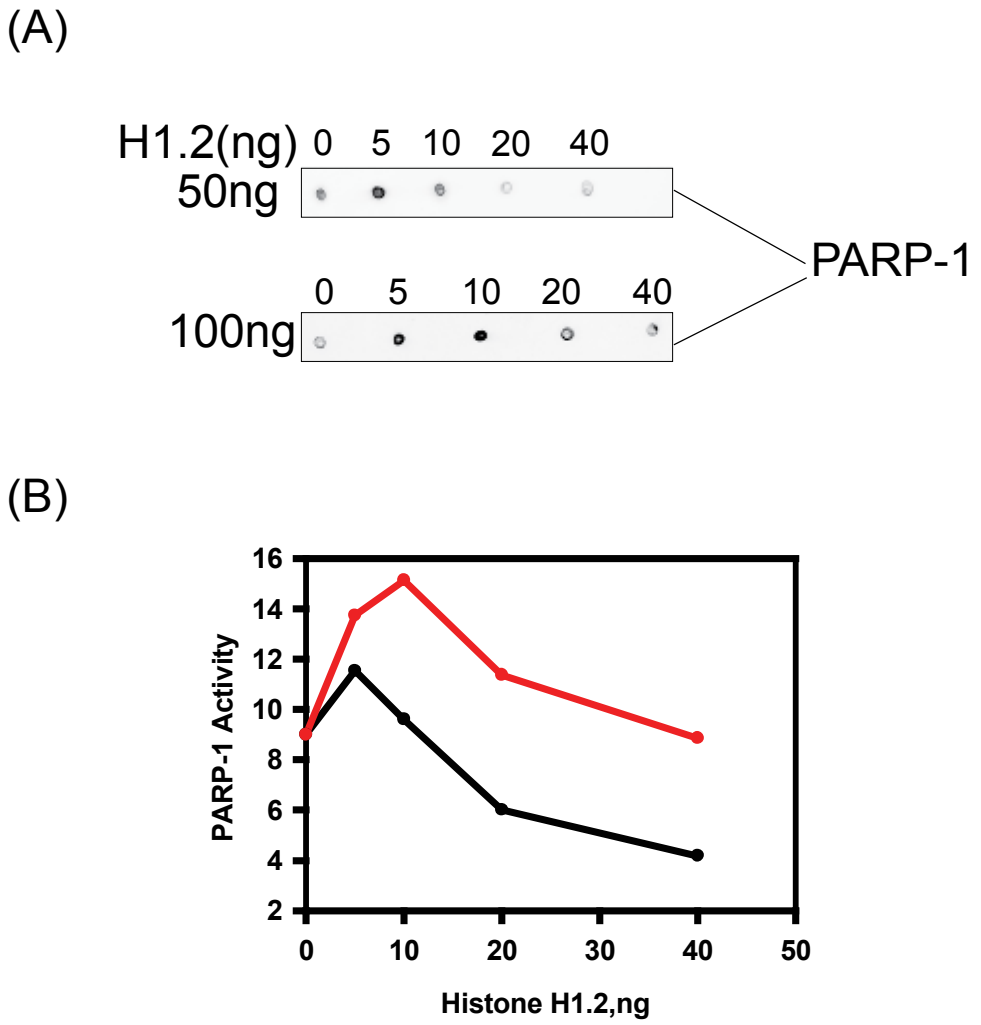

Figure 1.16

(B) Histone H1 activates PARP-1(Dot blot):

A) Dot Blot depicting PARP-1 activity which was measured by auto-poly-(ADP-ribosylation) and detected by an antibody against poly-(ADP-ribose) using 50 and 100 ng of purified PARP-1.

B) Line graph representing the densitometric quantification of results shown in the corresponding blot.

4. Discussion

The results presented here offer some novel insights into the role of Mre11 and Ku in DDR. The first part of the thesis focuses on the determination of the functional significance of the physical interaction between Mre11 and Ku and investigates whether this interaction is modulated by IR. The MRN complex is a well known sensor of DNA damage, functioning in signaling pathways that activate cell cycle checkpoints. Although the function of Mre11 is also known to be important for homologous recombination repair (HRR), recent studies have shown that this protein may have functions in non homologous end joining (D-NHEJ) as well. Indeed, in yeast, in addition to the Ku and Ligase IV homologs, also the MRN homologs are found to be involved in NHEJ.

4.1. Why Mre11 and Ku interact? What is the influence of IR on this interaction?

MRN and Ku are among the earliest molecule which recognizes DNA double strand breaks. The interaction of mammalian Ku heterodimer and Mre11 has already been reported in somatic cells [55]. However, the order of assembly onto DSB ends, their relationship and interdependency, as well as the regulation of this interaction by IR or DNA damage is not well understood. Our results confirmed the interaction between Mre11 and Ku though IP with antibodies raised against either protein. The interaction is resistant to EtBr and RNase suggesting that it is does not derive from independent binding to DNA or RNA of the two DNA binding proteins.

The crystal structure of Ku reveals an asymmetric ring conformation allowing the threading of the DNA that may facilitating the rejoining of the DNA ends. After completion of end joining, the Ku heterodimer is either immediately removed by degradation (ubiquitination), or it remains trapped, at least for some time, on the repaired DNA and may act as a marker or signal for subsequent steps of repair or signaling, including the possible recruitment of signaling factors such as MRN and possibly also of HRR components. In *Saccharomyces cerevisiae*, MRX facilitates NHEJ [127, 128]. To what extent mammalian MRN influences NHEJ of unprogrammed DSBs is not clear.

In the present thesis, we test the hypothesis that the MRN complex plays a bridging role between HRR and NHEJ. In vertebrates, the MRN complex controls important

aspects of the DNA damage response, at least at the early signaling steps [129], but its possible role in NHEJ remains uncharacterized. Recent studies show that MRN may contribute to the Ku-dependent NHEJ in mammalian cell-free extracts and both proteins participate in a complex that is formed immediately prior to rejoining [43, 130, 131]. It has been reported that silencing of Mre11 causes a reduction of NHEJ - both the classical and the alternative versions of the pathway [43]. There is also evidence that depletion of Mre11 suppresses end-resection in *Xrcc4*$^{-/-}$ */LigaseIV*$^{-/-}$ cells indicating a role in B-NHEJ [113]. One study suggests that Mre11 functions in NHEJ as a scaffold to support synapsis between the DNA ends. As NHEJ does not entail extensive end-resection (except for a role of Artemis in a subset of DNA breaks), this could be a function of Mre11 in this pathway, thereby promoting the re-ligation of a DSB [113, 132].

To address these issues in greater detail, we started by deciphering the interactions between Mre11 and Ku in cells exposed to IR. Our results clearly indicate that the interaction between Mre11 and Ku is DNA damage dependent and increases with increasing dose of IR. This suggests that both Mre11 and Ku are the earliest molecules to be recruited to DNA damage sites. Recent work from a group showed the accumulation of Mre11 in nuclear foci in human cells. Mre11 was found to be distributed throughout the nuclei of irradiated cells in CHO-K1-Xrs-6 cells, which are Ku80 deficient [55]. This suggests that Ku may be responsible for recruitment of Mre11 to DNA damage sites. Our experiments showed a dose- dependent interaction of Ku and Mre11 in wild type cells; of course this interaction was absent in Ku mutants.

4.2. Mre11 recruitment at DNA damage sites occurs within 10 min after IR

Next, we studied the Ku/Mre11 kinetics of interaction at different time points after IR. We observed that KU/Mre11 interaction is observable within 10 minutes after IR, consistent with prior observations which were IR induced Mre11/Ku interaction and known interactions between Mre11 and Ku in yeast [108]. In yeast, YFP-Mre11 recruitment was found to be the earliest detectable event at a DSB; it formed a focus peak within 6 min after IR. Also, delay in maximal MRX binding in the absence of Ku suggests a role of Ku in stabilizing MRX complex for NHEJ. However, it was also found that ligase binding strongly depends on Ku, while MRX loss only leads to a

delay in ligase binding. This allows the conclusion that Ku but not MTX is essential for the recruitment of ligase at the sites of DSBs [133, 134]. As a matter of fact, Ku and MRX binding were found to coexist immediately after the formation of a DSB, which might suggest that these proteins are not present in a preformed complex, but rather the binding of each might be intensified by the DSB substrate and the presence of the other. In yeast, it was also observed that the disappearance of Ku and DNA Ligase IV from unrepaired DSBs strongly depends on MRX, where a persistent signal of Ku was observed when MRX was not present [135]. Thus, MRN might be the factor responsible for post-translational modification of Ku, possibly also assisting in its unloading from repaired DNA. It has also been proposed that the removal of Ku happens by ubiquitination [50], but the mechanism is still unknown.

4.3. Players of Ku/Mre11 interaction

Our results clearly show that not only Mre11 but also Nbs1 and Rad50 are constituents of the Ku/Mre11 interaction, thus implicating the whole MRN complex in the process. Since it is known that the MRN complex controls ATM activation [129, 136], we thought of determining the possible role of ATM in this interaction. Notably, in the absence of ATM activity the interaction between Ku and Mre11 was abrogated. MRN was also recently found to be a prime candidate for B-NHEJ [113] raising the possibility that D-NHEJ and B-NHEJ share common steps. PARP-1 was also found to be present in the Ku/Mre11 complex providing thus further evidence for pathway cross talk and the possibility the Ku/Mre11 complex contributes to this phenomenon. It is known that DNA damage-dependent rapid accumulation of Mre11 and Nbs1 at the damage sites requires PARP-1, which provides further hints for DNA damage sensor protein cooperation [94]. Since Mre11 is known to interact with PARP-1 at the sites of DSBs [94], the role of Mre11 in B-NHEJ is also consistent with data that describe the role of PARP-1 in B-NHEJ [115, 137].

4.4. How do DNA-PKcs and ATM influence the Mre11/Ku interaction?

The DNA-PKcs is recruited to the Ku-DNA end complex to form the holoenzyme DNA-PK and activate the kinase. It was therefore reasonable to study the role of DNA-PKcs on the Mre11/Ku interaction. In vitro-studies show that DNA-PKcs phosphorylates both Ku and XRCC4 [131]. Autophosphorylation of DNA-PKcs also

appears to play a key role in NHEJ and is thought to induce a conformational change that allows end-processing enzymes to access the ends of the DSBs. However, phosphorylation could also modulate the interactions of Ku and XRCC4 with DNA-PKcs itself, or with other regulatory proteins, probably including the constituents of MRN complex. The results generated showed that in the absence of DNA-PKcs the IR-mediated interaction between Mre11 and Ku is down regulated.

As discussed earlier, the MRN complex is known to be involved in the activation of the ATM kinase in response to DSBs. Our results show the involvement of ATM kinase as well in the interaction of Ku with MRN. To analyze this interplay, we performed IP in ATM deficient cells and found a reduction of the IR-mediated Mre11/Ku interaction. Our data also suggests that Mre11 can affect NHEJ in an ATM dependent manner, as Mre11 could modulate end-joining by its nuclease-dependent or independent functions. Inhibition of ATM causes a delay in DNA repair [43] and there are reports which suggest that Mre11 can affect NHEJ, partly in an ATM dependent manner [43]. Thus, Mre11 could control end joining through both ATM dependent and ATM independent mechanisms [43].

It has been reported that deletion of Nbs1 in MEFs completely abrogates ATM target phosphorylation in response to IR [138]. These observations and striking similarities between syndromes caused by mutations in ATM, Nbs1 and Mre11 are consistent with a sensor function for the MRN complex. As observed from our results and as discussed above, the probable regulators for the DNA damage dependent interactions between Mre11 and Ku seem to be the DNA-PKcs and ATM kinases.

When we investigated in vitro the effect of phosphorylation and dephosphorylation on Mre11/Ku interaction, we observed that maintenance of phosphorylation retained the IR-dependent aspect of the interaction, whereas dephosphorylation completely abrogated the interaction.

4.5. How does phosphorylation influence the Mre11/Ku interaction?

We suspected that the IR dose dependent interaction between Mre11 and Ku is regulated by phosphorylation, as phosphorylation sites are abundant in Ku and Mre11 (known as well as unknown sites). Our results suggest that phosphorylation is critical for the Mre11/Ku interaction, but that this effect is a dynamic process. When we checked by BAP, no dose dependent enhancement or decrease in the interaction was observed. On the other hand, when the interaction was checked by phosphatase

inhibitors, a decrease in the constitutive interaction was observed, but the IR dose dependent increase in the interaction was retained.

Various reports provide valuable background information for this phenomenon. Thus, phosphorylation of SQ/TQ sites inactivates MRN and facilitates its dissociation from chromatin, thus allowing down regulation of DNA damage signalling and recovery from checkpoint response. According to this model, DSBs trigger rapid association coupled with the hyper-phosphorylation of Mre11. Hence, it is important to identify both proteins phosphorylated in response to DNA damage and the kinases responsible for this phosphorylation. As one report suggests that DNA-PK mediated phosphorylation of Ku is not required for DSB repair by NHEJ [139], the possible role of ATM/MRN as a main regulator is suggested.

4.6. Comparison of results from *in vivo* and *in vitro* systems

Despite the fact that Ku has a central role in NHEJ, we still have an incomplete picture of the interaction between Ku and DNA. Studies of the affinity of Ku to various DNA configurations demonstrated that Ku binding is specific for single to double stranded transitions [59, 140]. After loading on DNA ends, Ku can diffuse to internal positions in an energy independent manner.[141]. Issues such as the interaction of Ku with DNA when DNA length is sufficient for more than one Ku molecule to load, have recently been resolved, suggesting that Ku binds cooperatively to DNA when the DNA has sufficient length to accommodate two Ku molecules and this is sequence independent. This model suggests that Ku molecules may function by providing more sites for recruiting other factors that participate in other aspects of the DDR [142].

We also observed in *in vitro* experiments that Ku binding was directly proportional to the size of oligos when IP was performed with an anti-Mre11 Ab using A549 or Xrs-6 NE. Interestingly, Ku showed this pattern of binding only in NE of A549 cells but not in Xrs-6 cells. This difference in the binding pattern of Ku leads us to suggest two different models; first, A549 NE mimics the in vivo situation where all the cellular components and signalling molecules facilitate the dose dependent interaction between Mre11 and Ku, and second, the less efficient *in vitro* artificial system used to study the interactions between purified Mre11 and Ku70. Our results suggest that dose dependent interactions between Ku and Mre11 may be dependent on other components and processes, which may not take place in some mutants. The

possibility of competition between Ku and Mre11 for DNA ends can also not be ruled out. Finally the large difference in the levels of DNA-PKcs between hamster and human systems, may contribute to the different responses observed.

4.7. Intertwining of NHEJ pathways

When a DSB is induced in a repair proficient cell, the most likely scenario is that the Ku heterodimer will bind to the ends of the broken DNA replacing bound histone H1 (in cooperation with DNA-PK) and possibly also other components of chromatin in preparation for the recruitment of DNA-PKcs to the site. DNA-PKcs dependent phosphorylation events then will regulate and coordinate the end-joining process and ultimately lead to end ligation catalyzed by LigaseIV/XRCC4/XLF complex, with a possible role of Artemis in a subset of breaks. Activation of DNA-PKcs is expected to facilitate the removal of histone H1 from chromatin and to facilitate the productive functions of Ku at DNA ends.

If the DNA-PK-dependent pathway of NHEJ is compromised as a result of a defect in one of its components, histone H1 will probably remain bound and will act as an alignment factor to mediate end joining by LigaseIII/XRCC1 complex, possibly with the contribution of PARP-1. This pathway operates with slower kinetics and is normally suppressed by D-NHEJ. Regulation of DSB end processing via Ku/CtIP is a common step during B-NHEJ, SSA and HDR. Recently, it has also been shown that DSB end-processing factors Ku and CTIP affect all three pathways similarly.

4.8. How PARP-1 and histone H1 influence backup pathways?

Little is known about the potential consequences of B-NHEJ function, about the underlying mechanism and its regulation. Here we show interaction between PARP-1, Mre11 and Ku. Histone H1's role in B-NHEJ and its effect on PARP-1 activity has been reported [42]. A marked stimulation is observed at low concentrations of histone H1 reaching a maximum at about 10-20 ng with a decline at higher concentrations. These observations point to a cooperative interaction between PARP-1 and histone H1, which is compatible with a function in the same repair pathway. The effect in our experiments, particularly for inhibitory concentrations of histone H1, suggests that PARP-1 may have a role in relieving local inhibition of DSB repair by histone H1. It has been shown that the end-ligation activity of DNA Ligase III is strongly and relatively specifically enhanced by histone H1, albeit in a narrow range of

concentrations [42], which also explains some reports of inhibitory action of histone H1.

5. Concluding Remarks

The major observations and conclusions that can be drawn from this study are as follows:

In different types of cellular extracts we employed immunoprecipitation techniques to show the DNA damage dependent interaction between Mre11 and Ku.

1. We provided evidence that the MRN complex and Ku, the earliest known molecules to sense DSBs, physically interact with each other. We also found that this interaction is IR dose dependent.
2. We examined interdependency for this interaction and generated results suggesting that the Mre11/Ku interaction has a component that requires DNA and DNA damage, but also a component that is independent of DNA or DNA damage. We determined that the entire MRN complex is involved in this interaction, as well as PARP-1.
3. We measured the kinetics of Mre11/Ku interaction and show it to be detectable 10 min post irradiation.
4. We provided evidence that the dose dependent interaction of Mre11 with Ku depends on the PIKK-3 group of kinase family members like DNA-PKcs and ATM. The decline in interaction observed in DNA-PKcs and ATM mutant cell lines hints to possible connections between these kinases and the Mre11/Ku interaction.
5. Results from second part of the thesis helped in establishing that histone H1 enhances the activity of PARP-1 protein, whose possible role in backup pathways of NHEJ (B-NHEJ) is already documented.

6. Future Outlook

The data presented in this thesis provide new insights into the role of MRN complex and Ku in the repair of DSBs, as well as the role of other repair and signaling proteins in DDR. DNA damage induction and repair are associated with activation of a myriad of proteins and their sequential recruitment to damage sites. Although a great deal is known about NHEJ, the most prominent and prompt but error prone DSB repair pathway, knowledge about the functional aspects of the individual participating proteins is still lacking. For example, the significance and purpose of the interaction of Ku with signaling molecules like the MRN complex is still unanswered.

We speculate that this interaction could mediate post translation modifications in Ku leading to its unloading from the repaired DNA. This aspect of the interaction needs to be studied further. In addition, Mre11 and Ku interactions need to be studied in cell lines defective in individual MRN components using purified proteins with specific mutations that may help enlighten the specificity of this interaction.

It would also be useful to use various drugs like Wortmannin or Mirin to inhibit the function of specific partners and to study further the interactions between them. To further illustrate the critical role of phosphorylation and dephosphorylation, phospho-specific antibodies could be useful to determine activation and deactivation of proteins through their phosphorylation status immediately after DNA damage induction (IR) or during the repair process.

At last, a detailed investigation of the potential link between D-NHEJ and B-NHEJ, as well as the regulatory functions of proteins such as MRN complex, CtIP, PARP-1, histone H1 and LigaseIII/XRCC1 may prove useful in elucidating the DNA repair mechanisms and the factors affecting choice of a particular repair pathway by the cell.

7. References

1. Khanna, K.K. and S.P. Jackson, *DNA double-strand breaks: signaling, repair and the cancer connection.* Nature Genetics, 2001. **27**: p. 247-254.
2. van Gent, D.C., J.H.J. Hoeijmakers, and R. Kanaar, *Chromosomal stability and the DNA double-stranded break connection.* Nature Reviews. Genetics, 2001. **2**: p. 196-206.
3. Richardson, C., N. Horikoshi, and T.K. Pandita, *The role of the DNA double-strand break response network in meiosis.* DNA Repair, 2004. **3**: p. 1149-1164.
4. Rouse, J. and S.P. Jackson, *Interfaces between the detection, signaling, and repair of DNA damage.* Science, 2002. **297**: p. 547-551.
5. Shiloh, Y. and A.R. Lehmann, *Maintaining integrity.* Nature Cell Biology, 2004. **6**: p. 923-928.
6. Sancar, A., et al., *Molecular Mechanisms of Mammalian DNA Repair and the DNA Damage Checkpoints.* Annual Review of Biochemistry, 2004. **73**: p. 39-85.
7. Downs, J.A. and S.P. Jackson, *A means to a DNA end: The many roles of Ku.* Nature Reviews. Molecular Cell Biology, 2004. **5**: p. 367-378.
8. Ogawa, Y., et al., *Stimulation of Transcription Accompanying Relaxation of Chromatin Structure in Cells Overexpressing High Mobility Group 1 Protein.* Journal of Biological Chemistry, 1995. **270**: p. 9272-9280.
9. Zhou, B.B. and S.J. Elledge, *The DNA damage response: putting checkpoints in perspective.* Nature, 2000. **408**: p. 433-439.
10. Iliakis, G., et al., *DNA damage checkpoint control in cells exposed to ionizing radiation.* Oncogene, 2003. **22**: p. 5834-5847.
11. Wang, H., et al., *Replication Protein A2 Phosphorylation after DNA Damage by the Coordinated Action of Ataxia Telangiectasia-Mutated and DNA-dependent Protein Kinase.* Cancer Research, 2001. **61**: p. 8554-8563.
12. Balajee, A.S. and C.R. Geard, *Replication protein A and g-H2AX foci assembly is triggered by cellular response to DNA double-strand breaks.* Experimental Cell Research, 2004. **300**: p. 320-334.
13. Kastan, M.B. and D.-S. Lim, *The many substrates and functions of ATM.* Nature Reviews. Molecular Cell Biology, 2000. **1**: p. 179-186.
14. Kastan, M.B., *Checking two steps.* Nature, 2001. **410**: p. 766-767.
15. Durocher, D. and S.P. Jackson, *DNA-PK, ATM and ATR as sensors of DNA damage: variations on a theme?* Current Opinion in Cell Biology, 2001. **13**: p. 225-231.
16. Smith, G.C.M. and S.P. Jackson, *The DNA-dependent protein kinase.* Genes & Development, 1999. **13**: p. 916-934.
17. Jackson, S.P., *The DNA-damage response: new molecular insights and new approaches to cancer therapy.* Biochemical Society Transactions, 2009. **37**(3): p. 483-494.
18. Bakkenist, C.J. and M.B. Kastan, *DNA damage activates ATM through intermolecular autophosphorylation and dimer dissociation.* Nature, 2003. **421**: p. 499-506.
19. Brown, K.D., et al., *The mismatch repair system is required for S-phase checkpoint activation.* Nature Genetics, 2003. **33**: p. 80-84.
20. Pleschke, J.M., et al., *Poly(ADP-ribose) Binds to Specific Domains in DNA Damage Checkpoint Proteins.* Journal of Biological Chemistry, 2000. **275**(52):

p. 40974-40980.
21. Paques, F. and J.E. Haber, *Multiple pathways of recombination induced by double-strand breaks in Saccharomyces cerevisiae.* Microbiology and Molecular Biology Reviews, 1999. **63**: p. 349-404.
22. D'Amours, D. and S.P. Jackson, *The Mre11 Complex: At the Crossroads of DNA Repair and Checkpoint Signalling.* Nature Reviews, 2002. **3**: p. 317-327.
23. Roth, D.B. and J.H. Wilson, *Relative rates of homologous and nonhomologous recombination in transfected DNA.* Proceedings of the National Academy of Sciences of the United States of America, 1985. **82**: p. 3355-3359.
24. Critchlow, S.E. and S.P. Jackson, *DNA end-joining: from yeast to man.* Trends in Biochemical Sciences, 1998. **23**: p. 394-398.
25. Tsukamoto, Y. and H. Ikeda, *Double-strand break repair mediated by DNA end-joining.* Genes to Cells, 1998. **3**: p. 135-144.
26. Drouet, J., et al., *DNA-dependent Protein Kinase and XRCC4-DNA Ligase IV Mobilization in the Cell in Response to DNA Double Strand Breaks.* Journal of Biological Chemistry, 2005. **280**(8): p. 7060-7069.
27. McElhinny, S.A.N. and D.A. Ramsden, *Sibling rivalry: competition between Pol X family members in V(D)J recombination and general double strand break reapir.* Immunological Reviews, 2004. **200**: p. 156-164.
28. Paull, T.T. and M. Gellert, *The 3' to 5' exonuclease activity of Mre11 facilitates repair of DNA double-strand breaks.* Molecular Cell, 1998. **1**: p. 969-979.
29. Junop, M.S., et al., *Crystal structure of the Xrcc4 DNA repair protein and implications for end joining.* EMBO Journal, 2000. **19**(22): p. 5962-5970.
30. Lee, K.-J., et al., *DNA Ligase IV and XRCC4 Form a Stable Mixed Tetramer That Functions Synergistically with Other Repair Factors in a Cell-free End-joining System.* Journal of Biological Chemistry, 2000. **275**(44): p. 34787-34796.
31. Sibanda, B., et al., *Crystal structure of an Xrcc4-DNA ligase IV complex.* Nature Structural Biology, 2001. **8**: p. 1015-1019.
32. Takata, M., et al., *Homologous recombination and non-homologous end-joining pathways of DNA double-strand break.* EMBO Journal, 1998. **17**: p. 5497-5508.
33. West, S.C., *Molecular views of recombination proteins and their control.* Nature Reviews. Molecular Cell Biology, 2003. **4**: p. 1-11.
34. Riballo, E., et al., *XLF-Cernunnos promotes DNA ligase IV-XRCC4 re-adenylation following ligation.* Nucleic Acids Research, 2009. **37**(2): p. 482-492.
35. van Attikum, H. and S.M. Gasser, *The histone code at DNA breaks: A guide to repair?* Nature Reviews. Molecular Cell Biology, 2005. **6**: p. 757-765.
36. Lundin, C., et al., *Different Roles for Nonhomologous End Joining and Homologous Recombination following Replication Arrest in Mammalian Cells.* Molecular and Cellular Biology, 2002. **22**: p. 5869-5878.
37. Wang, H., et al., *Biochemical evidence for Ku-independent backup pathways of NHEJ.* Nucleic Acids Research, 2003. **31**: p. 5377-5388.
38. Löbrich, M., B. Rydberg, and P.K. Cooper, *Repair of x-ray-induced DNA double-strand breaks in specific Not I restriction fragments in human fibroblasts: Joining of correct and incorrect ends.* Proceedings of the National Academy of Sciences of the United States of America, 1995. **92**: p. 12050-12054.
39. Nevaldine, B., J.A. Longo, and P.J. Hahn, *The scid defect results in much slower repair of DNA double-strand breaks but not high levels of residual*

breaks. Radiation Research, 1997. **147**: p. 535-540.
40. DiBiase, S.J., et al., *DNA-dependent protein kinase stimulates an independently active, nonhomologous, end-joining apparatus.* Cancer Research, 2000. **60**: p. 1245-1253.
41. Wang, H., et al., *Efficient rejoining of radiation-induced DNA double-strand breaks in vertebrate cells deficient in genes of the RAD52 epistasis group.* Oncogene, 2001. **20**: p. 2212-2224.
42. Rosidi, B., et al., *Histone H1 functions as a stimulatory factor in backup pathways of NHEJ.* Nucleic Acids Research, 2008. **36**(5): p. 1610-1623.
43. Rass, E., et al., *Role of Mre11 in chromosomal nonhomologous end joining in mammalian cells.* Nature Structural & Molecular Biology, 2009. **16**(8): p. 819-825.
44. Wu, W., et al., *Repair of radiation induced DNA double strand breaks by backup NHEJ is enhanced in G2.* DNA Repair, 2008. **7**(2): p. 329-338.
45. Difilippantonio, M.J., et al., *DNA repair protein Ku80 suppresses chromosomal aberrations and malignant transformation.* Nature, 2000. **404**: p. 510-514.
46. Chen, S., et al., *Accurate in Vitro End Joining of a DNA Double Strand Break with Partially Cohesive 3'-Overhangs and 3'-Phosphoglycolate Termini. EFFECT OF Ku ON REPAIR FIDELITY.* Journal of Biological Chemistry, 2001. **276**(26): p. 24323-24330.
47. Baumann, P. and S.C. West, *DNA end-joining catalyzed by human cell-free extracts.* Proceedings of the National Academy of Sciences of the United States of America, 1998. **95**: p. 14066-14070.
48. Paillard, S. and F. Strauss, *Analysis of the mechanism of interaction of simian Ku protein with DNA.* Nucleic Acids Research, 1991. **19**: p. 5619-5624.
49. Walker, J.R., R.A. Corpina, and J. Goldberg, *Structure of the Ku heterodimer bound to DNA and its implications for double-strand break repair.* Nature, 2001. **412**: p. 607-614.
50. Postow, L., et al., *Ku80 removal from DNA through double strand break-induced ubiquitylation.* Journal of Cell Biology, 2008. **182**(3): p. 467-479.
51. Wasko, B.M., et al., *Inhibition of DNA double-strand break repair by the Ku heterodimer in mrx mutants of Saccharomyces cerevisiae.* DNA Repair, 2009. **8**(2): p. 162-169.
52. Fattah, F., et al., *Ku Regulates the Non-Homologous End Joining Pathway Choice of DNA Double-Strand Break Repair in Human Somatic Cells.* PLoS Genetics, 2010. **6**(2): p. e1000855.
53. Wang, H., et al., *Characteristics of DNA-binding proteins determine the biological sensitivity to high-linear energy transfer radiation.* Nucleic Acids Research, 2010. **38**(10): p. 3245-3251.
54. Rupnik, A., M. Grenon, and N. Lowndes, *The MRN complex.* Current Biology, 2008. **18**(11): p. R455-R457.
55. Goedecke, W., et al., *Mre11 and Ku70 interact in somatic cells, but are differentially expressed in early meiosis.* Nature Genetics, 1999. **23**: p. 194-198.
56. Dynan, W.S. and S. Yoo, *Interaction of ku protein and DNA-dependent protein kinase catalytic subunit with nucleic acids.* Nucleic Acids Research, 1998. **26**: p. 1551-1559.
57. Gell, D. and S.P. Jackson, *Mapping of protein-protein interactions within the DNA-dependent protein kinase complex.* Nucleic Acids Research, 1999. **27**: p. 3494-3502.
58. Mahaney, B.L., K. Meek, and S.P. Lees-Miller, *Repair of ionizing radiation-*

induced DNA double-strand breaks by non-homologous end-joining. Biochemical Journal, 2009. **417**: p. 639-650.
59. Falzon, M., J.W. Fewell, and E.L. Kuff, *EBP-80, a transcription factor closely resembling the human autoantigen Ku, recognizes single-to double-strand transitions in DNA.* Journal of Biological Chemistry, 1993. **268**: p. 10546-10552.
60. Ono, M., P.W. Tucker, and J.D. Capra, *Production and characterization of recombinant human Ku antigen.* Nucleic Acids Research, 1994. **19**: p. 3918-3924.
61. Blier, P.R., et al., *Binding of Ku protein to DNA. Measurement of affinity for ends and demonstration of binding to nicks.* Journal of Biological Chemistry, 1993. **268**: p. 7594-7601.
62. Muller, C., et al., *The Double Life of the Ku Protein: facing the DNA breaks and the extracellular environment.* Cell Cycle, 2005. **4**(3): p. 438-441.
63. Mimori, T., J.A. Hardin, and J.A. Steitz, *Characterization of the DNA-binding protein antigen Ku recognized by autoantibodies from patients with rheumatic disorders.* Journal of Biological Chemistry, 1986. **261**: p. 2274-2278.
64. Allaway, G.P., et al., *Characterization of the 70KDA component of the human Ku autoantigen expressed in insect cell nuclei using a recombinant baculovirus vector.* Biochemical and Biophysical Research Communications, 1990. **168**: p. 747-755.
65. Zhang, W.-W. and M. Yaneva, *On the mechanisms of Ku protein binding to DNA.* Biochemical and Biophysical Research Communications, 1992. **186**: p. 574-579.
66. Griffith, A.J., et al., *Ku polypeptides synthesized in vitro assemble into complexes which recognize ends of double-stranded DNA.* Journal of Biological Chemistry, 1992. **267**: p. 331-338.
67. Johzuka, K. and H. Ogawa, *Interaction of Mre11 and Rad50: Two proteins required for DNA repair and meiosis-specific double-strand break formation in Saccharomyces cerevisiae.* Genetics, 1995. **139**: p. 1521-1532.
68. Jeggo, P.A., *Identification of genes involved in repair of DNA double-strand breaks in mammalian cells.* Radiation Research, 1998. **150 (Suppl)**: p. S80-S91.
69. Haber, J.E., *The many interfaces of Mre11.* Cell, 1998. **95**: p. 583-586.
70. Rupnik, A., N. Lowndes, and M. Grenon, *MRN and the race to the break.* Chromosoma, 2009. **in press**: p. doi:10.1007/s00412-009-0242-4.
71. Mirzoeva, O.K. and J.H.J. Petrini, *DNA damage-dependent nuclear dynamics of the Mre11 complex.* Molecular and Cellular Biology, 2001. **21**(1): p. 281-288.
72. Bartek, J., J. Bartkova, and J. Lukas, *DNA damage signalling guards against activated oncogenes and tumour progression.* Oncogene, 2007. **26**(56): p. 7773-7779.
73. Harper, J.W. and S.J. Elledge, *The DNA Damage Response: Ten Years After.* Molecular Cell, 2007. **28**(5): p. 739-745.
74. Kanaar, R. and C. Wyman, *DNA Repair by the MRN Complex: Break It to Make It.* Cell, 2008. **135**(1): p. 14-16.
75. Zhu, W.-G., et al., *Translocation of MRE11 from the Nucleus to the Cytoplasm as a Mechanism of Radiosensitization by Heat.* Radiation Research, 2001. **156**: p. 95-102.
76. Stewart, G.S., et al., *The DNA double-strand break repair gene hMRE11 is mutated in individuals with an ataxia-telangiectasia-like disorder.* Cell, 1999.

99(6): p. 577-587.
77. Nakada, D., K. Matsumoto, and K. Sugimoto, *ATM-related Tel1 associates with double-strand breaks through an Xrs2-dependent mechanism.* Genes & Development, 2003. **17**: p. 1957-1962.
78. Di Virgilio, M., C.Y. Ying, and J. Gautier, *PIKK-dependent phosphorylation of Mre11 induces MRN complex inactivation by disassembly from chromatin.* DNA Repair, 2009. **8**(11): p. 1311-1320.
79. Dolganov, G.M., et al., *Human Rad50 Is Physically Associated with Human Mre11: Identification of a Conserved Multiprotein Complex Implicated in Recombinational DNA Repair.* Molecular and Cellular Biology, 1996. **16**: p. 4832-4841.
80. Dong, Z., Q. Zhong, and P.-L. Chen, *The Nijmegen breakage syndrome protein is essential for Mre11 phosphorylation upon DNA damage.* Journal of Biological Chemistry, 1999. **274**: p. 19513-19516.
81. Paull, T.T. and M. Gellert, *Nbs1 potentiates ATP-driven DNA unwinding and endonuclease cleavage by the Mre11/Rad50 complex.* Genes & Development, 1999. **13**: p. 1276-1288.
82. Usui, T., S.S. Foster, and J.H.J. Petrini, *Maintenance of the DNA-Damage Checkpoint Requires DNA-Damage-Induced Mediator Protein Oligomerization.* Molecular Cell, 2009. **33**(2): p. 147-159.
83. Furuse, M., et al., *Distinct roles of two separable in vitro activities of yeast Mre11 in mitotic and meiotic recombination.* EMBO Journal, 1998. **17**: p. 6412-6425.
84. Paull, T.T. and M. Gellert, *A mechanistic basis for Mre11-directed DNA joining at microhomologies.* Proceedings of the National Academy of Sciences of the United States of America, 2000. **97**(12): p. 6409-6414.
85. Williams, R.S., J.S. Williams, and J.A. Tainer, *Mre11-Rad50-Nbs1 is a keystone complex connecting DNA repair machinery, double-strand break signaling, and the chromatin template.* Biochemistry and Cell Biology, 2007. **85**: p. 509-520.
86. Williams, R.S., et al., *Mre11 Dimers Coordinate DNA End Bridging and Nuclease Processing in Double-Strand-Break Repair.* Cell, 2008. **135**(1): p. 97-109.
87. Stracker, T.H., et al., *The Mre11 complex and the metabolism of chromosome breaks: the importance of communicating and holding things together.* DNA Repair, 2004. **3**: p. 845-854.
88. de Jager, M., et al., *Human Rad50/Mre11 Is a Flexible Complex that Can Tether DNA Ends.* Molecular Cell, 2001. **8**: p. 1129-1135.
89. van den Bosch, M., R.T. Bree, and N.F. Lowndes, *The MRN complex: coordinating and mediating the response to broken chromosomes.* EMBO Reports, 2003. **4**(9): p. 844-849.
90. Alani, E., S. Subbiah, and N. Kleckner, *The yeast RAD50 gene encodes a predicted 153-kD protein containing a purine nucleotide-binding domain and two large heptad-repeat regions.* Genetics, 1989. **122**: p. 47-57.
91. Tauchi, H., et al., *Nbs1 is essential for DNA repair by homologous recombination in higher vertebrate cells.* Nature, 2002. **420**: p. 93-98.
92. Tauchi, H., et al., *Nijmegen breakage syndrome gene, NBS1, and molecular links to factors for genome stability.* Oncogene, 2002. **21**: p. 8967-8980.
93. Sartori, A.A., et al., *Human CtIP promotes DNA end resection.* Nature, 2007. **450**: p. 509-514.
94. Haince, J.-F., et al., *PARP1-dependent Kinetics of Recruitment of MRE11 and*

NBS1 Proteins to Multiple DNA Damage Sites. Journal of Biological Chemistry, 2008. **283**(2): p. 1197-1208.
95. Takeda, S., et al., *Ctp1/CtIP and the MRN Complex Collaborate in the Initial Steps of Homologous Recombination.* Molecular Cell, 2007. **28**(3): p. 351-352.
96. White, C. and J. Haber, *Intermediates of recombination during mating type switching in Saccharomyces cerevisiae.* EMBO Journal, 1990. **9**(3): p. 663-673.
97. Sugiyama, T., E.M. Zaitseva, and S.C. Kowalczykowski, *A single-stranded DNA-binding protein is needed for efficient presynaptic complex formation by the saccharomyces cerevisiae Rad51 protein.* Journal of Biological Chemistry, 1997. **272**(12): p. 7940-7945.
98. Symington, L.S., *Role of Rad52 epistasis group genes in homologous recombination and double-strand break repair.* Microbiology and Molecular Biology Reviews:MMBR, 2002. **66**: p. 630-670.
99. Hopkins, B.B. and T.T. Paull, *The P. furiosus Mre11/Rad50 Complex Promotes 5' Strand Resection at a DNA Double-Strand Break.* Cell, 2008. **135**(2): p. 250-260.
100. Moore, J.K. and J.E. Haber, *Cell Cycle and Genetic Requirements of Two Pathways of Nonhomologous End-Joining Repair of Double-Strand Breaks in Saccharomyces cerevisiae.* Molecular and Cellular Biology, 1996. **16**: p. 2164-2173.
101. Boulton, S.J. and S.P. Jackson, *Components of the Ku-dependent non-homologous end-joining pathway are involved in telomeric length maintenance and telomeric silencing.* EMBO Journal, 1998. **17**: p. 1819-1828.
102. Kanaar, R. and J.H. Hoeijmakers, *Recombination and joining: different means to the same ends.* Genes and Function, 1997. **1**: p. 165-174.
103. Moreau, S., J.R. Ferguson, and L.S. Symington, *The nuclease activity of Mre11 is required for meiosis but not for mating type switching, end joining, or telomere maintenance.* Molecular and Cellular Biology, 1999. **19**: p. 556-566.
104. Petrini, J.H.J., D.A. Bressan, and M.S. Yao, *The RAD52 epistasis group in mammalian double strand break repair.* Seminars in Immunology, 1997. **9**: p. 181-188.
105. Gatei, M., et al., *ATM-dependent phosphorylation of nibrin in response to radiation exposure.* Nature Genetics, 2000. **25**: p. 115-119.
106. Boulton, S.J. and S.P. Jackson, *Saccharomyces cerevisiae Ku70 potentiates illegitimate DNA double-strand break repair and serves as a barrier to error-prone repair pathways.* EMBO Journal, 1996. **15**(18): p. 5093-5103.
107. Murnane, J.P., *Cell cycle regulation in response to DNA damage in mammalian cells: A historical perspective.* Cancer and Metastasis Reviews, 1995. **14**: p. 17-29.
108. Wu, D., L.M. Topper, and T.E. Wilson, *Recruitment and Dissociation of Nonhomologous End Joining Proteins at a DNA Double-Strand Break in Saccharomyces cerevisiae.* Genetics, 2008. **178**(3): p. 1237-1249.
109. Lee, S.E., et al., *Saccharomyces Ku70, Mre11/Rad50, and RPA proteins regulate adaptation to G2/M arrest after DNA damage.* Cell, 1998. **94**: p. 399-409.
110. Zhang, Z., et al., *Homology-driven chromatin remodeling by human RAD54.* Nature Structural & Molecular Biology, 2007. **14**(5): p. 397-405.
111. Yang, Y.-G., et al., *Conditional deletion of Nbs1 in murine cells reveals its role in branching repair pathways of DNA double-strand breaks.* EMBO Journal, 2006. **25**: p. 5527-5538.

112. Hopfner, K.-P., et al., *Structural biochemistry and interaction architecture of the dna double-strand break repair mre11 nuclease and rad50-atpase.* Cell, 2001. **105**(4): p. 473-485.
113. Xie, A., A. Kwok, and R. Scully, *Role of mammalian Mre11 in classical and alternative nonhomologous end joining.* Nature Structural & Molecular Biology, 2009. **16**(8): p. 814-818.
114. Deriano, L., et al., *Roles for NBS1 in Alternative Nonhomologous End-Joining of V(D)J Recombination Intermediates.* Molecular Cell, 2009. **34**(1): p. 13-25.
115. Wang, M., et al., *PARP-1 and Ku compete for repair of DNA double strand breaks by distinct NHEJ pathways.* Nucleic Acids Research, 2006. **34**(21): p. 6170-6182.
116. D'Amours, D., et al., *Poly(ADP-ribosyl)ation reactions in the regulation of nuclear functions.* Biochemical Journal, 1999. **342**: p. 249-268.
117. Kim, M.Y., T. Zhang, and W.L. Kraus, *Poly(ADP-ribosyl)ation by PARP-1: `PAR-laying' NAD+ into a nuclear signal.* Genes & Development, 2005. **19**(17): p. 1951-1967.
118. Allinson, S.L., I.I. Dianova, and G.L. Dianov, *Poly(ADP-ribose) polymerase in base excision repair: always engaged, but not essential for DNA damage processing.* Acta Biochimica Polonica, 2003. **50**: p. 169-179.
119. Okano, S., et al., *Spatial and Temporal Cellular Responses to Single-Strand Breaks in Human Cells.* Molecular and Cellular Biology, 2003. **23**: p. 3974-3981.
120. Fattah, K.R., B.L. Ruis, and E.A. Hendrickson, *Mutations to Ku reveal differences in human somatic cell lines.* DNA Repair, 2008. **7**(5): p. 762-774.
121. Tanaka, T., et al., *ATM activation accompanies histone H2AX phosphorylation in A549 cells upon exposure to tobacco smoke.* BMC Cell Biology, 2007. **8**: p. 26.
122. Jeggo, P.A. and L.M. Kemp, *X-ray-sensitive mutants of Chinese hamster ovary cell line. Isolation and cross-sensitivity to other DNA-damaging agents.* Mutation Research, 1983. **112**: p. 313-327.
123. Stiff, T., et al., *ATM and DNA-PK function redundantly to phosphorylate H2AX after exposure to ionizing radiation.* Cancer Research, 2004. **64**: p. 2390-2396.
124. Luo, C.-M., et al., *High frequency and error-prone DNA recombination in ataxia telangiectasia cell lines.* Journal of Biological Chemistry, 1996. **271**: p. 4497-4503.
125. Knight, M.I. and P.J. Chambers, *Production, Extraction, and Purification of Human Poly (ADP-ribose) Polymerase-1 (PARP-1) with High Specific Activity.* Protein Expression and Purification, 2001. **23**: p. 453-458.
126. Ruis, B.L., K.R. Fattah, and E.A. Hendrickson, *The Catalytic Subunit of DNA-Dependent Protein Kinase Regulates Proliferation, Telomere Length, and Genomic Stability in Human Somatic Cells.* Molecular and Cellular Biology, 2008. **28**(20): p. 6182-6195.
127. Ma, J.-L., et al., *Yeast Mre11 and Rad1 Proteins Define a Ku-Independent Mechanism To Repair Double-Strand Breaks Lacking Overlapping End Sequences.* Molecular and Cellular Biology, 2003. **23**: p. 8820-8828.
128. Mimitou, E.P. and L.S. Symington, *Sae2, Exo1 and Sgs1 collaborate in DNA double-strand break processing.* Nature, 2008. **455**(7214): p. 770-774.
129. Lee, J.-H. and T.T. Paull, *Direct Activation of the ATM Protein Kinase by the Mre11/Rad50/Nbs1 Complex.* Science, 2004. **304**: p. 93-100.
130. Di Virgilio, M. and J. Gautier, *Repair of double-strand breaks by*

nonhomologous end joining in the absence of Mre11. Journal of Cell Biology, 2005. **171**(5): p. 765-771.
131. Huang, J. and W.S. Dynan, *Reconstruction of the mammalian DNA double-strand break end-joining reaction reveals a requirement for an Mre11/Rad50/NBS1-containing fraction.* Nucleic Acids Research, 2002. **30**: p. 1-8.
132. Zhang, X. and T.T. Paull, *The Mre11/Rad50/Xrs2 complex and non-homologous end-joining of incompatible ends in S. cerevisiae.* DNA Repair, 2005. **4**(11): p. 1281-1294.
133. Zhang, Y., et al., *Role of Dnl14-Lif1 in nonhomologous end-joining repair complex assembly and suprresion of homologous recombination.* Nature Structural & Molecular Biology, 2007. **14**(7): p. 639-646.
134. Lisby, M., et al., *Choreography of the DNA Damage Response: Spatiotemporal Relationships among Checkpoint and Repair Proteins.* Cell, 2004. **118**: p. 699-713.
135. Mari, P.-O., et al., *Dynamic assembly of end-joining complexes requires interaction between Ku70/80 and XRCC4.* Proceedings of the National Academy of Sciences of the United States of America, 2006. **103**(49): p. 18597-18602.
136. Lee, J.H. and T.T. Paull, *Activation and regulation of ATM kinase activity in response to DNA double-strand breaks.* Oncogene, 2007. **26**(56): p. 7741-7748.
137. Audebert, M., B. Salles, and P. Calsou, *Involvement of Poly(ADP-ribose) Polymerase-1 and XRCC1/DNA Ligase III in an Alternative Route for DNA Double-strand Breaks Rejoining.* Journal of Biological Chemistry, 2004. **279**: p. 55117-55126.
138. Difilippantonio, S., et al., *Role of Nbs1 in the activation of the Atm kinase revealed in humanized mouse models.* Nature Cell Biology, 2005. **7**(7): p. 675-685.
139. Douglas, P., et al., *DNA-PK-dependent phosphorylation of Ku70/80 is not required for non-homologous end joining.* DNA Repair, 2005. **4**(9): p. 1006-1018.
140. Smider, V., et al., *Failure of hairpin-ended and nicked DNA to activate DNA-dependent protein kinase: Implications for V(D)J recombination.* Molecular and Cellular Biology, 1998. **18**: p. 6853-6858.
141. de Vries, E., et al., *HeLa nuclear protein recognizing DNA termini and translocating on DNA forming a regular DNA-multimeric protein complex.* Journal of Molecular Biology, 1989. **208**: p. 65-78.
142. Ma, Y. and M.R. Lieber, *DNA Length-Dependent Cooperative Interactions in the Binding of Ku to DNA.* Biochemistry, 2001. **40**: p. 9638-9646.

8. Appendix

Buffers and Solutions

Appendix 1: Cell flow cytometry and tissue culture

1. **1X Phosphate Buffered Saline (PBS)**

   Dissolve the following in 800ml Double distilled water (ddH_2O).

   - 8 g of NaCl
   - 0.2 g of KCl
   - 1.44 g of Na_2HPO_4
   - 0.24 g of KH_2PO_4

   Adjust pH to 7.4, Adjust volume to 1L with additional ddH_2O. Sterilize by autoclaving and store at 4°C.

2. **Trypsin-EDTA (Trypsin 0.05%, EDTA 0.02%)**

   0.5 g of Trypsin

   0.2 g of EDTA

   Adjust the volume to 1 L with 1X PBS.

   Sterilize by passing through 0.22 µm filter and store at -20 °C.

3. **Sodium azide (NaN_3 0.02%)**

   10 g of NaN_3

   Adjust the volume to 100 ml with ddH_2O.

   Store at RT.

4. **BrdU stock solution (10mM)**

   0.307 g of BrdU

   Adjust the volume to 100 ml with 1X PBS.

   Sterilize by passing through 0.22 µm filter and store at -20 °C in dark.

5. **100X Propidium iodide (4 mg/ml)**

   400 mg of PI

   Adjust the volume to 100 ml with ddH_2O.

   Store at -20°C in dark.

6. **100X RNase (6.2 mg/ml)**

   620 mg of BrdU

   Adjust the volume to 100 ml with MQ

   Store at -20°C in dark.

7. **1M HCl**

   Add 10 ml 12M HCl to 50 ml ddH_2O.

   Adjust the volume to 120ml with ddH_2O.

   Store at RT.

Appendix 2: Electrophoresis

8. **4x Tris/SDS pH 6.8 stacking gel buffer**

   Dissolve 6.05 g Tris-base in 40ml ddH_2O.

   Adjust pH to 6.8 with 1 N HCl.

   Add H20 to 100 ml.

   Add 0.4 g SDS.

   Store at 4°C.

9. **4x Tris/SDS pH 8.8 resolving gel buffer**

   Dissolve 91 g Tris-base in 300 ml ddH_2O.

   Adjust to pH 8.8 with 1 N HCl.

   Add H2O to 500 ml.

   Add 2 g SDS. Store at room temperature

10. 5x SDS electrophoresis buffer

15.1 g Tris-base

72.0 g glycine

5.0 g SDS

Add ddH_2O to 1000 ml.

Store at room temperature.

11. 6x SDS sample buffer

7 ml 4x Tris/SDS pH 6.8 stacking gel buffer

3.0 ml glycerol

1 g SDS

0.93 g DTT (dithio-threitol)

1.2 mg bromophenol blue

Add ddH_2O to 10 ml.

Store in 1 ml aliquots at -20°C.

12. 1X Transfer Buffer (Western blot transfer buffer)

Dissolve the following in 1600ml ddH_2O.

- 28.8 g of glycine
- 6.04 g Tris base

Add 200 ml methanol.

Adjust the volume to 2000 ml with ddH_2O.

Store at 4°C.

13. Tween-20 20%

200 ml Tween-20

Adjust the volume to 1000ml with ddH_2O.

Store the solution at RT in dark.

14. TBST (PBS-0.05% Tween-20, washing buffer)

2.5 ml 20% Tween-20

Adjust the volume to 1000 ml with PBS.

Store the solution at RT in dark.

15. PBST-milk (PBST-5% ,Tween-20, washing buffer)

5g of milk (blot grade)

Adjust the volume to 1000 ml with ddH_2O.

Store the solution at 4 °C in dark.

16. Coommassie – staining Solution

0.02% Coommassie Brilliant Blue G250

2% (w/v) Phosphoric acid

5% Aluminium sulphate

10% Ethanol

Appendix 3: Immunoprecipitation

17. IP buffer

50mM Tris HCl pH 8.0

150mM NaCl

1% NP-40 (Igepal CA-630)

18. True-Blot Buffer (TBST)

50mMTris HCl pH 7.3

150mM NaCl

0.1 % Tween20

Appendix 4: Cell Fractionation

19. Hypotonic Buffer

10mM HEPES, pH 7.5

1.5mM $MgCl_2$

5mM KCl

0.2mM PMSF

0.5mM DTT

20. Low Salt Buffer

20mM HEPES, pH 7.9 at 4°C

1.5mM $MgCl_2$

0.02M KCl

0.2mM EDTA

0.2mM PMSF

0.5mM DTT

21. High Salt Buffer

10mM HEPES, pH 7.9 at 4°C

1.6 M KCl

1.5 mM $MgCl_2$

22. Dialysis Buffer

25mM Tris/HCl pH 7.5 at 4°C

10% Glycerol

50mM EDTA

1mM EDTA

0.5 mM DTT

0.2mM PMSF

Appendix 5: EMSA

23. 10X EMSA Buffer

10mM Tris-HCl, pH 7.5

1mM

1mM DTT

150 mM NaCl

24. 6% EMSA Non Denaturizing gel

Acrylamide/Bis acryl amide (30:1) - 10ml

0.5X TBE (Stock-5X) - 5ml

H_2O - 35ml

10% APS - 300µl

TEMED - 90µl

25. 10X NHEJ Buffer

20mM Hepes-KOH (pH 7.5)

10mM $MgCl_2$

80mM KCl

1mM ATP

1mM DTT

Appendix 6: Protein Purification

26. PARP Purification Buffers

Homogenization Buffer

25mM Tris-HCl, pH 8.0

50mM Glucose

10mM EDTA

1mM β-mercaptoethanol

1mM DTT

0.1mM PMSF

10% glycerol

PARP chromatography Buffer A

50mM Tris-HCl, pH8.0

1mM EDTA

25mM $Na_2S_2O_3$

10mM 2-Mercaptoethanol

1mM DTT

0.1mM PMSF

10% glycerol

Buffer B

Buffer A + 1M NaCl

Dialysis Buffer

0.25 M NaCl in Buffer A

27. Ku70/80 Purification buffers

Homogenization Buffer

50 mM Tris-HCl (pH 7.5)
100 mM NaCl
0.1% Igepal CA-630
2 mM EDTA
0.5 mM DTT
1 mM Phenylmethanesulfonyl fluoride (PMSF)
1 mM Benzamidine-HCl
1 µg/ml Leupeptin
2 µg/ml Aprotinin
1 µg/ml Pepstatin

Ku-Chromatography Buffer A

50mM Tris-HCl, pH 7.9
1mM EDTA
0.02% Tween-20
5% Glycerol
1mM DTT
10ug/ml PMSF

Buffer B

Buffer A + 1M NaCl

9. Acknowledgements

It is a pleasure to thank all the honorable people who have supported and inspired me in any respect in the completion of my thesis work.

They say, success is a journey and not a destination. But I believe that the dream of success begins with a teacher who believes in you, who tugs and pushes and leads you to the next plateau, sometimes poking you with a sharp stick called "truth." And my journey of completion of thesis is no exception.

I would like to express my deep and sincere gratitude to my supervisor, Professor Dr. George Iliakis, whose encouragement, guidance and support from the initial to the final level enabled me to develop an understanding of the subject and to complete my thesis. His wide knowledge and his logical way of thinking have been of great value for me. I thank him for providing me an opportunity to work under him by offering me this position in the institute. His detailed and constructive comments and his important support throughout this work have played a pivotal role in completion of this work.

I would also like to thank Prof. Dr. Wolfgang-Ulrich Müller and Dr. Peter Tamulevicius for giving me insights into radiation protection, dosimetry and laboratory safety.

I am extremely thankful to Frau Müller for her excellent and timely administrative assistance during my stay in the institute.

I am very thankful to Dr. Bustanur Rosidi for introducing to me the basic principles of purification technique on ÄKTA FPLC system which helped me in studying various in-vitro aspects of the project. I would also like to convey my sincere thanks to Dr. Emil Mladenov who played an important role in getting my thesis completed. I am extremely grateful to him for his generous and timely help for my experiments. I would like to also thank Dr. Minli Wang for introducing various laboratory techniques in the lab in initial days of my Ph.D. thesis.

I would like to thank Malihe Mesbah, Anita Hollenbeck, Tamara Musßfeldt, and Frau Lander for their constant wonderful technical assistance and endless effort in providing materials, chemicals and equipments needed for experimental purposes. I owe special thanks to all my past and present group members who helped and made our laboratory a convivial place to work. I would like to thank them all for their constant motivation and care extended during the years of my stay in Germany. Without their help and timely support this journey would have never been so

pleasant.

My deep regards to my Indian friends who have provided me a great company in Essen. Their social activities and moral support made my stay very congenial and convenient in this city. I extend my special thanks to Pooja, Savita, Pratima, Nisha, Preet, Aruna, Meenakshi, Pankaj, Janpriya, Satyendra, Aashish, Kunal, Shreenath, Manoj, Hemant. Special thanks to Janpriya and Satyendra who helped me in making appropriate corrections and in formatting my thesis.

I would like to thank my loving parents and younger brother Bhavesh for their love and encouragement, as well as for supporting me in all my pursuits.

Lastly, I offer my regards to all those who supported me in any respect during the completion of the project.

The financial support of the University of Duisburg Essen is gratefully acknowledged.

10. Curriculum Vitae

Aparna Sharma
Institute for Medical Radiation Biology,
Medical School of University of Duisburg-Essen.
Tel: 0176-24854260

Personal Details

Name:	Aparna Sharma
Date of Birth:	December 12, 1980
E-mail address:	aparna.sharma@uk-essen.de

Research Experience

January 2006 onwards:	Ph.D. Student, Institute for Medical Radiation Biology (IFMSB), Medical School of University of Duisburg-Essen, Essen, Germany.
2004 – 2005:	Research Fellow, National Institute for Immunology, Jawaharlal Nehru University, New Delhi, India.
2002 – 2003:	Master Thesis dissertation titled “Cloning DHFR Gene in plasmid internal Ribosomal Entry Site Bicistronic Vector.”

Education and Qualifications

2001 – 2003:	Masters in Biotechnology, Faculty of Life Sciences, Extol College, Barkatullah University, Bhopal, Madhya Pradesh, India.
1999 – 2001:	Graduation in Basic Sciences, SRJ Girls Govt College, Vikram University, Ujjain, Madhya Pradesh, India.
Until 1998:	Kendriya Vidyalaya, Neemuch, Madhya Pradesh, India.

Aparna Sharma
Institute for Medical Radiation Biology,
Medical School of University of Duisburg-Essen.
Tel: 0176-24854260

Training:

2002 — Summer training at Reliance Life Sciences, Mumbai under the guidance of Dr. Venkata Ramana, Associate Research Director.

Accomplishments and Activities:

2009 — Participated in 12th GBS (Gesellschaft fuer Biologische Strahlenforschung) Jahrestagung, Essen.

2003 — Secured Third position in order of Merit in the University examination in M.Sc. Biotechnology.

2002 — Won 1st prize in Extol TechnoGlimpse, Bhopal, India - an annual state level science model competition and exhibition on topic-“Cryopreservation”.

Poster Presentation:

12.Jahrestagung/12th Annual Conference Der/of the Gesellschaft für Biologische Strahlenforschung – GBS 30.9. – 2.10.2009, Essen, Germany titled “DNA damage dependent interactions between Mre11 and Ku heterodimer.”

Publications:

Rosidi B., Wang M., Wu W., **Sharma A.,** Wang H., Iliakis G**.** “Histone H1 functions as a stimulatory factor in backup pathways of NHEJ.” Nucleic Acids research, 2008 Mar; 36(5):1610-23

Singh S.M., **Sharma A.,** Panda A.K. “High throughput purification of recombinant human growth hormone using radial flow chromatography.” Protein expression and Purification, 2009 Nov; 68(1):54-9.

Aparna Sharma
Institute for Medical Radiation Biology,
Medical School of University of Duisburg-Essen.
Tel: 0176-24854260

Computer Knowledge:

MS Windows

Microsoft Office

BLAST, Vector NTI

Languages Known:

English	Fluent
Hindi	Mother Tongue
Hindi	Native language
German	Basic knowledge

Date: September 16, 2010 Aparna Sharma

11. Publications and Conferences

Publications

1. Rosidi B., Wang M., Wu W., **Sharma A.,** Wang H., Iliakis G**.** "Histone H1 functions as a stimulatory factor in backup pathways of NHEJ." Nucleic Acids research, 2008 Mar; 36(5):1610-23

2. Singh S.M., **Sharma A.,** Panda A.K. "High throughput purification of recombinant human growth hormone using radial flow chromatography." Protein expression and Purification, 2009 Nov; 68(1):54-9.

Poster Presentations

12.Jahrestagung/12th Annual Conference Der/of the Gesellschaft für Biologische Strahlenforschung – GBS 30.9. – 2.10.2009, Essen, Germany titled "DNA damage dependent interactions between Mre11 and Ku heterodimer."

12. Declaration

Erklärung:

Hiermit erkläre ich, gem. § 6 Abs. 2, Nr. 7 der Promotionsordnung der Math.-Nat.-Fachbereiche zur Erlangung der Dr. rer. nat., dass ich das Arbeitgebiet, dem das Thema *„Studies on Mre11-Ku interaction and its modulation by ionizing radiation“* zuzuordnen ist, in Forschung und Lehre vertrete und den Antrag von Frau Aparna Sharma befürworte.

Essen, den _____ _____ _____

Name des wissenschaftl. Betreuers/Mitglieds der Universität Duisburg-Essen	Unterschrift d. wissenschaftl. Betreuers/Mitglieds Universität Duisburg-Essen

Erklärung:

Hiermit erkläre ich, gem. § 6 Abs. 2, Nr. 6 der Promotionsordnung der Math.-Nat.-Fachbereiche zur Erlangung des Dr. rer. nat., dass ich die vorliegende Dissertation selbständig verfasst und mich keiner anderen als der angegebenen Hilfsmittel bedient habe.

Essen, den _____ _____

Unterschrift des/r Doktoranden/in

Erklärung:

Hiermit erkläre ich, gem. § 6 Abs. 2, Nr. 8 der Promotionsordnung der Math.-Nat.-Fachbereiche zur Erlangung des Dr. rer. nat., dass ich keine anderen Promotionen bzw. Promotionsversuche in der Vergangenheit durchgeführt habe und dass diese Arbeit von keiner anderen Fakultät abgelehnt worden ist.

Essen, den _____ _____

Unterschrift des Doktoranden